NASA CONTRACTOR REPORT

NASA CR-

NASA CR-2707

SPACE SHUTTLE ELECTROMAGNETIC ENVIRONMENT EXPERIMENT

Phase A: Definition Study

Fred Haber, R. M. Showers,
C. Kocher, and L. A. Forrest, Jr.

Prepared by
THE MOORE SCHOOL OF ELECTRICAL ENGINEERING
Philadelphia, Pa. 19174
for Goddard Space Flight Center

NATIONAL AERONAUTICS AND SPACE ADMINISTRATION • WASHINGTON, D. C. • JUNE 1976

TECHNICAL REPORT SI

1. Report No.	2. Government Accession No.	3. Recipient's Catalog No.
NASA CR-2707		

4. Title and Subtitle
SPACE SHUTTLE ELECTROMAGNETIC ENVIRONMENT EXPERIMENT, Phase A: Definition Study

5. Report Date
June 1976

6. Performing Organization Code

7. Author(s)
Fred Haber, R. M. Showers, C. Kocher, L. A. Forrest, Jr.

8. Performing Organization Report No.
Moore School 76-03

9. Performing Organization Name and Address
The Moore School of Electrical Engineering
University of Pennsylvania
Philadelphia, Pa. 19174

10. Work Unit No.

11. Contract or Grant No.
NAS 5-20707

12. Sponsoring Agency Name and Address
GODDARD SPACE FLIGHT CENTER
National Aeronautics & Space Administration
Communication & Navigation Division
Greenbelt, Md. 20771

13. Type of Report and Period Covered
Final Report
9/3/74-9/30/75

14. Sponsoring Agency Code
953

15. Supplementary Notes

16. Abstract

The results of a study aimed at developing methods for carrying out measurements of earth electromagnetic environment using the space shuttle as a measurement system platform are herein reported. The goal is to provide means for mapping intentional and nonintentional emitters on earth in the frequency range 0.4 to 40 GHz.

To guide in the system development, a survey was made of known emitters using available data from national and international regulatory agencies, and from industry sources. The spatial distribution of sources, power levels, frequencies, degree of frequency re-use, etc., found in the survey, are here presented.

A concept is developed for scanning the earth using a directive antenna whose beam is made to rotate at a fixed angle relative to the nadir; the illuminated area swept by the beam is of the form of cycloidal annulus over a sphere. During the beam's sojourn over a point, the receiver sweeps in frequency over ranges in the order of octave width using sweeping filter bandwidths sufficient to give stable readings. Special means are proposed for dealing with low-duty cycle emissions. General formulas and curves are presented to allow the user to choose

Continued

17. Key Words (Selected by Author(s))
Electromagnetic Environment
Satellite Survey
Radio Frequency Interference

18. Distribution Statement
Unclassified - Unlimited
Cat. 70

19. Security Classif. (of this report)	20. Security Classif. (of this page)	21. No. of Pages	22. Price*
Unclassified	Unclassified	176	$7.00

For sale by the National Technical Information Service, Springfield, Virginia 22161

Abstract (Continued)

spatial and frequency scan modes to suit his need, and specific cases are also presented. Special emphasis is put on a horizon scanning mode which allows earth transmitter powers to be measured along their main beams.

Techniques for determining the frequency with which points on earth will be illuminated are developed and specific results for the horizon scanning mode are worked out. The probability that the receiver will erroneously respond to powerful emitters not in the direction of the receiver's main beam is analyzed,and proposals for dealing with this problem are made. Finally, the problem of data handling is examined. Estimates of the rate of the generation of data and storage requirements are made, and alternatives for data processing are discussed.

TABLE OF CONTENTS

Continued

Continued TABLE OF CONTENTS

LIST OF FIGURES

LIST OF FIGURES - (continued)

LIST OF FIGURES - (continued)

LIST OF FIGURES - (continued)

LIST OF TABLES

Continued

LIST OF TABLES (continued)

1.0 INTRODUCTION

1.1 Objective and Background Information

The principal objective of the work reported here was to develop a plan for a comprehensive measuring system capable of systematically surveying electromagnetic emissions from the earth, and suitable for accommodation on the space shuttle.

The use of satellites for surveying electromagnetic emissions from the earth's surface has been under discussion for about 10 years [1-6] and, indeed, a number of measurements have been and are being made [7-11]. The experiments actually carried out have been of a restricted nature designed either to demonstrate the feasibility of such measurements or to obtain a specific kind of information. The Space Shuttle Electromagnetic Environment Experiment (EEE) is intended to provide more comprehensive results and, where it is advantageous, to make use of the crew members in carrying out measurements.

In designing the experiment, it is essential to determine who will be principal users of the data. A recent paper by R. E. Taylor, R. E. Prince, and D. N. McGregor [12] lists national and international bodies concerned with spectrum use and management, as well as NASA itself. Accordingly, the measurement methods proposed here have in mind various possible users. Principally, however, the orientation of this work is to applications in space. In a recent article surveying the state of domestic satellites [13] it is pointed out that interference problems associated with the satellite-to-earth link are not usually important, since control can be exercized through proper siting of the ground station.* The satellite, however (in the case under discussion synchronous satellites were in mind), is subject to interference from widely dispersed points, so that proper choice of the earth-to-satellite frequency is important. Emissions from ground-based sources affecting satellite operations can be categorized as follows: intentional emissions whose fundamental frequencies lie in or close to the bands allocated for satellite operations; intentional emissions whose fundamental frequencies are not in those bands but whose harmonics or spurious emissions are; and unintentional emissions that may come from ignition systems, Industrial, Scientific, and Medical (ISM) equipment, welding equipment, or hitherto unsuspected sources.

There are three principal ways to obtain information about some of these emissions: (1) by examination and correlation of data on emitters listed by such agencies as the Electromagnetic Compatibility Analysis Center (ECAC) and the Federal Communications Commission (FCC); (2) by direct measurement with ground-based or aircraft-based monitoring equipment; (3) by direct measurement from a satellite.

Other investigators [14] have concluded that the first approach is of limited value in large part because files do not include actual use of licensed devices and because of time lag in additions to and deletions from

---

* An exception is down link commands to data collection balloons (SMS geostationary satellite and communications directly to ships, aircraft and satellites in low orbits).

the file. A point in favor of this approach is that the potential exists for calculating field strength in any direction from the source. Programs for this purpose are available at ECAC. A measuring system has the advantage of updating emitters not yet listed in the files, and in also giving much needed information on unintentional and spurious emitters.

Ground-based measuring equipment is very commonly used particularly for site surveying and for determining radio station coverage. But the data so obtained will not be immediately useful for determining fields in space nor can one hope to be thorough on the ground. Measurements made on-board aircraft do not suffer from these deficiencies and may be better than satellite measurements in some respects. The limited region in view from aircraft serves to limit the number of sources to which the measuring receiver is exposed at any one time as compared with a satellite. This problem of "satellite overexposure" is discussed further below. The rate of coverage by aircraft is, however, much less than with satellites and the cost over a long period of time for a systematic monitoring system may favor satellites. The subject of cost effectiveness was not part of this study but is an important issue to be determined once optimum methods are developed.

In favor of the satellite-borne monitor is its capability of more directly examining the RFI environment as it would be seen by subsequent satellites. It would be impossible for a satellite monitor in a low earth orbit to continuously monitor single sources for prolonged periods, but it could examine such sources for short periods at different times of day, and from different angles, and it might identify sources that are worthy of more intensive examination by ground-based or airborne monitors. Two satellites, the LES-5 and LES-6, have monitored portions of the spectrum from 255 to 280 and from 290 to 315 MHz. The ATS-6 geo-stationary satellite is now making measurements in the vicinity of 6 GHz.* Except for this, none have investigated the many bands reserved for earth-satellite communications in the 0.4-40 GHz range and none have provided high geographic resolution. A cost/benefit study [14] has indicated that a survey of these bands would improve the performance of subsequent missions, particularly space shuttle missions.

The effort was carried out with attention to the following steps:

1. Examinations of the expected environment, including the numbers, types, and intensities of emitters as seen at the satellite

2. Choice of a measuring concept

3. Analysis of the technical parameters of possible measurements conducted from an orbiting vehicle at the expected altitude. This includes a trade-off analysis accounting for such factors as sensitivity, area coverage, and detection probability.

---

* An experiment is being conducted by the NASA Communication and Navigation Division to measure radio frequency interference (RFI) in the vicinity of 1.6 and 2.25 GHz using the ATS-6 satellite at synchronous altitude. Recent information will be found in NASA-GSFC Preliminary Report,"ATS-6 Electromagnetic Environment Survey Manual Data Reduction," 30 September 1975, by Westinghouse Electric Corporation.

4. Optimum parameter selection

5. Examinations of hardware feasibility including the antenna, RF components, frequency sweep systems, and data recording and display systems (hardware implementation is to be carried out elsewhere)

6. Data processing in the satellite and on the ground, and programming for access to the stored data,

1.2 Measurables and System Capabilities

A 1967 study by General Dynamics [15] gives the following as the output of an ideal experiment:

1. Exact location of every transmitter on earth
2. Its frequency
3. Power radiated
4. Antenna pattern and polarization
5. Transmitter modulation and duty cycle
6. Whether the transmitter is stationary, rotating, or mobile
7. Variations of transmitter output
8. Probability that a mobile transmitter is in a specific location

To these we may add:

9. Probability that a known transmitter is transmitting at a given time

The list is drawn up with the idea that only intentional transmissions need to be measured. Tests with aircraft carried out by Lincoln Laboratories [16] showed that when an area of more than three miles across is viewed (their measurements were made at frequencies between 200 and 400 MHz) the urban noise field observed has the characteristics of Gaussian random noise when intentional emitters are eliminated from the data. The receiver sees many minute noncoherent sources simultaneously, the effect of which is an increase in the receiver noise level.

Intentional communication channels are deliberately spread out spectrally, spatially, and/or temporally to avoid interference among them. One would like the space-borne measuring system to be sufficiently discriminating so as to identify individual intentional emitters. This does not imply that every transmitter will be detected by the measuring system. Factors affecting the probability of detection are transmitter on-time, antenna directivity, power output, shuttle/spacelab orbit, etc. These factors can be taken into account in estimating the probability that a given transmitter will be detected. Clearly, if measurements are made over a sufficiently long time, every emitter with enough power in the area surveyed will ultimately be observed.

2.0 SUMMARY OF PRINCIPAL CONCLUSIONS AND RECOMMENDATIONS

1. The space shuttle provides an excellent opportunity to demonstrate the "efficiency" of the satellite technique for collection of data on emissions from the earth's surface in the radio frequency range. The efficiency can be defined in terms of:

(a) ability to survey substantial portions of the earth's surface

(b) effective sensitivity of feasible sensors at orbital altitudes

(c) probability of intercept of various types of emissions.

2. Simultaneous scanning of both the frequency spectrum and the earth's surface is quite feasible and can provide large output data rates. However, probability of intercepting a given source depends upon its output power, antenna directivity and pointing discipline, duty cycle, and other factors. A flexible system would be one providing for both nodding (with adjustable scanning width and rate) and conical scan (with adjustable scanning rate and inclination angle). The capability of fixing the antenna relative to the satellite, particularly for nadir looking, and the capability of tracking sources using the man in space would be useful.

3. The selection of detailed modes of system operation (scan rate and inclination angle) is critically dependent on the ultimate uses for which the data are gathered, which in turn defines the characteristics of those emissions which are to be identified, location information, exact frequency times of operation, etc.

4. Side-and-backlobe characteristics of both satellite mounted and ground emitting antennas will cause ambiguities in emitter location information as the satellite circles the earth in orbit. For this reason, techniques for processing video data must be very carefully designed. Because of item (3) above, as much data processing as possible should be done on a real time basis.

5. The hardware and software required to carry out the experiment are feasible. The development of detailed technical specification and subsequent equipment development and construction should be initiated.

6. Continuing evaluation should be carried out to firm up detailed plans for conduct of experiments and data processing in order to optimize the use of the equipment and to maximize the value of the information obtained.

3.0 SURVEY OF AIRCRAFT ELECTROMAGNETIC ENVIRONMENT MEASUREMENTS

For the purpose of this survey, electromagnetic radiation has been divided into two groups: that arising from intentional emitters and unintentional emitters generating coherent RF energy, and that arising from multiple natural or man-made noncoherent sources (incidental broadband emitters). A limited number of coherent and noncoherent emission measurements have been made using both airborne and spaceborne platforms. Measurements of noncoherent emissions avoided frequencies at which there were intentional sources. Measurements of coherent emissions were actually composite surveys - surveys of total radio frequency radiation measured continuously over a frequency band. In these cases, the apparent baseline radiation was treated as the noncoherent radiation component with the amplitude salients treated as coherent radiation. Because the measured data are limited, estimated information on the numbers of major sources in various services, location, and frequencies has been assembled.

3.1 Incidental Emissions

Noncoherent noise radiation from cities at UHF frequencies has been modeled by Ploussios [16] on the basis of aircraft based surveys at 226.2 MHz, 305.5 MHz, and 369.2 MHz made over 7 cities in the Eastern United States: Miami, Jacksonville, Orlando, Baltimore, Philadelphia, New York City (Manhattan and Brooklyn), and Boston. It was noted that above 5,000 ft. where more than 3 square miles were observed, urban spectra cease to appear to originate from discrete sources, and approach random noise. The measurements are reported in terms of antenna temperature noise and shown in Table 1.

Table 1. Noise Temperature Recorded on C-131 Over Eastern U.S. Cities

City	Altitude		Antenna Temperature (K)		
		(Ft.)	226.2 MHz	305.5 MHz	369.2 MHz
Boston		8k	22,000	8,000	*
Baltimore		18k	23,000	7,000	*
Jacksonville		14k	14,000	3,400	*
Miami	(Cold)	18k	14,000	4,600	*
	(Hot)	10k-18k	27,000	10,500	*
Orlando		9k	9,000	4,000	2,200
Philadelphia		8k-18k	26,000	9,000	6,000
Brooklyn		8k-18k	60,000	19,000	9,500
Manhattan		8k-18k	75,000	30,000	16,000

* Accurate values not obtained due to ground RFI

Measurements were made using total power radiometers having a 1.2 MHz bandwidth and a 2 ms integration time. The antenna was a 2 dipole array matched at the three frequencies to a VSWR of less than 1.5:1.

The half power beamwidths of the antenna ranged from 42° to 112°.

Two measurements are reported for Miami, showing a significant difference between temperatures during the tourist season (hot) and the "off" season (cold). Ploussios observed that the brightness temperatures of different cities are not substantially different, excepting New York. A plot of brightness temperature profile of Philadelphia is shown in Fig. 1. From his findings, Ploussios modeled a city as an aperture having the dimension of the city within which are random sources having a uniform power density as shown in Fig. 2. The power density was found to range from 3×10^{-18} $(W/m^2)/Hz$ to 1×10^{-18} $(W/m^2)/Hz$ over the UHF band during weekdays. However, New York City has a level from 5 to 6 dB higher.

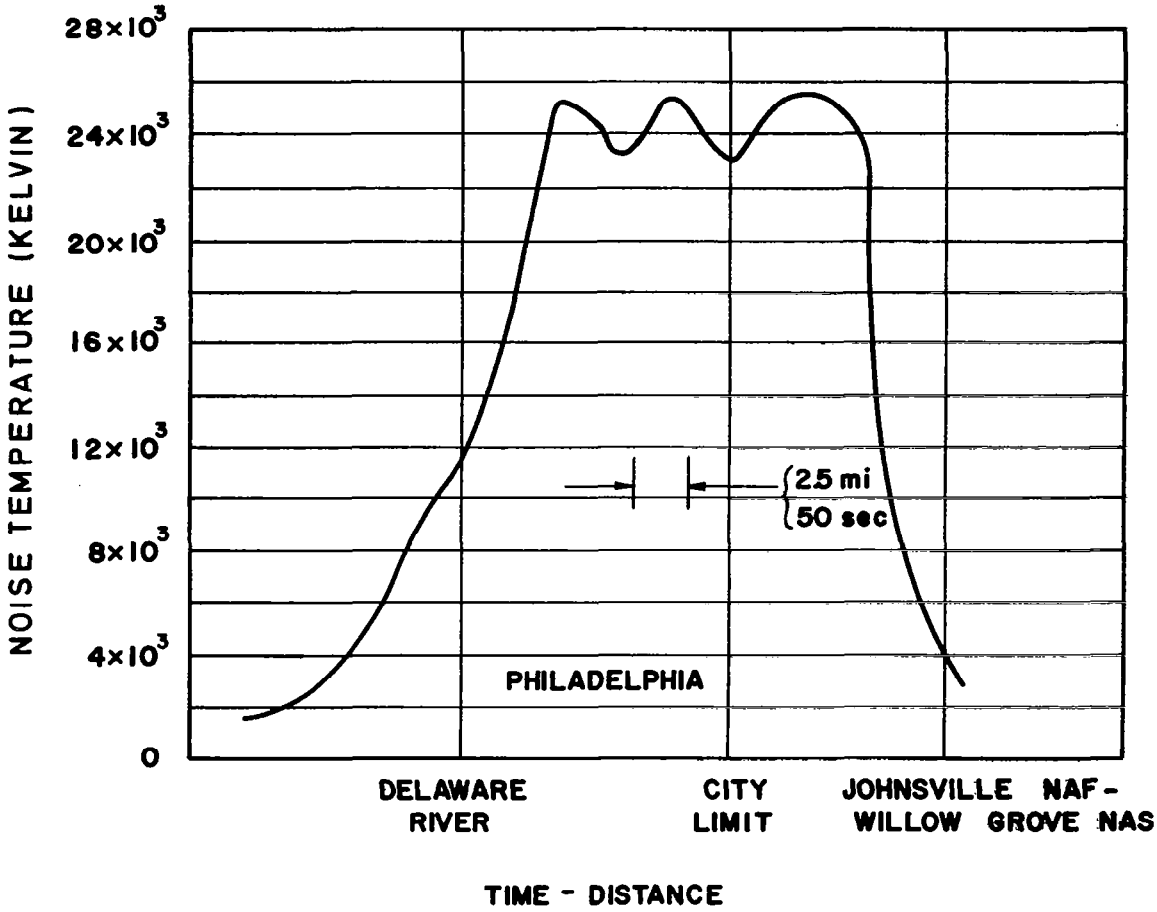

Fig. 1 Temperature Profile of Philadelphia at 226.2 MHz, Measured Traveling North at 18,000 ft, 18 Nov. 1965 (from Ref. 16).

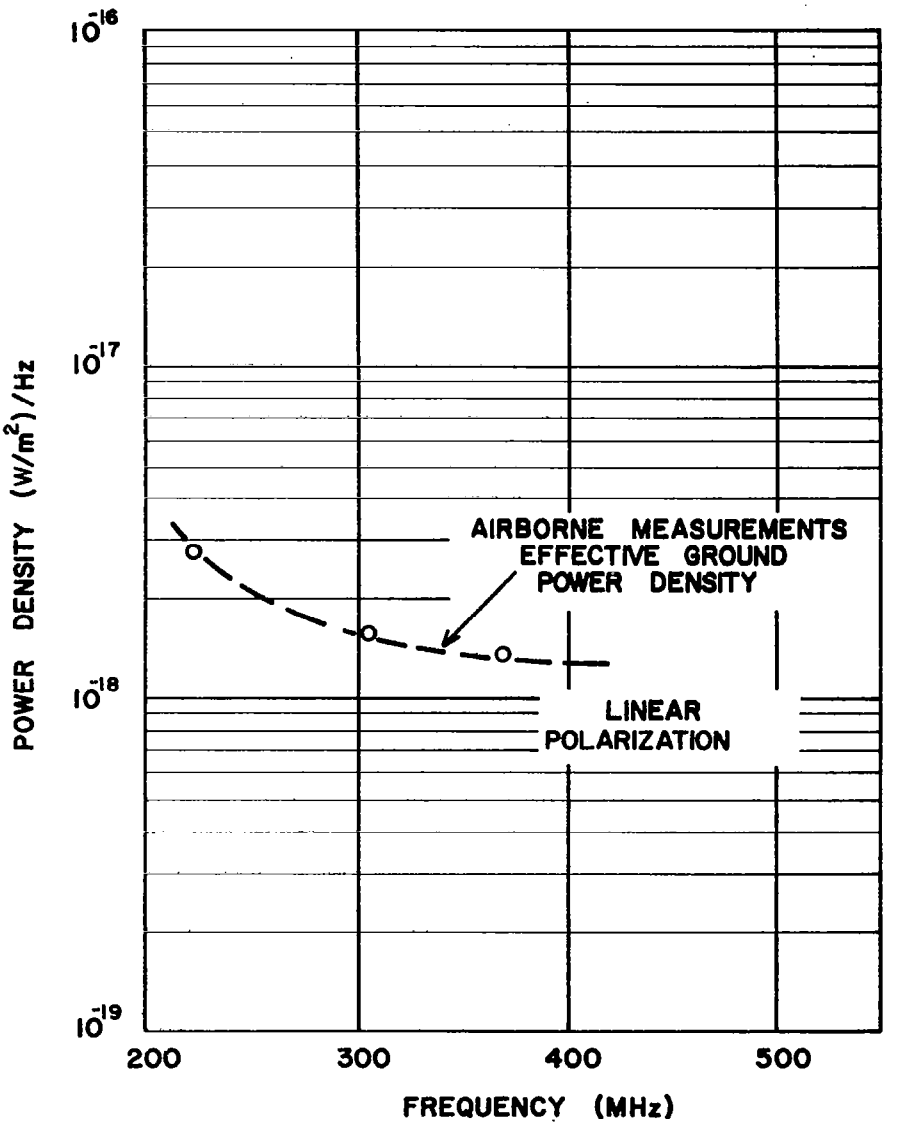

Fig. 2 Effective Noise Power Density as Measured in Aircraft over a City (from Ref. 16).

A series of surveys of urban, suburban, and rural man-made incidental noise in the UHF frequency range was made by Mills [17,18] and analyzed by Anzic [19-22]. The sites surveyed were: Cleveland, where noise was measured on the ground at 480 MHz and 950 MHz; Phoenix, where noise was measured on the ground and from an aircraft near 0.3 GHz, 1.0 GHz, and 3.0 GHz; and Akron, where noise was measured from an aircraft, also at 0.3 GHz, 1.0 GHz, and 3.0 GHz. Only the results of the aircraft based surveys are presented here since, as Ploussios concluded, these are more representative of vertically propagated noise.

The Phoenix survey was conducted using receivers having a bandwidth of 2.7 MHz, and noise figures less than 4 dB. The antenna characteristics are shown below:

Table 2. Antenna Characteristics

Freq. GHz	Type	Polarization	Gain	Half power Beamwidth	Front to back ratio-greater than
0.3	Quad Dipole	circular	11.2 dB	48°	19 dB
1	Helical	circular	11 dB	$34^{\circ} \times 47^{\circ}$	18 dB
3	Helical	circular	13 dB	$33^{\circ} \times 26^{\circ}$	20 dB

Measurements were made only on weekdays, and in the morning, at noon, and in the evening, from an altitude of 1000 and 4000 ft. at a speed of 100 ± 10 knots. The parameters measured were rms noise voltage and average noise envelope voltage.

Data were reported in terms of dB above kTB. Average noise levels were observed to vary in a daily pattern as shown in Table 3.

Table 3. Daily Variation of Noise Levels Over Phoenix

Time of Measurement	Average level 0.3 GHz at 4000 feet * (dB above kTB)
Morning	19
Noon	17
Late Evening	13

Typical 1.0 GHz noise levels measured during morning rush hours were 5 to 6 dB below those measured at 0.3 GHz. Rms noise profiles of Phoenix, prepared from measurements made at 0.3 and 1.0 GHz during morning, noon, and evening flights, are shown in Fig. 3. The profile shown in Fig. 3a is along an east-west path crossing the city hub, while Fig. 3b shows the profile made along a north-south profile, also crossing the city hub. It is noted that the levels measured at 1.0 GHz show little variation from place to place in the city, but do show a variation of about 10 dB at different times of day. The evening profile at 0.3 GHz, made at 2119 hr, similarly is relatively flat, while a considerable variation is seen in profiles made at 0653, 0817 and 1115. No results were reported at 3.0 GHz since most data obtained were found to be unreliable because of receiver limitations. The data indicated that the RF noise level was near the system threshold most of the time (4 dB above kTB).

Measurements were made over Akron at 0.3 GHz, 1.0 GHz, and 3.0 GHz using the same equipment that was used in Phoenix, somewhat modified to take into account experience gained there. As in the Phoenix survey, the rms level measured at 3.0 GHz remained near or below the receiving system threshold, less than 4 dB above kTB, and no significant data were gathered.

The noise levels at 1.0 GHz were found to range from about 7 dB above kTB to below 4 dB above kTB, the receiving system threshold, with the exception of one narrow salient of about 20 dB above kTB, which appears on one of the profiles. The received noise level remained above the receiver threshold in urban areas and for the most part in suburban areas, while remaining below the receiver threshold most of the time in rural areas.

* Levels noted include internal noise of measuring system = 4 dB above kTB.

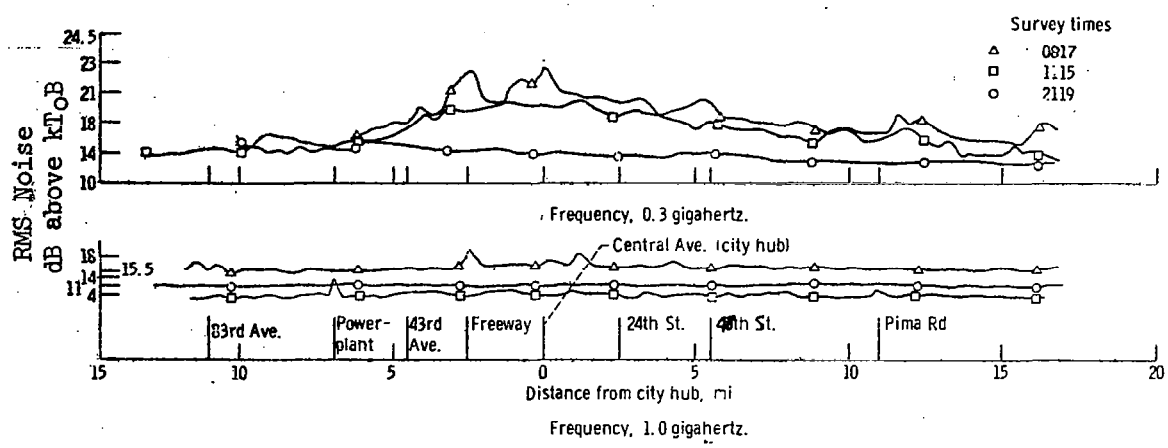

a. East-West Flight Path

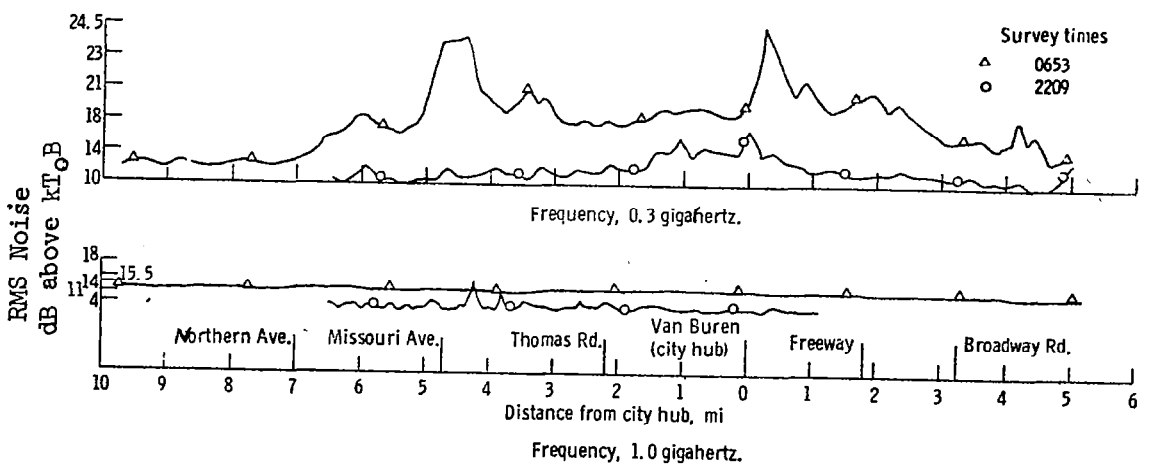

b. North-South Flight Path

Figure 3. Noise Level Variations Over Phoenix (from Ref. 19).

The noise levels at 0.3 GHz were, as expected, substantially higher than those measured at 1.0 GHz. The measurements range from a high of about 37 dB above kTB to a low of less than 10 dB above kTB, the lower measurement appearing on one of the profiles in an area indicated as rural. Within the urban/suburban areas, the levels remained above 20 dB above kTB. A sample profile is shown in Fig. 4.

Aircraft based surveys were also performed by Barnard [23] and Buehler, King, and Lunden [24]. Barnard surveyed cities in the United Kingdom including London, Birmingham, Manchester, and Liverpool, but only at VHF frequencies, 118 MHz. Buehler et.al., surveyed Seattle, again at VHF frequencies, measuring urban, suburban, and rural radio-frequency noise at 49, 73, and 137 MHz.

Skomal [25,26] has analyzed the results of these surveys, with emphasis on the prediction of noise level depending on altitude and frequency. He notes that at altitudes above 1 mile over metropolitan areas, the impulsive character of surface incidental noise disappears and is replaced by the noise patterns which appear similar to thermal noise, eg. Gaussian. Since these surveys were not in the UHF band, they will not be further discussed.

Aircraft based surveys of composite noise covering extended geographical areas were conducted by Zamites and Hurlbut [27]. The receiver measured average and peak power in the frequency bands from 233 to 258 MHz and 290 to 315 MHz. The reported measurements are averages of those recorded along extended strips such as from Cape Cod to Dayton (Fig. 5), the Mideast, Europe, and the Eastern United States (Fig. 6). Measurements which were made in Vietnam and Southeast Asia showed very high levels of emissions, probably due to the war. The baseline of the plot of the noise density averaged, over the Eastern United States, the Mideast, and Europe ranges between -120 dBm/kHz, and what appears to be the system noise density, about -125 dBm/kHz. Noise levels tended to reside in the lower end of this range much of the time, and fell below this level over significant parts of the spectrum surveyed, especially in the range 290 to 315 MHz. This set of surveys also included data concerning maximum and mean peak levels. The baseline of the maximum peak level plot, 290 to 315 MHz, ranges from about -70 dBm/kHz to about -90 dBm/kHz, in the average of noise observed in the Mideast, Europe, and Eastern United States. These high peak levels may be the result of coherent sources being found in such large number over the large geographical areas surveyed to take on the nature of continuous spectra, as occurred with city incidental noise sources when a sufficiently large area was viewed. The baseline of maximum peak levels, 233 to 258 MHz, observed in the Mideast, Europe, and Eastern United States ranges from -70 dBm/kHz to about -95 dBm/kHz.

Noise power and occupancy was measured by Madison, Kuehn, and Bode [28] in the frequency band 100 MHz through 500 MHz over Northern Europe, including Northeastern France, Central West Germany, Belgium, The Netherlands, and Luxemburg. The results presented are averages over this

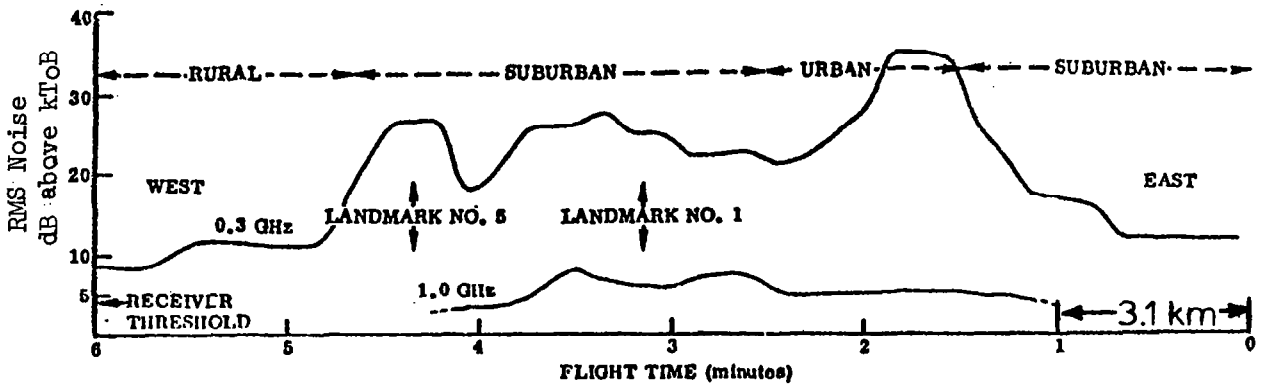

Figure 4. Noise Level Variations on Flight Path over Akron, Ohio (from Ref. 18).

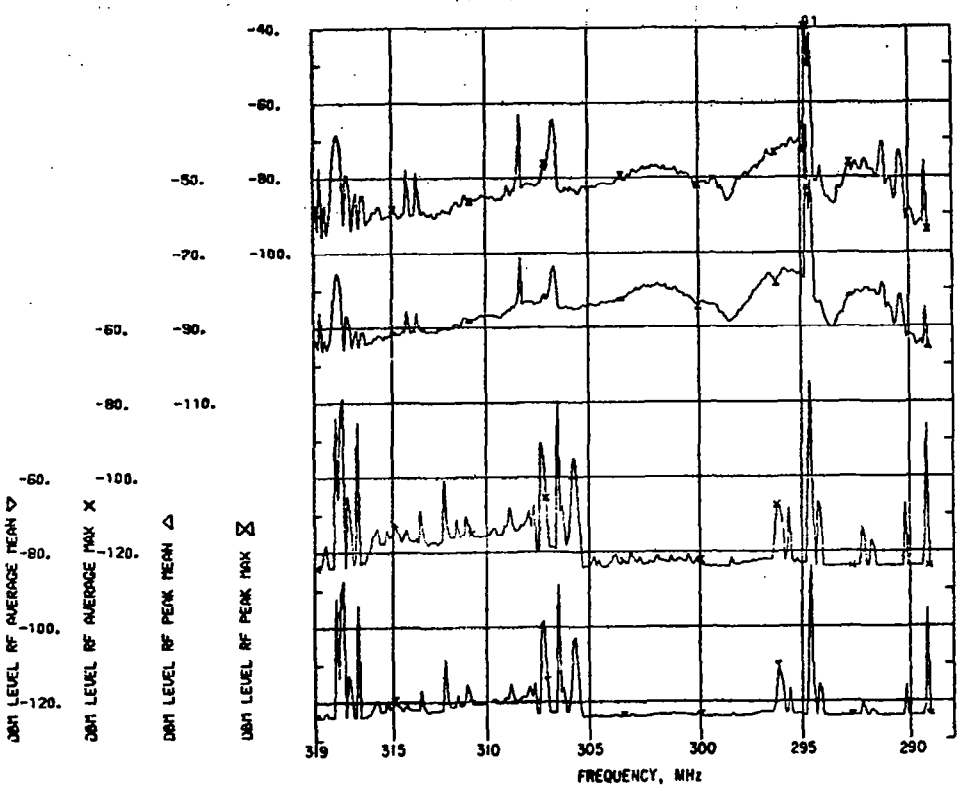

Fig. 5 Noise Level as a Function of Frequency (Eastern United States - Cape Cod to Dayton) (from Ref 27).

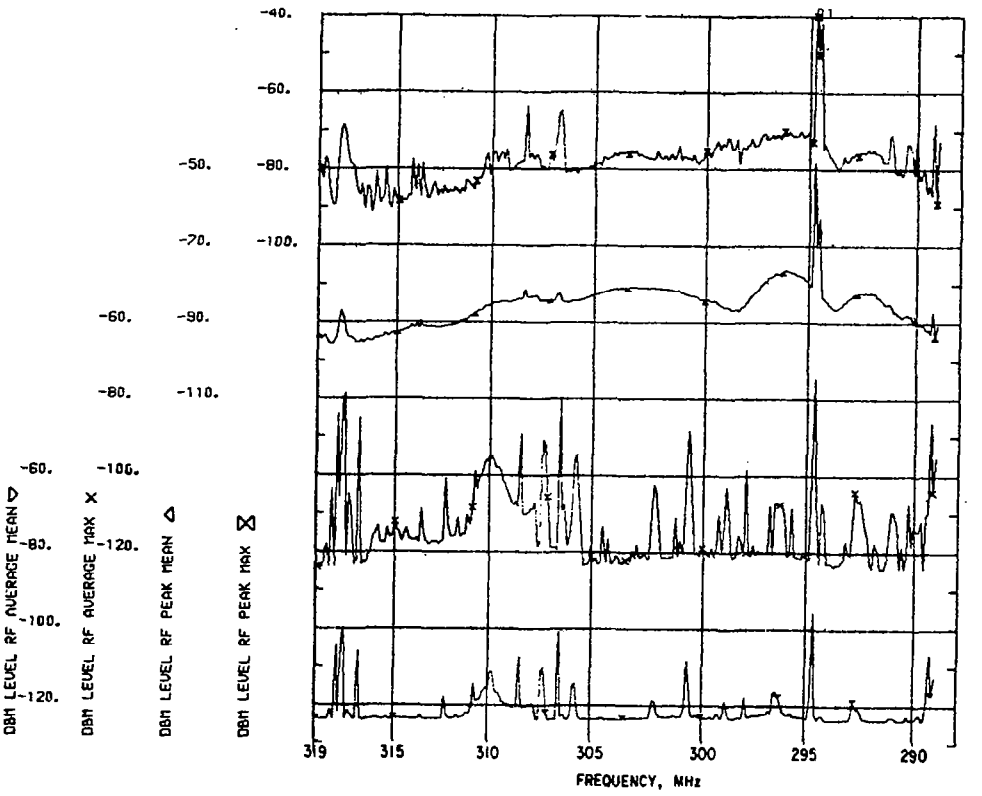

Fig. 6 Noise Level as a Function of Frequency--Mideast, Europe, and Eastern United States (from Ref. 27).

entire region. This survey measured peak and average power at an altitude of 30,000 ft., quantized in steps of 5 dBm in each 30 kHz channel from 100 to 500 MHz using a computer controlled spectrum analyzer mounted in a KC-135. The view of the log periodic antennas was 360 miles wide. The measurements were made viewing a wide angle looking forward from the aircraft with the center of the main lobe about 0.2^{o} below the horizon. Various bands in this portion of the spectrum are allocated for fixed mobile operation, aeronautical radio-navigation, broadcast, and space and meterological aids. The report includes graphs of average power levels in each channel, and graphs of channel occupancy, and the text and accompanying tables note hourly or day to day variations. Figure 7 shows the results of measurements of average power levels from 400 to 410 MHz. The baseline of noise was at about -108 dBm for most of the surveys made in the 400-406 MHz band (ITU Meteorological). Occupancy is defined as the percent of time that the level in a 30 kHz channel is above -99 dBm. This band was occupied less than 10% of the time, except on the occasion where the average level went to -115 dBm/kHz, when the occupancy rose to nearly 100%. This was possible due to a signal near 404 MHz.

The 450 to 470 band (ITF Fixed Mobile) was found to be in much more intensive use. The levels of average power in this band are shown in Figs. 8 and 9. The baseline level here ranged from about -100 dB to about -110 dBm.

The distribution of received power levels for several flights is shown on Fig. 13. The received level never rose above -80 dBm and remained below -90 dBm for more than 90% of the time. In this survey, no attempt was made by the investigators to separate coherent sources from noncoherent sources.

According to this survey, the 400-406 MHz band showed the lowest occupancy and average power levels of all the bands above 400 MHz, with average power levels typically around -110 dBm.

Occupancy and average power in the various fixed mobile bands was varied, albeit evenly distributed within each band. Average power levels extended as high as -80 dBm.

Average power levels across the 470 to 500 MHz UHF broadcast band (Figs. 10-12) were substantially higher (up to -56 dBm) but very regular: one sees virtually the same set of peaks for each TV channel. A survey looking at the continental U.S. might see a similar set of peaks repeated every 6 MHz across the entire 470-806 MHz portion of the spectrum.

One set of information from a satellite, Nimbus -4 [29] reports levels of radio interference at 401.5 MHz (down-link) and 466 MHz (up-link) (Fig. 14). Up-link interference ranges from above -110 dBm to below -130 dBm. No data are given on area of view, receiver characteristics, or how the measurements were made.

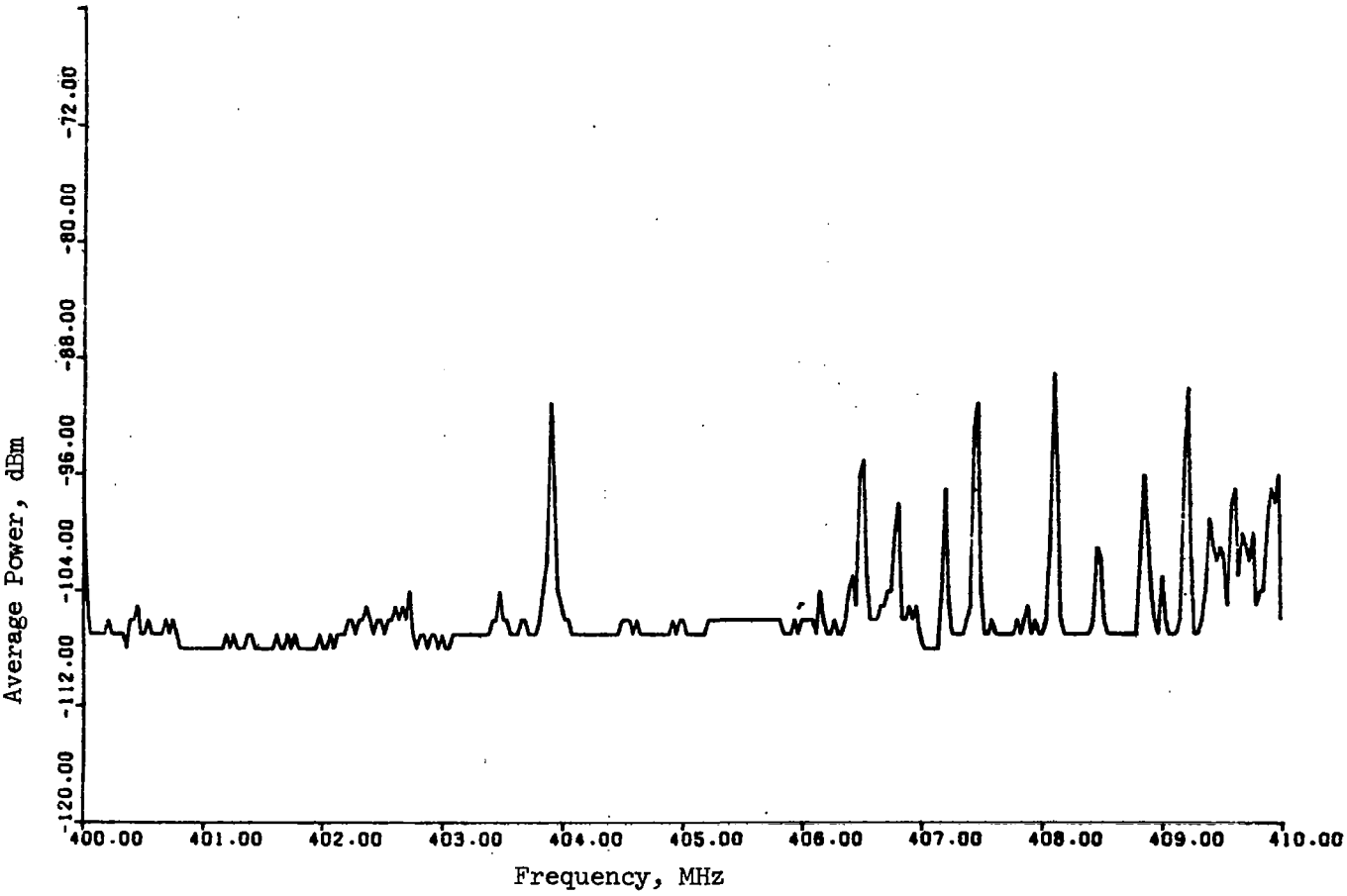

Fig. 7 Average Power Levels over Europe in the 400-410 MHz Band as Measured at 30,000 ft with Antenna Looking Forward (from Ref. 28).

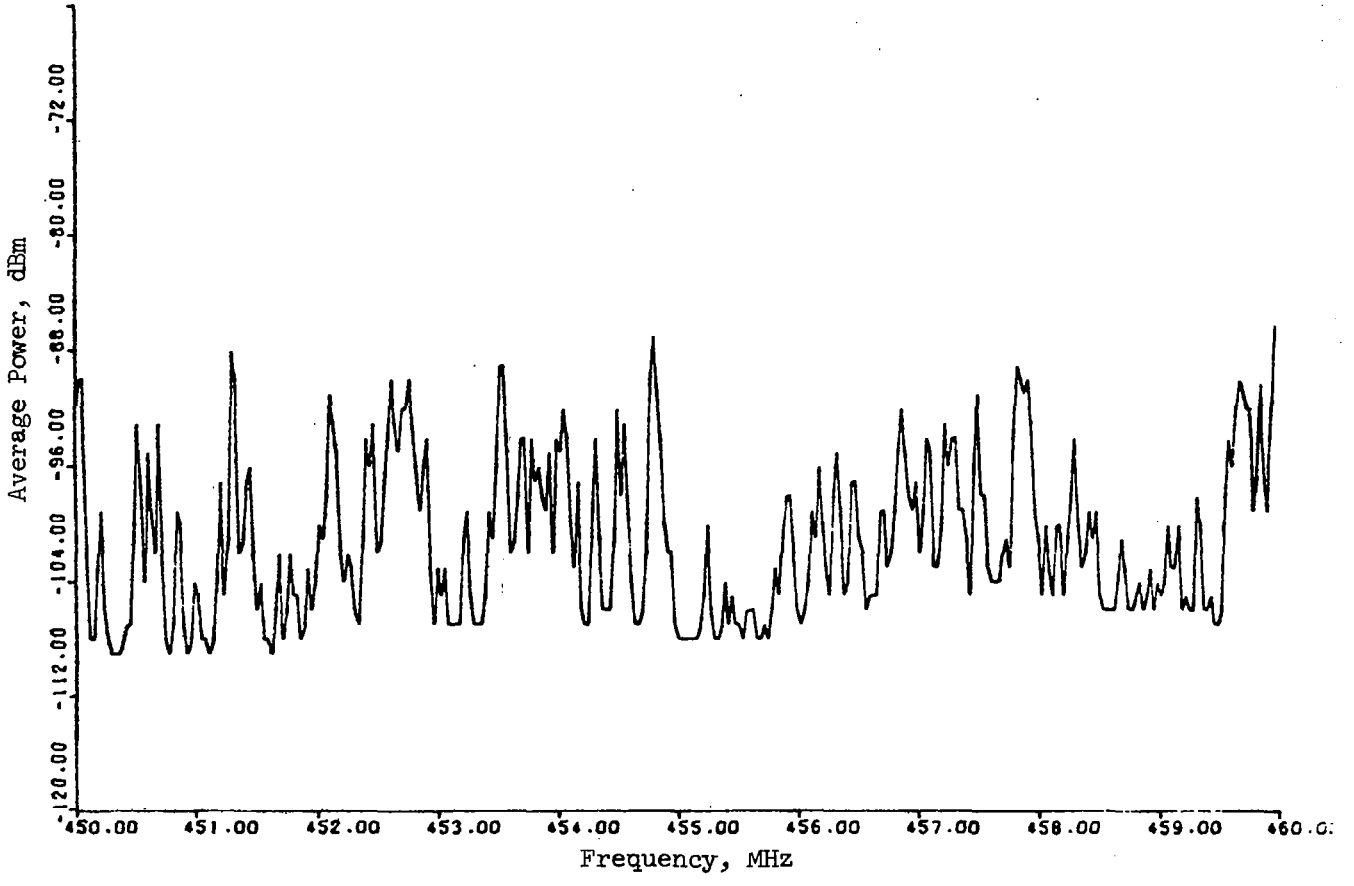

Fig. 8 Average Power Levels over Europe in the 450-460 MHz Band as Measured at 30,000 ft with Antenna Looking Forward (from Ref 28).

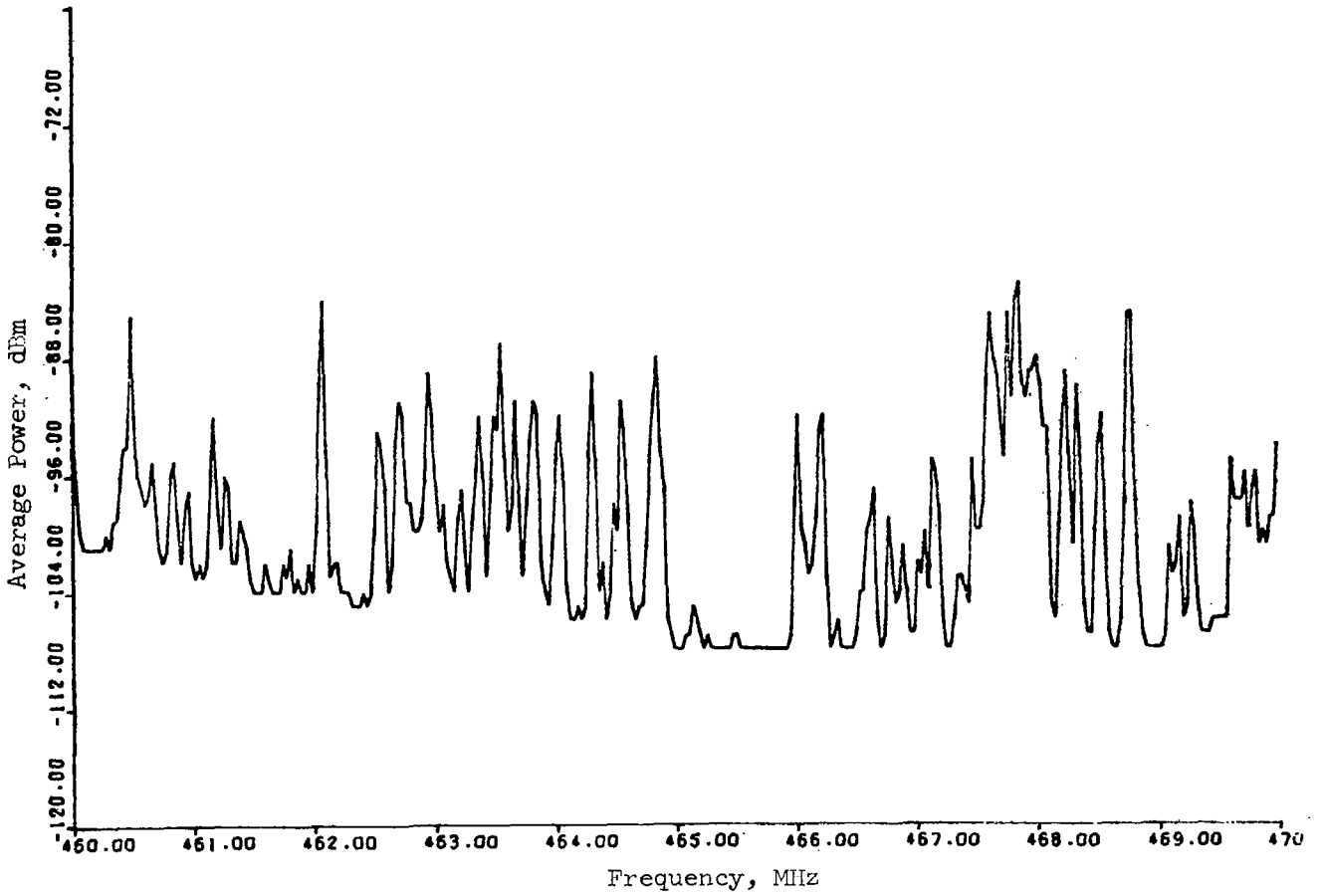

Fig. 9 Average Power Levels over Europe in the 460-470 MHz Band as Measured at 30,000 ft with Antenna Looking Forward (from Ref. 28).

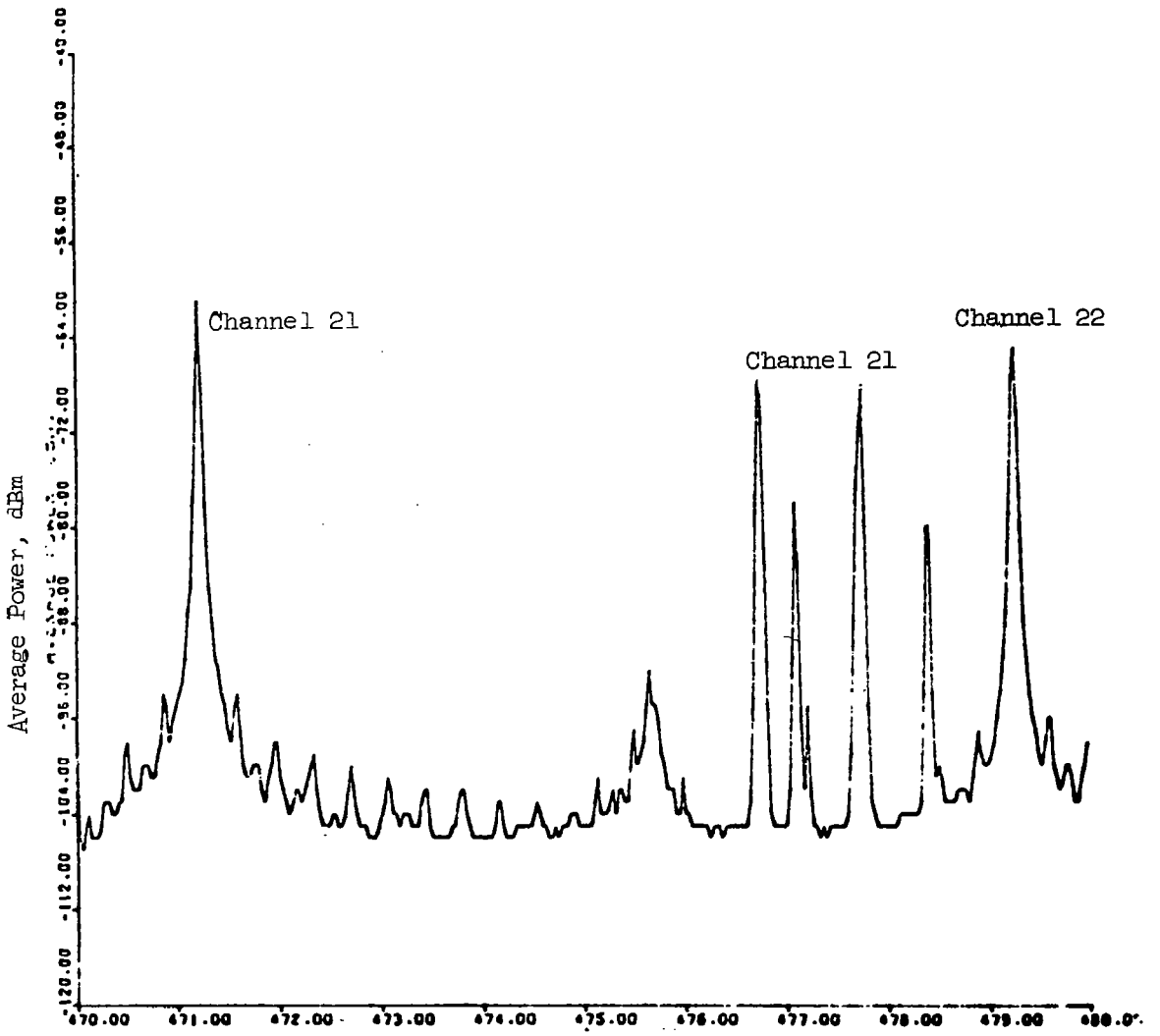

Fig. 10. Average Power Levels Over Europe in the 470-480 MHz Band as Measured at 30,000 ft. With Antenna Looking Forward (from Ref. 28)

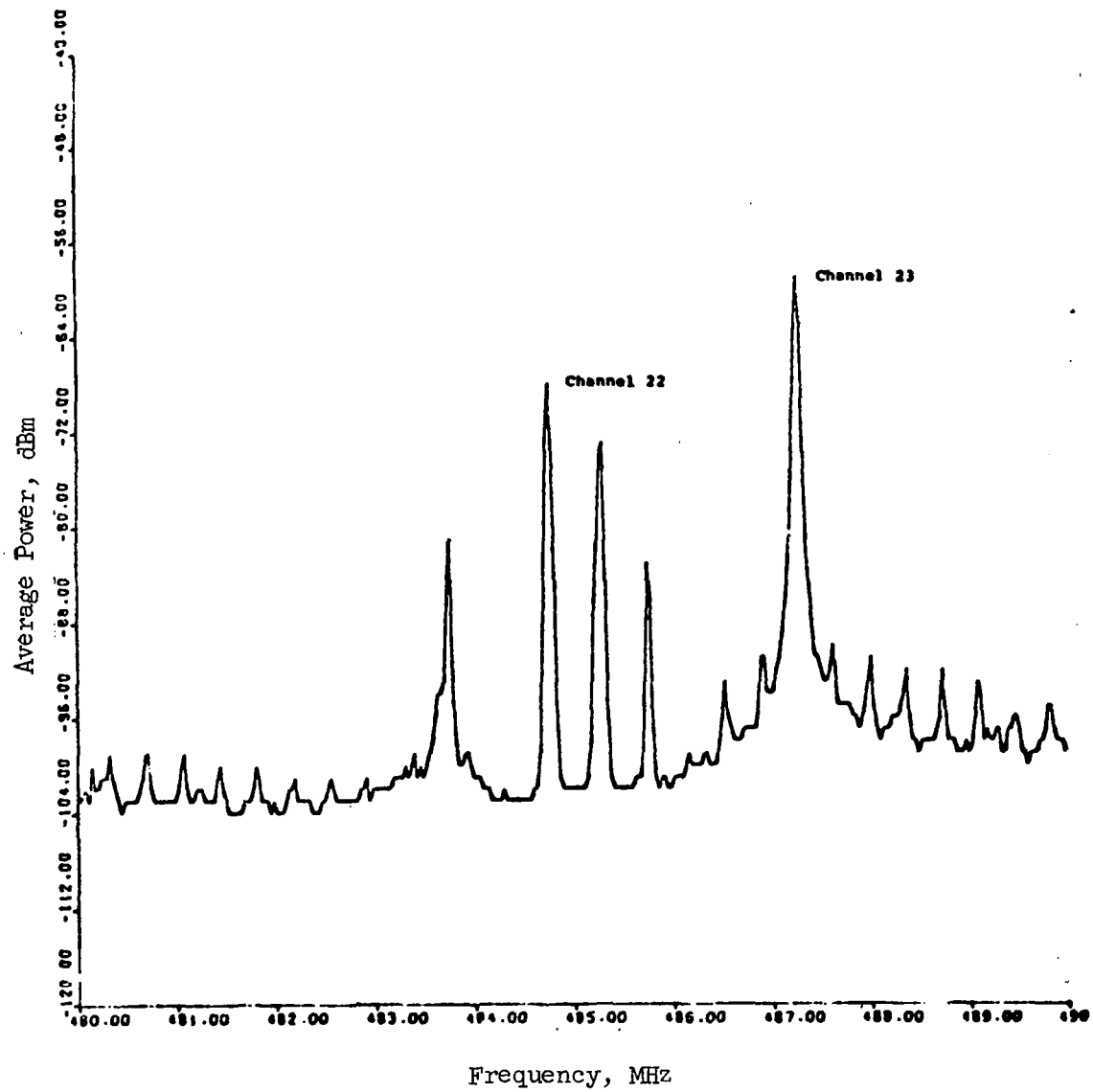

Fig. 11. Average Power Levels Over Europe in the 480-490 MHz Band as Measured at 30,000 Ft. With Antenna Looking Forward (from Ref. 28)

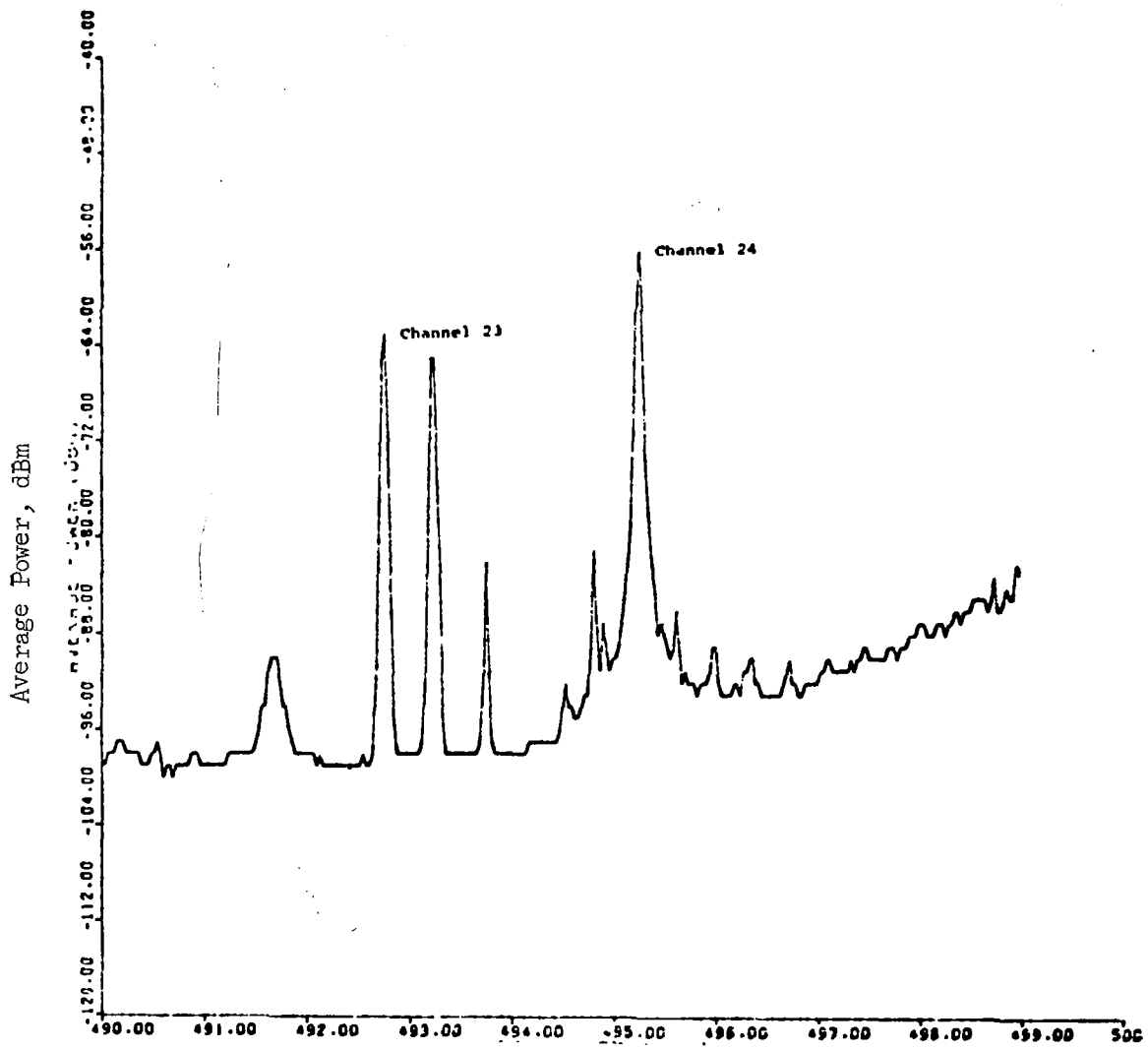

Fig. 12. Average Power Levels Over Europe in the 490-500 MHz Band as Measured at 30,000 Ft. with Antenna Looking Forward (from Ref. 28)

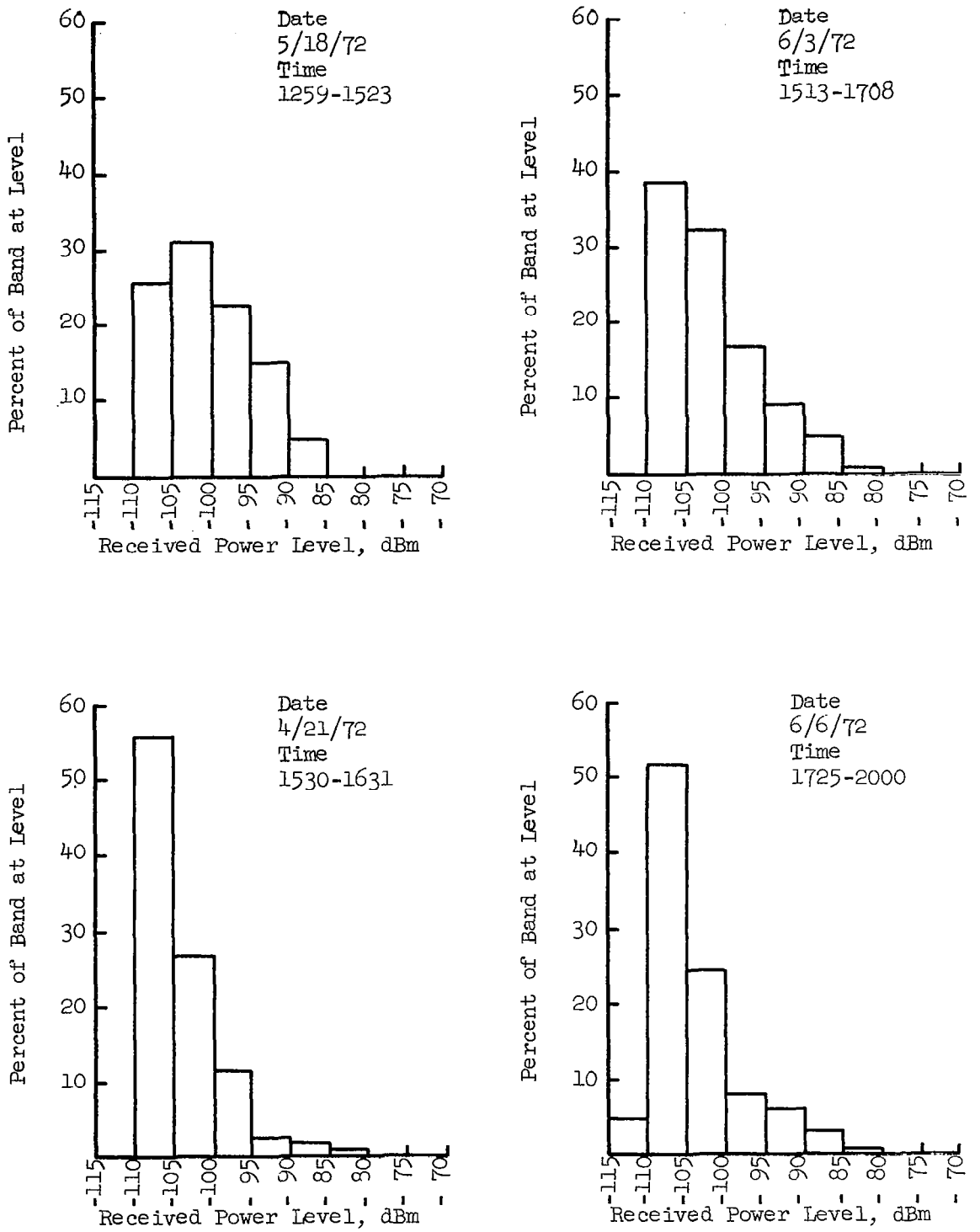

Fig. 13. Power Level Distribution of Emissions Measured over Europe at 450-470 MHz (B.W. 30 kHz) (from tabulations in Ref. 28).

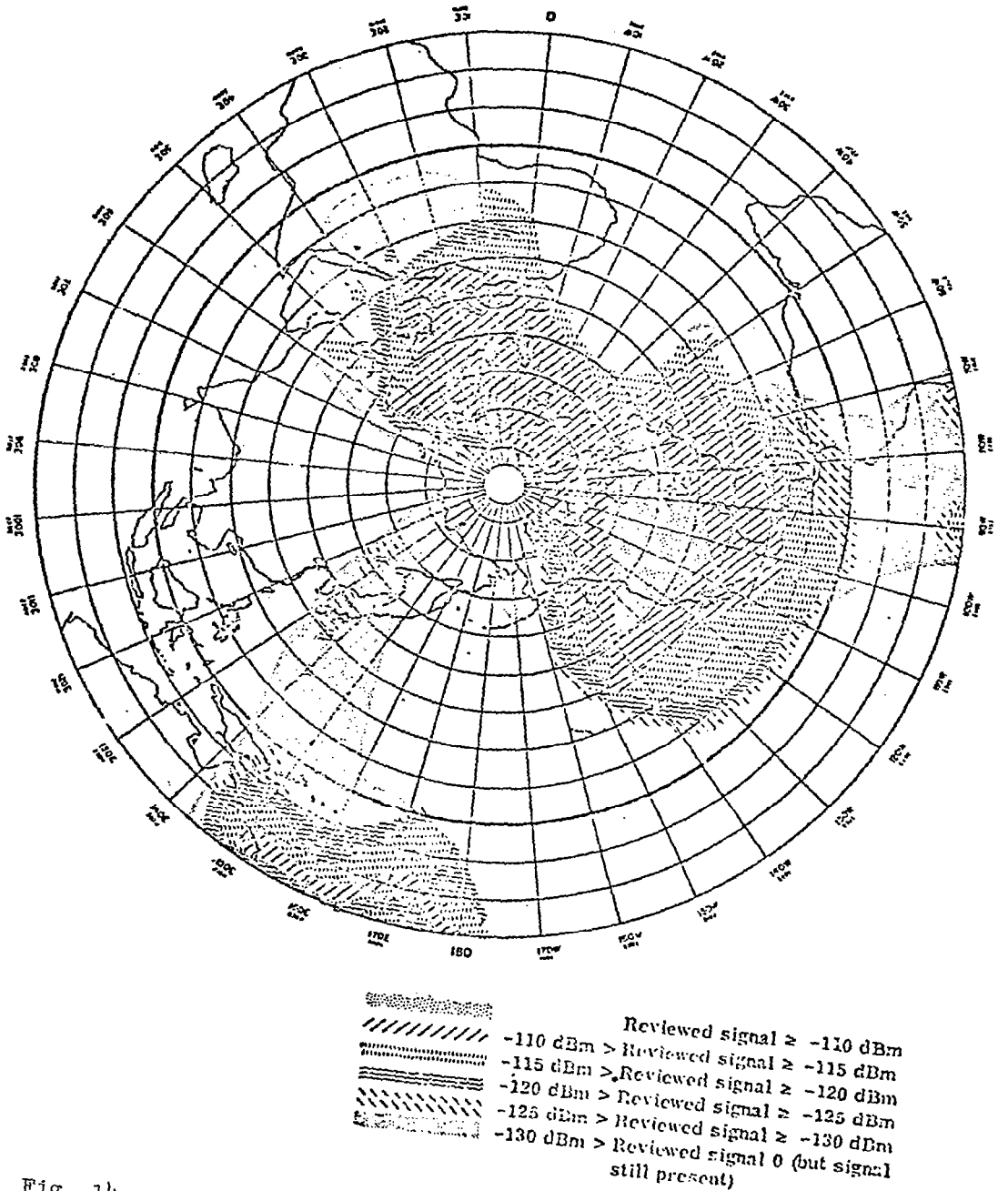

Fig. 14. Geographical Distribution of Power Levels of Interfering Signals Observed By NIMBUS-4 at 466 MHz (from Ref. 29).

Currently the ATS-6 satellite is surveying the 6 GHz region over the continental United States from a synchronous orbit. A preliminary report of data gathered by this satellite has been received only recently, and has not been fully evaluated, as yet.

The results of satellite based RFI measurements made from LES-5 and LES-6 have been reported by W. W. Ward et.al. [7, 8].

LES-5, which surveyed the radio frequency environment from 253 to 283 MHz was located in a quasi-stationary subsynchronous 33,400 km orbit, drifting slowly eastward so that the entire earth, excepting the polar regions, was viewed during the nine months of the experiment. The results of these measurements are presented as frequency versus strongest signal plots and frequency versus average signal plots covering the entire period of the experiment, and for each of five geographical areas: United States; United States and Europe; Europe and Asia; United States, Asia, and Pacific; and North, Central and South America. The weakest observable source was 100 W (isotropic radiator) suggesting that all of the radiation observed was from coherent sources.

The LES-5 antenna has a gain of 2 dB, its beam being in the shape of a torus symmetrical about the axis of rotation of the satellite with a half-power beamwidth of 30° about the plane normal to it. The receiver bandwidth was 120 kHz with a sensitivity of -120 dBW and a noise figure of 3 dB at 255 MHz. The noise figure was a minimum at this frequency. Strongest signals were observed in the U.S. ranging from about -110 dBm to about -90 dBm (referenced to an isotropic antenna), most occurring in the frequency range between 254 MHz and 262 MHz where the system noise is low, and two occurring in the band between 276 MHz and 279 MHz. Similar results were recorded in the U.S. and Europe. The strongest signals observed in the Asia-Pacific-and-U.S. and the North-South-and Central Americas were similarly distributed in frequency but at a level 5 to 10 dB lower.

The LES-6, which surveyed the radio frequency environment from 290 to 315 MHz, was located in a synchronous, station-kept orbit near 90° West longitude from November 1968 through July 1969, and repositioned eastward thereafter with data being reported until October when it has reached about 60° East longitude. The results of these measurements are presented in four plots: (1) average signal power observed between 0600 and 2200 Central Standard Time, (2) average signal power observed between 2200 and 0600 Central Standard Time, (3) peak signal power observed between 0600 and 2200 Central Standard Time, and (4) peak signal power observed between 2200 and 0600 Central Standard Time. The antenna had a gain of 10 dB and half power beamwidths of 34° (parallel with the earth's axis) and 54° (normal to the earth's axis), which allowed LES-6 to view the entire visible portion of the earth. The receiver had a bandwidth of 120 kHz, a sensitivity of -120 dBm and a noise figure of 3 dB. The weakest observable signal was 25 W (isotropic radiator). Data were presented, corrected to equivalent noise power received by an isotropic antenna.

The average power plot shows a baseline level near the system noise level throughout most of the band with some salients rising from 10 to 15 dB higher. The average peak power plot shows a baseline ranging from about -100 dBm at 288 MHz to about -110 dBm at 300 MHz and above. The strongest peak power signals in the band rose to about -80 dBm with the baseline of the plot of strongest peak power being at about -105 dBm.

3.2 INTENTIONAL EMITTERS

3.2.1 Introduction

Estimates of the densities of intentional emitters and their expected emitted powers and antenna characteristics have been greatly extended since the publication of the Preliminary Report (Ref. 30). The data assembled to date are displayed in Table 4.

The portion of the spectrum under consideration has been segmented into frequency bands and types of services within these bands according to the major frequency allocations appearing in Part 2 of the FCC Rules and Regulations. Following this plan, transmitters in each table entry are all subject to the same technical requirements and limits, which is expected to have the effect of minimizing spreads of equipment characteristics represented by each entry. Military equipment has not been included (except for long-range radars operating in bands coordinated by the FAA); however, government bands dedicated only to military use are included so that no gaps appear in the list. It is expected that the use of allocated bands in segmenting the data will assure that transmitters which do not share frequencies will not appear to do so.

National average densities of emitters located in the contiguous 48 states have been determined, as well as weighting factors in three frequency decades for each state, to permit estimating geographic variations. Typical values or ranges of values of emitter power levels and antenna characteristics have been assembled in preparation for calculation of expected effective radiated powers.

These data covering all emitters have been augmented by a more detailed consideration of a number of special cases such as the actual distribution of long-range radars on a single frequency and the distribution of main beam azimuths of microwave transmitters in a selected area.

The data presented in Table 4 have been collected from a number of sources, predominantly International Frequency List (Ref. 31), the FAA Radar Frequency List (Ref. 32), Spectrum Engineering - Key to Progress (Ref. 33) and, in the case of antennas, Antenna Engineering by Jasik (Ref. 34). The references are keyed to Table 4 on an item by item basis in Table 5.

Table 4 DENSITIES, POWER, AND ANTENNA CHARACTERISTICS OF EMITTERS LOCATED IN U.S.

Band (MHz)	Ref. Item	Usage	Emitter Density (per 1000 mi^2)	Total Radiated Power (W) Exceptions noted	Antenna	
					gain (dB)	Beamwidth (degrees)
400-406	1	Meteorological Aids (Radiosonde gnd site)	0.026	NA*	32	4.5
	2	Space	NA	NA	NA	NA
406-420	3	Government	0.048-0.803 (2)	20-60	10-16	NA some omni
420-450	4	Government Amateur-Satellite	NA (3)	NA	NA	NA
	5	Amateur	NA	1000	NA	NA
450-470	6	Land mobile, fixed base	0.682	20-600	2-13	omni
	7	Land Mobile, mobile base	69.40	20-600	2-10	omni
470-512	8	UHF Television Broadcast	0.020	5MW EIRP Max (6)	17 Max	omni
	9	Land Mobile	152.2	30 dBW EIRP max (6)	2-10	omni
512-806	10	UHF Television Broadcast	0.144	5 MW EIRP Max	17 max	omni
806-928	11	Land Mobile	0.014	10-20	Assume 2-10	NA
928-947	12	Land Mobile	9.126	10-20	Assume 2-10	omni
947-952	13	Aural STL	0.247	10-20	19	17
952-960	14	International Fixed	0.143	110 (max)	20 to 40	NA some omni

Table 4 (cont.)

Band (MHz)	Ref. Item	Usage	Emitter Density (per 1000 mi^2)	Total Radiated Power (W) Exceptions noted	Antenna gain (dB)	Antenna Beamwidth (degrees)
960-1215		Air Traffic Control Radar Beacon (ATCRBS)				
	15	Ground Site 1030 MHz	0.285	0.5-2 kW (peak)	22	17
	16	Aircraft 1090 MHz	3.330	400-750 (peak)	1-4	Omni
		TACAN (includes VORTAC)				
	17	Ground Site	0.036	6 or 10 kW	8	Omni
	18	Aircraft 1025-1150 MHz	6.67	1.5 kW (peak)	1-9	Omni
		Distance Measuring Equipment (DME)				
	19	Ground Site (not part of VORTAC)	0.017	15 kW	NA	NA
	20	Aircraft	Same Equipment Cited for TACAN	-	-	-
1215-1250		Government	NA	NA	NA	NA
	21	Amateur	NA	1 kW	NA	NA
1250-1350	22	Long Range Radar	0.034	4 MW (peak)	34	1.5 x 5-30
1350-1535		Government	NA	NA	NA	NA
	23	Aeronautical Telemetry	NA	NA	NA	NA

Table 4 (cont.)

Band (MHz)	Ref. Item	Usage	Emitter Density (per 1000 mi^2)	Total Radiated Power (W) Exceptions noted	Antenna gain	Antenna Beamwidth (degrees)
1535-1700	24	Space (one system)	NA	28.5 dBW EIRP 18.5 dBW EIRP	NA	NA
	25	Aeronautical Navigation Collision Avoidance	NA	1000 W to 1.6kW (peak)	-2	Omni
	26	Altimeter	NA	500 to 1000 (peak)	8-12dB	NA
	27	Radiosonde	0.026	0.25 to 0.5	0 to 2.2	Omni
1700-1850	28	Government Ground Site (Space)	NA	NA	NA	NA
1850-2290	29	Microwave Point-to-Point	0.121	2-80	20-30	NA
	30	Troposcatter-2000MHz band	0.002	1-10kW	37-49	0.6 to 2
	31	Mobile (Domestic)	NA	NA	NA	NA
2290-2450	32	Space	NA	NA	NA	NA
2450-2500	33	Police Radar	0.236	12	24 (min)	10 (max)
	34	T.V. Aux	0.121	NA	NA	NA
2500-2700	35	Instructional Television	0.620	90	28-30	5 to 6
2700-2900	36	Weather Radar	0.033	0.5 MW (peak)	34	1.5 X 5-30
	37	Short Ranged Radar (FAA)	0.037	0.5 MW (peak)	34	1.5 X 5-30
2900-3100	38	Maritime Radar	NA	50W - 50 kW(peak)	NA	NA
3100-3700	38a	Government	NA	NA	NA	NA
3700-4200	39	Microwave Point-to-Point Common Carrier	1.85	1	35	2.7
	40	Television STL	NA	1 to 2	35	2.7

Table 4 (cont.)

Band (MHz)	Ref. Item	Usage	Emitter Density (per 1000 mi^2)	Total Radiated Power (W) Exceptions noted	Antenna	
					gain (dB)	Beamwidth (degrees)
4200-4400	41	Altimeter	NA	NA	NA	NA
4400-5000	42	Government Point-to-Point	NA	500	NA	NA
5000-5650	43	FAA Radar	0.001	250 kW (peak)	45	0.9
	44	Aircraft Radar (commercial)	0.786 max (4)	150 kW (peak)	NA	NA
	45	Maritime Radar	2.67 max (5)	NA	NA	NA
5650-5925		Radar	NA	NA	NA	NA
	46	Satellite Communication	NA	NA	NA	NA
5925-6425	47	Microwave Point-to-Point Common Carrier	0.513	1 to 2	40	1.5
	48	Satellite	NA	NA	NA	NA
6425-7125	49	Microwave Point-to-Point Mobile 6425-6575 MHz	68.67	7 max	27dB(min)	7^{o} (max)
	49a	Television Auxiliary	0.493	1-2	35	
	50	Fixed 6575-7125 MHz	0.170	> 200	40	1.5
7125-8400	51	Microwave Point-to-Point Government	0.033	1-10	Assume 35	NA
8400-8500	52	Space	NA	NA	NA	NA
	53	Mobile (Land Transportation)	NA	NA	NA	NA
8500-9300	54	Radar (FAA-PAR)	0.005	22 or 35kW(peak)	40	1.5
	55	Satellite	NA	NA	NA	NA

Table 4 (cont.)

Band (MHz)	Ref. Item	Usage	Emitter Density (per 1000 mi^2)	Total Radiated Power (W) Exceptions noted	Antenna	
					Gain (dB)	Beamwidth (degrees)
9300-9500	56	Coast Guard Radar	0.116	30-50 kW (peak)	39-41	1.5
	57	Maritime Radar	2.67 (5)	30-50 kW (peak)	NA	NA
	58	Airborn Radar	0.786 (4)	75 kW (peak)	35	2.7
	59	Land Mobile (Response Freq.)	NA	NA	NA	NA
9.5 - 10		Government Radar	NA	NA	NA	NA
10 - 10.5		Government Radar	NA	NA	NA	NA
		Amateur	NA	NA	NA	NA
10.5 - 10.7	60	Police Radar	2.472	5 (max)	32 min	4° max
10.7 - 11.7	61	Domestic Point-to-Point	0.102	1	38	2°
		Space	NA	NA	NA	NA
11.7 - 12.2		Broadcasting Satellite	NA	NA	NA	NA
	62	Mobile	6.181	NA	NA	NA
12.2 - 12.7	63	Operational	NA	10-80	45	0.9
	64	Industrial	NA	5	32 min	4° max
12.7 - 13.25	65	Common Carrier	NA	1-2	Assume 38	NA
	66	Community Antenna Television	0.067	1-2	NA	NA
	67	Television BDCST Auxiliary	0.021	1-2	NA	NA

Table 4 (cont.)

Band (GHz)	Ref. Item	Usage	Emitter Density ($per\ 1000\ mi^2$)	Total Radiated Power (W) Exceptions noted	Antenna	
					Gain (dB)	Beamwidth (degrees)
13.25 - 13.4	68	Airborne Doppler Radar	0.786 max(4)	NA	NA	NA
13.4 - 23.6		Various Allocations	NA	NA	NA	NA
23.6 - 24	69	Radar (FAA...SDR)	0.005	50 kW (peak)	45	0.25 X 25
24 - 40		Various Allocations	NA	NA	NA	NA

* NA - not available.

NOTES

(1) The data presented in this table include only non-military sources located in the contiguous 48 states of the U.S., except long range military radars which are coordinated by FAA.

(2) The first entry includes stations being transferred into this band from the 162-174 MHz band, and assumes that all mobile stations were transferred, while the second entry assumes that no stations were transferred.

(3) An aircraft band measurement (Ref. 35) over the Northeastern United States found this band to be less than 10% occupied for more than 90% of the time.

(4) This maximum density is based on 2,3 commercial aircraft (total for U.S.) (Ref. 36) all having equipment operating in this band.

(5) This maximum density is based on there being 6,200 vessels (Ref. 33) which regularly call at U.S. ports being in U.S. coastal waters at the same time.

(6) These are limits set in terms of effective radiated power.

TABLE 5 REFERENCE SOURCES FOR TABLE 4

Reference Item	References		
	Density	Power	Antenna
1	33	54	54
2	-	-	-
3	33, *	31	31
4	-	-	-
5	-	55	-
6	56	31	31
7	57	34	34
8	56	34 & 55	31
9	57	58	34
10	56	34 & 55	34
11	57	*	-
12	57	31	-
13	36	31	58
14	56	31	31
15	32	32	32
16	33	32	59
17	33	33	33
18	33	33	59
19	59	31	
20	59	59	59
21	-	58	-
22	32	32	32
23	-	-	-
24	-	54	-
25	-	60	60
26	-	60	60
27	54	54	54
28	-	-	-
29	33	31	31
30	31 & 61	31 & 61	31 & 61
31	-	-	-
32	-	-	-
33	62	62	58

* Private communication from staff members of FCC

Continued

Reference Item	References		
	Density	Power	Antenna
34	33	-	-
35	36	31	31
36	33	32	32
37	32	32	32
38	-	31	-
39	31 & 34	31	31
40	-	*	31
41	-	-	-
42	-	33	-
43	32	32	32
44	36	59	-
45	33	-	-
46	-	-	-
47	31 & 56	31	31
48	-	-	-
49	57	58	58
49a	33	33	33
50	31 & 56	31	31
51	33	31	-
52	-	-	-
53	-	-	-
54	32	32	32
55	-	-	-
56	33	32	32
57	33	33	32
58	36	59	59
59	-	-	-
60	62	58	58
61	56	31	**
62	57	-	-
63	-	31	31
64	-	58	58
65	-	31	-
66	*	*	-
67	33	31, *	-
68	36	-	-
69	32	32	32

** Private communication from Microwave Communication, Inc.

3.2.2 Emitter Power

The powers of emitters occupying the 0.4 to 40 GHz band, as available at this time, are displayed in Fig. 15. As would be expected, the highest power levels are those emitted by radars: up to 4 MW. Other prominent sources of high level signals are Troposcatter and TACAN/DME systems.

The effective radiated powers of the strongest emitters are shown in Table 6. The lower power levels are emitted by point-to-point microwave communication transmitters (1-2 W typically) and radiosondes. The lowest emitted level identified to date is that of a radiosonde emitting 0.25 W. By comparing these power levels it may be expected that the total range of signal levels will be 72 dB.

When antenna gains are considered, this range is expanded considerably since the gain of long range radar antenna is typically 34 dB and that of the radiosonde emitting the lowest level is from 0 dB to 2.2 dB. Thus, the expected range of signal levels to be measured is 106 dB.

The expected range of signal levels at a single frequency must also be considered. This range is expected to be greatest where frequencies are shared by dissimilar radio services. The bands where frequencies are shared below 13 GHz are shown in Table 7.

Television broadcast transmitters and land mobile communications systems share the band ranging from 470 MHz through 512 MHz. Since large differences exist in the emitted power levels permitted in these two services, and a large number of transmitters appear in both, this band has been considered in more detail.

The FCC has limited the EIRP and antenna height of installations in the Land Mobile Service to protect the Television Broadcast Service which is the primary service. Spatial limits have also been applied to the Land Mobile Service. From these limits the worst case of geographic separation and differences in EIRP between transmitters in the two services may be established.

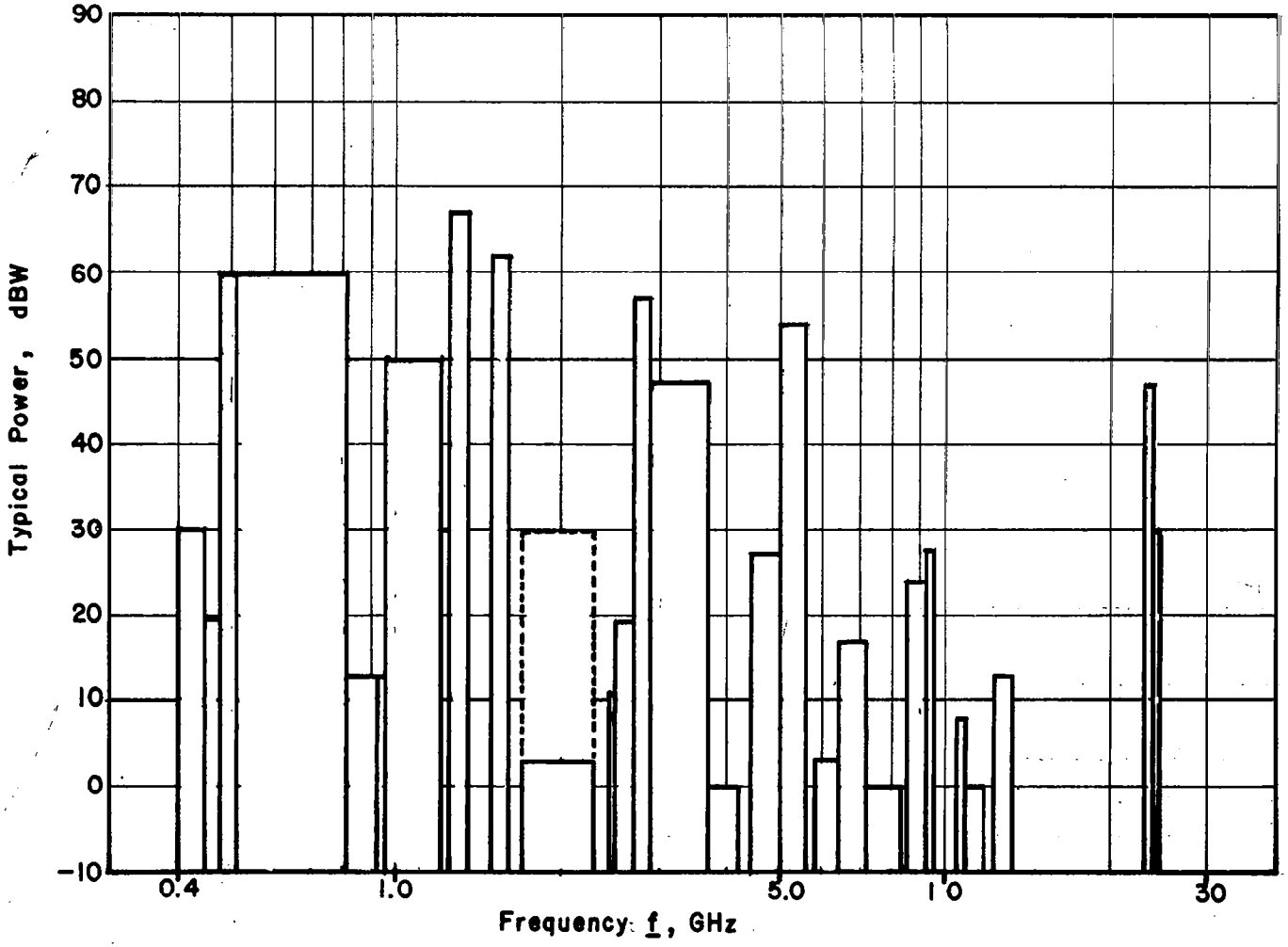

Figure 15 - Typical Transmitter Power Levels

TABLE 6 . EFFECTIVE RADIATED POWER OF SOURCES IN U.S.

Equipment Type	EIRP (dBW)	Ref. No. (from Table 4)
Long Range Radar	100	22
FAA Radar (5 GHz)	99	43
Surface Detection Radar	92	69
Short Range Radar	91	37
Weather Radar	91	36
Troposcatter	67-89	30
Maritime Radar	83-88	57
Coast Guard Radar	83-88	56
Precision Approach Radar	83-85	54
Airborne Weather Radar	84	58
Maritime Radar	50-81	38
Television	67	8 and 10
Operational Fixed (12 GHz)	55-64	63
Operational Fixed (7 GHz)	> 63	50
International Fixed (952 MHz)	40-60	14
Beacon Radar	49-55	15
Distance Measuring Equipment	50	19
Instructional TV	48-50	35
TACAN	48	17
Microwave, point-to-point (2 GHz)	23-49 (27-37 typical)	29
Microwave, point-to-point (8 GHz)	35-45	51
Common Carrier (6 GHz)	40-43	47
TV Auxiliary (13 GHz)	38-41	67
Community Antenna TV	38-41	66
Common Carrier (13 GHz)	38-41	65
DME/TACAN Transponder	33-41	18
Industrial Radio	39	64
Police Radar	39	60
Common Carrier	38	61
TV Auxiliary	35-38	49a
TV, STL	35-38	40
Land Mobile, fixed base	15-37	6
Land Mobile, mobile	15-37	7
Police Radar	35	33
Common Carrier	35	39
Mobile	35	49
Beacon Radar Transponder	27-33	16
Government	23-33	3
Aural STL	29-32	13
Land Mobile	30	9
Space	18.5-28.5	24
Collision Avoidance Radar	28	25
Altimeter	7.5-12	26
Radiosonde	(-6)-(-0.8)	27

TABLE 7 FREQUENCY SHARING BETWEEN 0.4 and 13 GHZ
(Earth and Airborne Emitters only)

Band (MHz)	Primary User	Secondary User
400.15 - 401	Radiosonde	Space Telemetry and Tracking
401 - 402	Radiosonde	Meteorological-Satellite
420 - 450	Radar	Amateur, Amateur-Satellite
450 - 460	Fixed Mobile	Space telecommand & space research (earth to space)
460 - 470	Land Mobile	Meteorological-Satellite (space to earth)
470 - 512	Television	Land Mobile
1215 - 1300	Radar	Amateur
1592.5-1622.5	Aircraft Collision Avoidance Systems	Altimeters
1644 - 1645	Aeronautical-Satellite	Maritime-Satellite
1690 - 1700	Radiosonde	Space
2062 - 2110	Fixed: Domestic Public & Broadcast Auxiliary	Space Research
2110 - 2130	Fixed: Domestic Public & Broadcast Auxiliary	International Fixed in Florida
2300 - 2450	Radar	Amateur
2450 - 2500	Fixed and Mobile	Radar
2500 - 2690	Broadcasting-Satellite, Instructional Television Broadcasting Satellite	Fixed Satellite
2.7 - 2.9	Aeronautical Navigational Aids	Radar
2.9 - 3.1	Maritime Navigational Aids	Radar
3.3 - 3.5	Radar	Amateur
3.7 - 4.2	Domestic Public	Space
5.0 - 5.25	Microwave Landing System (beginning about 1976)	Fixed Satellite
5.65 - 5.925	Radar	Amateur
5.925 - 6.425	Domestic Public	Space
6.875 - 7.125	Broadcast Auxiliary	Space
9.0 - 9.2	Aeronautical Navigational Aids	Radar
10 - 10.5	Radar	Amateur
10.95 - 11.2	Domestic Public	Fixed Satellite
11.7 - 12.2	Broadcast Satellite Fixed Satellite	Domestic Public
12.5 - 12.7	Fixed (International Control)	Fixed Satellite
12.7 - 12.75	Fixed/Mobile Broadcast Auxiliary	Fixed Satellite

The most restrictive geographic limit applied in this band is that it may be used by the Land Mobile Service only in the ten largest urban population centers. FCC rules allow a minimum separation (with a couple of exceptions) of 90 miles between a base station and a co-channel television and 112 miles between a mobile transmitter and a co-channel TV. The allowed EIRP for land mobile transmitters are at a minimum at these distances and increase at greater distances to a maximum of 1000 W.

Though the base station is allowed closer to the protected TV transmitter than is the mobile or control station, it is felt that this will be an unusual situation since the related mobile units must be clustered in one small part of the base station coverage area. A more likely situation will be where the separation between base station and the protected TV transmitter will equal or exceed that of the closest mobile unit. This implies that the worst case condition will be that of sharing between a mobile transmitter and a TV transmitter at a minimum separation. The expected range of levels and spatial separation would be as follows:

Television transmitter level	67 dBW
Mobile or control station transmitter level	7 dBW
range	60 dB
minimum separation	112 mi
maximum angular separation as seen from orbit (receiver looking at horizon; 250 mi. altitude)	4.7^{o}

At a distance of 155 miles or more from the protected television transmitter a mobile transmitter or control station is allowed to emit a level of 23 dBW ERP. Here:

Television transmitter level	67 dBW
Mobile or control station transmitter level	23 dBW
range	44 dB
minimum separation	155 mi
maximum angular separation as seen from orbit (receiver looking at horizon; 250 mi. altitude)	6.2^{o}

3.2.3 Emitter Densities

It is expected that in many if not most of the bands in the range of frequencies 400 MHz - 40 GHz there will be a considerable geographic variation from the densities shown in Table 4. In addition there will be apparent variations due to the use of directional antennas which will cause the number of transmitters observed in an area and from a point in space to be fewer than are actually there.

The actual distribution of some of the higher level emitters (on a single selected frequency) has been investigated as an important special case. Similarly, the distribution of azimuths of a point-to-point microwave network has been studied.

The range of emitter densities is shown in Table 8.

3.2.3.1 Variation of Densities from Average

Geographical variation of equipment densities have been estimated on the basis of installation counts published by the Joint Technical Advisory Committee (Ref. 33). These counts were made by the Electromagnetic Compatibility Analysis Center (ECAC) and included all installations from 100 MHz to 100 GHz except the 150 - 170 MHz land mobile band and were given state-by-state (including the District of Columbia) in three frequency decades. The installation density for each state in installations (an installation is defined as a transmitter, transmitter/receiver combination, or receiver) per 1000 mi^2 is shown in Table 9. A weighting factor consisting of the ratio of the density of installations in a given state and in a given frequency decade to the average national density of installations in that frequency decade are proportioned among the states in the same way as are the installations. The average equipment density in a state and in a particular band may be determined by multiplying the average national density of transmitters in that band by the appropriate weighting factor. No allowance is made for equipments in a given frequency decade not being distributed the same way geographically.

The weighting factors reflect the extent of the unevenness of transmitter distributions. The Northeastern states (except D.C.) show the highest densities, all except Maine, New Hampshire, and Vermont, being well above national average (range 1.8 to 6.0) while the mountain states showed the lower densities (Wyoming having only 0.116). The range of densities is from 6.029 (Maryland) to 0.116 (Wyoming).

The highest densities of transmitters are expected to be located in the cities. An effort was made to determine if these could be estimated by use of an installation-per-capita ratio; however, when this ratio was calculated for the 48 contiguous states the ratios were found to vary by more than 10:1. An indication of equipment densities for urban areas may be gained from the District of Columbia, since it is completely urban. Here the weighting factor rose to 466.8.

3.2.3.2 Distribution of Radars

Fixed ground radars are not very numerous, making it desirable to consider their actual distributions rather than estimating them. Since a prime concern is distribution of equipments (or separations) on a single frequency, distributions have been calculated for long range, short range, and beacon radars listed by FAA.

TABLE 8. DENSITIES OF U.S. SOURCES IN ORDER OF DENSITY

Equipment Type	Density (per 1000 mi^2)	Ref. No. (from Table 4)
Land Mobile	152.2	9
Land Mobile	69.40	7
Land Mobile	68.67	49
Land Mobile	9.126	12
DME/TACAN Transponder	6.67	18
Land Mobile	6.181	62
Beacon Radar Transponder	3.330	16
Maritime Radar (5 GHz)	2.67 max	45
Maritime Radar (9.3-9.5 GHz)	2.67 max	57
Police Radar	2.472	60
Common Carrier	1.85	39
Government	0.048-0.803	3
Aircraft Radar (commercial)	0.786 max	44
Aircraft Radar (commercial)	0.786 max	58
Aircraft Doppler Radar	0.786 max	68
Land Mobile Fixed Base	0.682	6
Instructional TV	0.620	35
Common Carrier	0.513	47
TV Auxiliary	0.493	49a
Radar Beacon	0.285	15
Aural STL	0.247	13
Police Radar	0.236	33
Fixed (6575-7125)	0.170	50
Television	0.144	10
International Fixed (952-960)	0.143	14
Microwave point-to-point	0.121	29
TV Auxiliary	0.121	34
Coast Guard Radar	0.116	59
Common Carrier	0.102	61
Community Antenna TV	0.067	66
Short Range Radar	0.037	37
Long Range Radar	0.034	22
Weather Radar	0.033	36
Government point-to-point	0.033	51
TV Auxiliary	0.021	67
DME (not part of TACAN)	0.017	19
Precision Approach Radar	0.005	54
Surface Detection Radar	0.005	69
FAA Radar (5 GHz)	0.001	43

Table 9. State Installation Densities and Weighting Factors

State	Installation Density in State			Weighting Factor		
	0.1-1GHz	1-10GHz	10-100GHz	0.1-1GHz	1-10GHz	10-100 GHz
ME	34.262	3.011	0,602	0.429	0.312	0.471
NH	49.011	4.300	0.430	0.614	0.445	0.336
VA	15.090	3.122	2.081	0.189	0.323	1.627
MA	479.835	26.644	9.689	6.010	2.758	7.575
RI	395.387	24.712	8.237	4.952	2.558	6.440
CT	156.918	21.960	19.964	1.965	2.273	15.609
NY	446.930	18.759	2.017	5.597	1.942	1.577
NJ	364.982	42.113	17.866	4.571	4.359	13.969
PA	149.578	13.988	0.184	1.873	1.448	0.144
OH	148.610	24.259	7.278	1.861	2.511	5.690
IN	98.867	16.809	2.204	1.238	1.740	1.723
IL	329.007	20.567	4.255	4.121	2.129	3.327
MI	252.388	8.073	2.577	3.161	0.836	2.015
WI	30.131	7.123	2.493	0.377	0.737	1.949
MN	174.775	5.591	1.784	2.189	0.579	1.395
IA	14.265	7.106	1.421	0.179	0.736	1.111
MO	55.664	10.619	1.148	0.697	1.099	0.898
ND	13.047	4.670	0.425	0.163	0.483	0.332
SD	11.850	2.726	0.260	0.148	0.282	0.203
NE	17.546	5.180	0.518	0.219	0.536	0.405
KS	31.411	10.940	1.459	0.393	1.132	1.141
DE	142.927	9.723	4.861	1.790	1.006	3.801
MD	481.422	46.327	1.891	6.029	4.795	1.478
D.C.	37,268.7	1044.78	14.925	466.757	108.144	11.669
VA	94.250	18.620	2.940	1.180	1.927	2.299
WV	7.030	10.339	1.241	0.088	1.070	0.970
NC	44.784	9.886	0.761	0.561	1.023	0.595
SC	52.423	16.744	0.644	0.657	1.733	0.504
GA	55.252	12.908	0.510	0.692	1.336	0.399
FL	215.113	24.590	0.683	2.694	2.545	0.534
KY	42.852	0.941	0.495	0.537	0.097	0.387

continued

Table 9 (continued)

State	Installation Density in State			Weighting Factor		
	0.1-1GHz	1-10GHz	10-100GHz	0.1-1GHz	1-10GHz	10-100GHz
TN	49.545	8.706	1.420	0.621	0.901	1.095
AL	39.276	10.657	0.775	0.492	1.103	0.606
MS	22.697	10.898	0.419	0.284	1.128	0.328
AR	17.645	3.390	0.753	0.221	0.351	0.589
LA	50.141	10.717	0.206	0.628	1.109	0.161
OK	28.948	7.294	0.715	0.363	0.755	0.559
TX	47.827	8.154	0.598	0.599	0.844	0.468
MT	15.849	2.651	1.087	0.198	0.274	0.850
ID	14.553	4.428	1.197	0.182	0.458	0.936
WY	9.273	4.085	1.021	0.116	0.423	0.798
CO	34.984	8.921	0.767	0.438	0.923	0.600
NM	21.756	7.890	0.493	0.272	0.817	0.385
AZ	33.650	4.390	1.229	0.421	0.454	0.961
UT	20.797	6.713	1.178	0.260	0.695	0.921
NV	16.275	5.066	0.362	0.204	0.524	0.283
WA	71.431	14.518	1.613	0.895	1.503	1.261
OR	22.076	6.187	0.825	0.276	0.640	0.645
CA	388.694	23.189	2.332	4.868	2.400	1.823

3.2.3.2.1 Long Range Radars

These equipments occupy channels in the 1250 MHz - 1350 MHz band. Long-range radars are more evenly spread geographically than are the beacon radars and a number of channels are available, though channel assignments are repeated many times. The largest concentration of long-range radars on a single frequency as shown in the FAA radar list is on 1250 MHz, where 22 are entered. The average density of these equipments taken nationally is 0.005/1000 mi^2.

The locations of long-range radars assigned to 1250 MHz are shown in Fig. 16. Separation distances indicated by lines between sites and number keys are listed in Table 10. The average minimum separation between a radar and its nearest neighbor is about 234 miles; however, 71% of these minimum separations equal or are less than 200 miles.

Table 10. Long Range Radar Minimum Separations

Item	Separation (mi)	Item	Separation (mi)
1	280	10	200
2	200	11	100
3	200	12	100
4	200	13	200
5	150	14	300
6	150	15	300
7	180	16	400
8	200	17	630
9	180		

3.2.3.2.2 Short Range Radars

These equipments occupy channels in the 2.7 GHz through 2.9 GHz band and are used to observe air traffic in the vicinity of airports. The FAA radar lists indicate that 155 short range radars are assigned to the same frequency, 2.7 GHz, the bulk of these being in the central or eastern part of the United States (Fig. 17). These equipments are not clustered as tightly as are beacon radars, but their density is much higher than that of long range radar.

To assess the variation of emitter density of these equipments, densities were calculated for contiguous geographical areas enclosed by 5° of latitude and 5° of longitude (see Table 11). Densities ranged from 0.123/1000 mi^2 to 0.000/1000 mi^2. The densities in these areas are shown in Table 10. The distribution of these densities in increments of 0.010/1000 mi^2 are shown in Fig. 18.

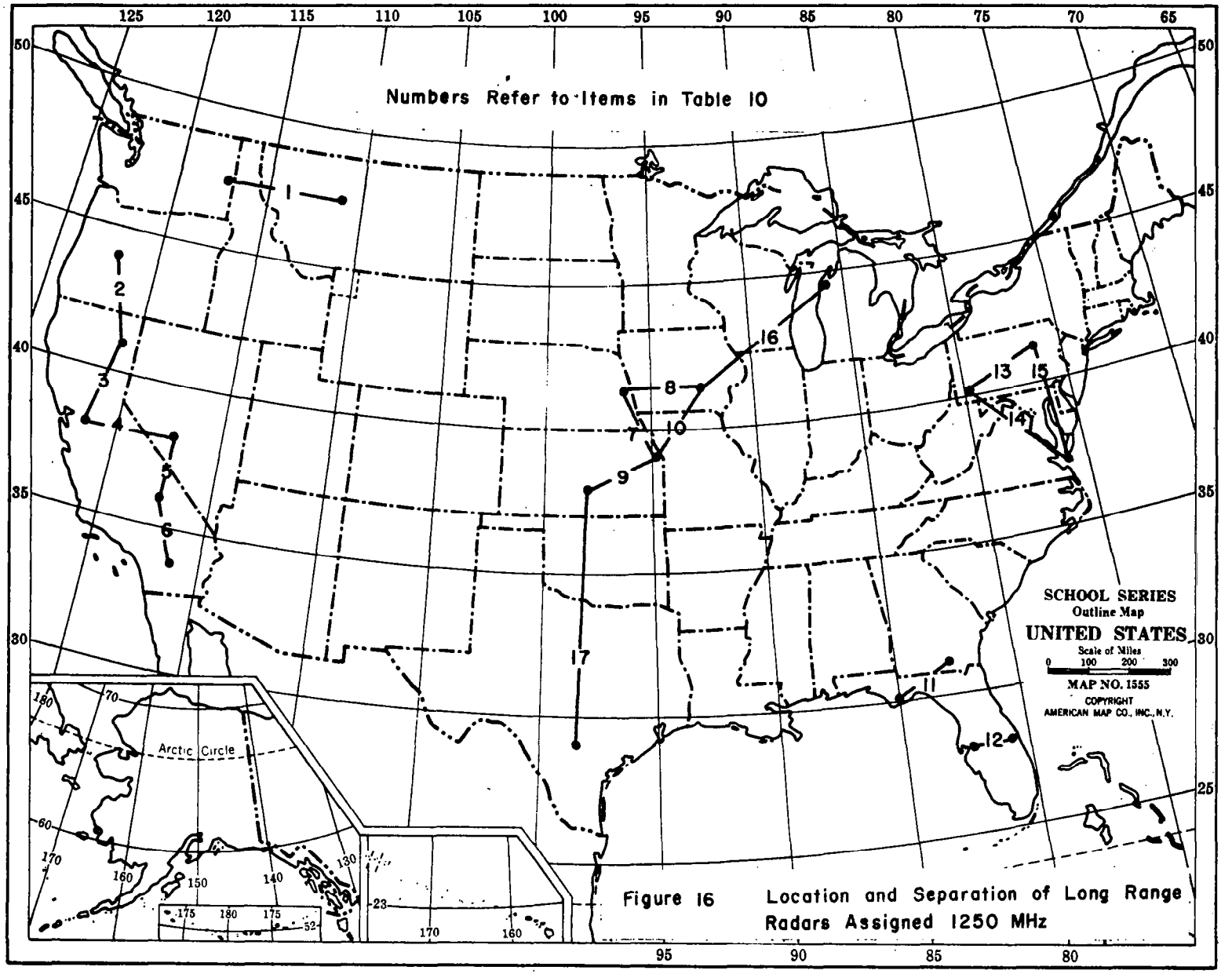

Figure 16 Location and Separation of Long Range Radars Assigned 1250 MHz

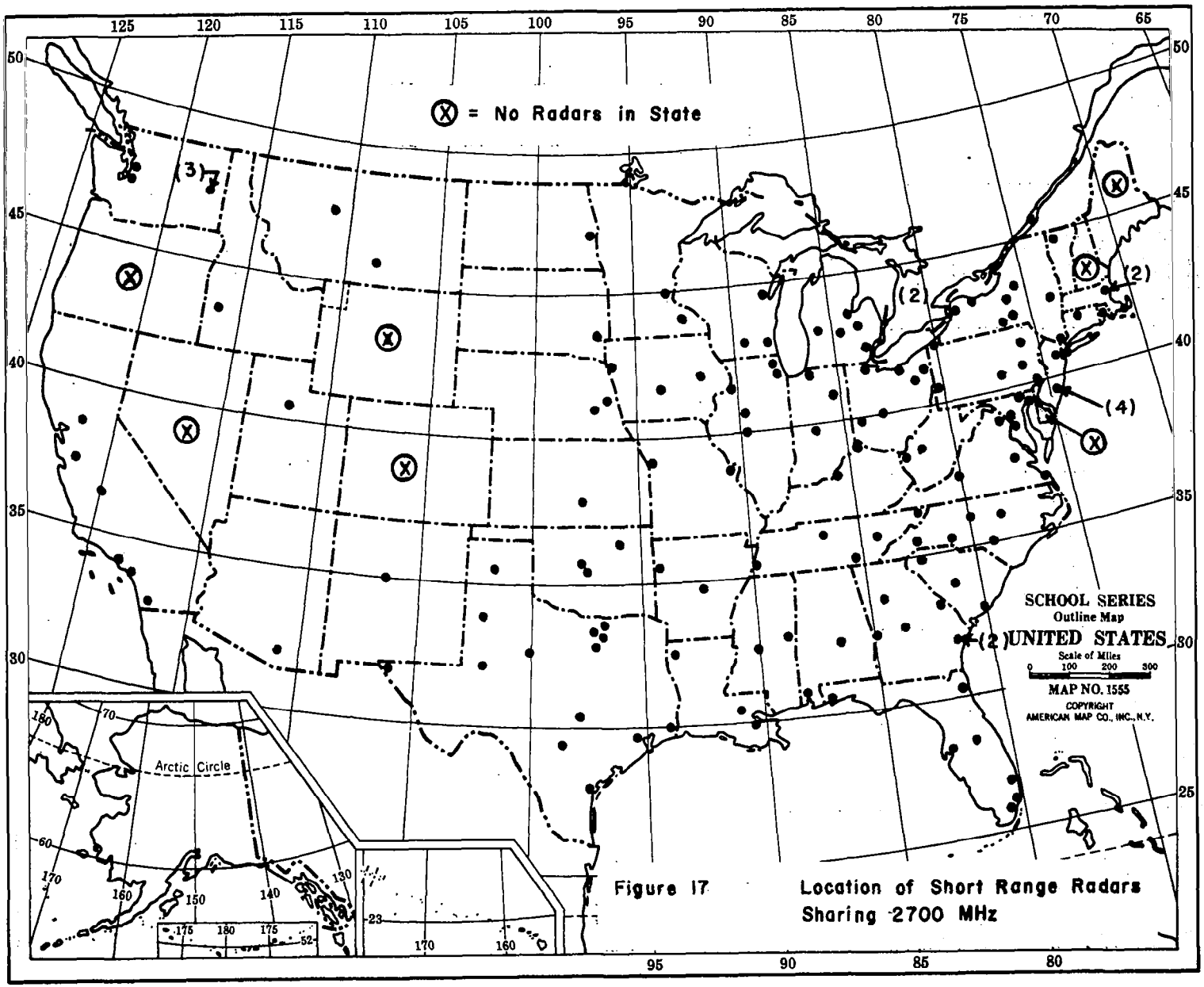

Figure 17 Location of Short Range Radars Sharing 2700 MHz

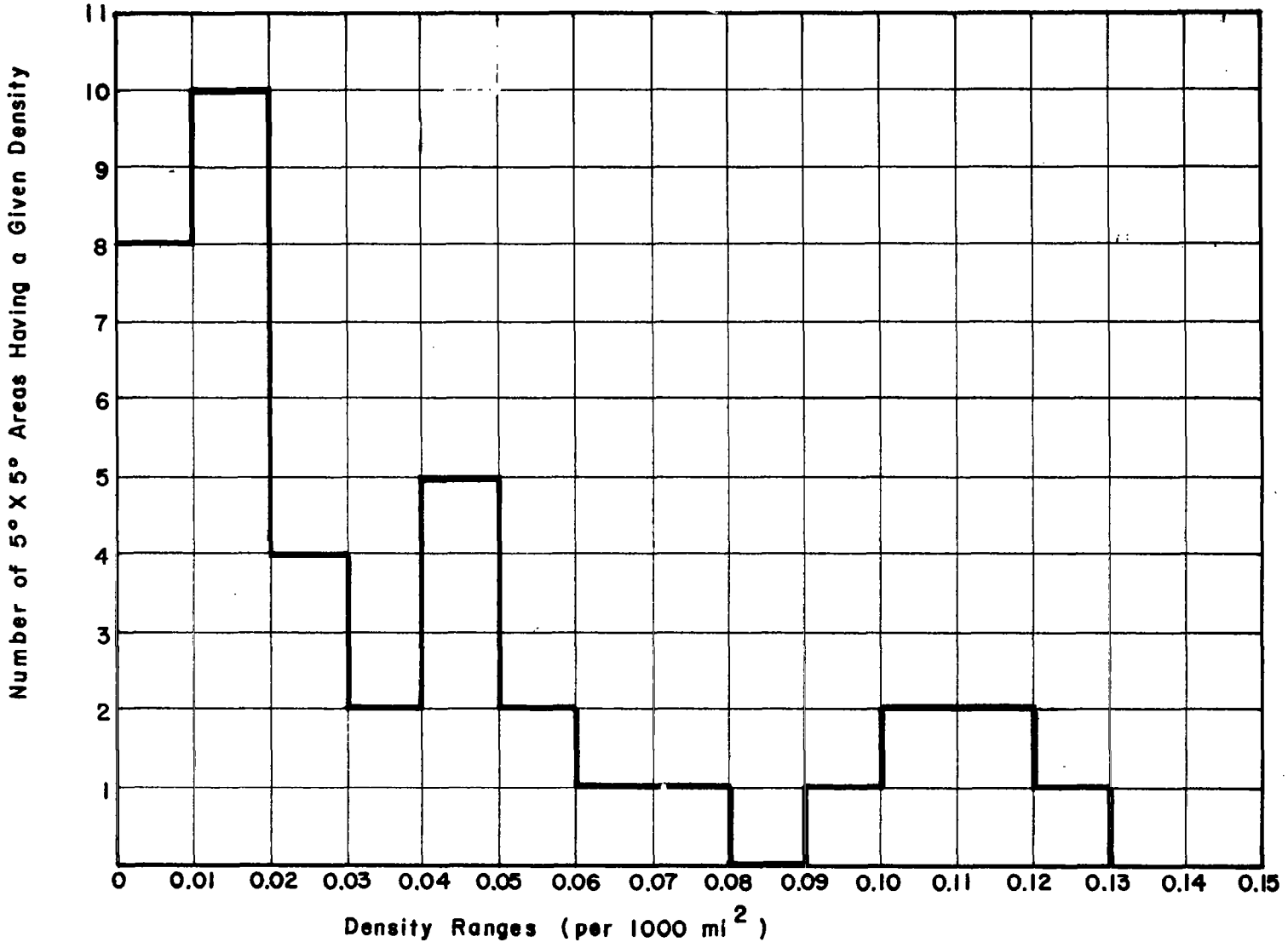

Figure 18 Distribution of Densities of Short Range Radar in Contiguous Areas Bounded by 5° Latitude and 5° Longitude

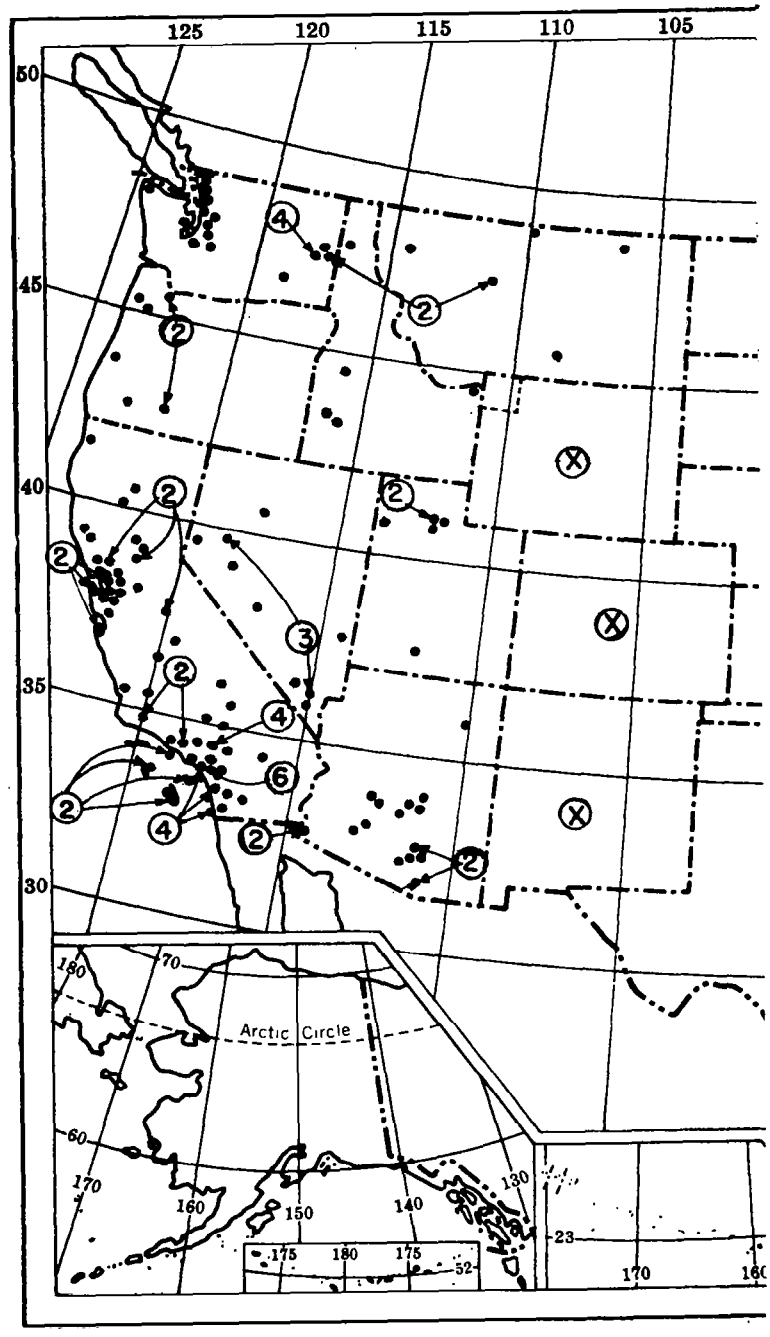

Figure 19 Location of Radar Beacon Sites (⊗ Non Plotted in These States)

Table 11 Densities of Short Range Radars

Longitude Range	Latitude Range				
	25°- 30°	30°- 35°	35°- 40°	40°- 45°	45°- 50°
70°- 75°	-	-	-	0.100	-
75°- 80°	-	-	0.114	0.123	-
80°- 85°	0.046	0.078	0.093	0.111	-
85°- 90°	-	0.049	0.062	0.100	0.000
90°- 95°	-	0.049	0.031	0.056	0.000
95°-100°	0.028	0.058	0.041	0.045	0.012
100°-105°	-	0.019	0.010	0.000	0.000
105°-110°	-	0.019	0.000	0.000	0.012
110°-115°	-	0.010	0.000	0.011	0.012
115°-120°	-	0.029	0.010	0.011	0.036
120°-125°	-	-	0.021	0.000	0.024

Note:
1. Densities are per 1000 mi^2.
2. Blanks indicate areas which lie mostly outside of U.S. or land areas for which no density was determined.

3.2.3.2.3 Beacon Radars (ATC RBS)

There are 856 Beacon Radar ground sites (interrogators) included in the FAA list (Ref. 32). These include not only FAA equipments but military equipments operating the band. It has been estimated (Ref. 33) that there are 10,000 civilian aircraft equipped to use this service. All beacon radar interrogators are assigned to precisely the same frequency, 1030 MHz, while the transponders are all assigned to 1090 MHz. The interrogators operate continuously excepting those used for training (a relatively small number).

Beacon sites are clustered about population centers, and areas where there is considerable aircraft activity. The locations of Beacon radars in 8 western states are shown in Fig. 19, with details of the Los Angeles area shown in Fig. 20 (Ref. 37), where the emitter density reaches 1.164/1000 mi^2. In Montana the density falls to 0.045/1000 mi^2. These are taken to be representative of the radar beacon densities to be encountered.

Since the transponders carried by aircraft operate only when interrogated by the beacon radars, it is assumed that the density of transmissions, though not of equipments will follow.

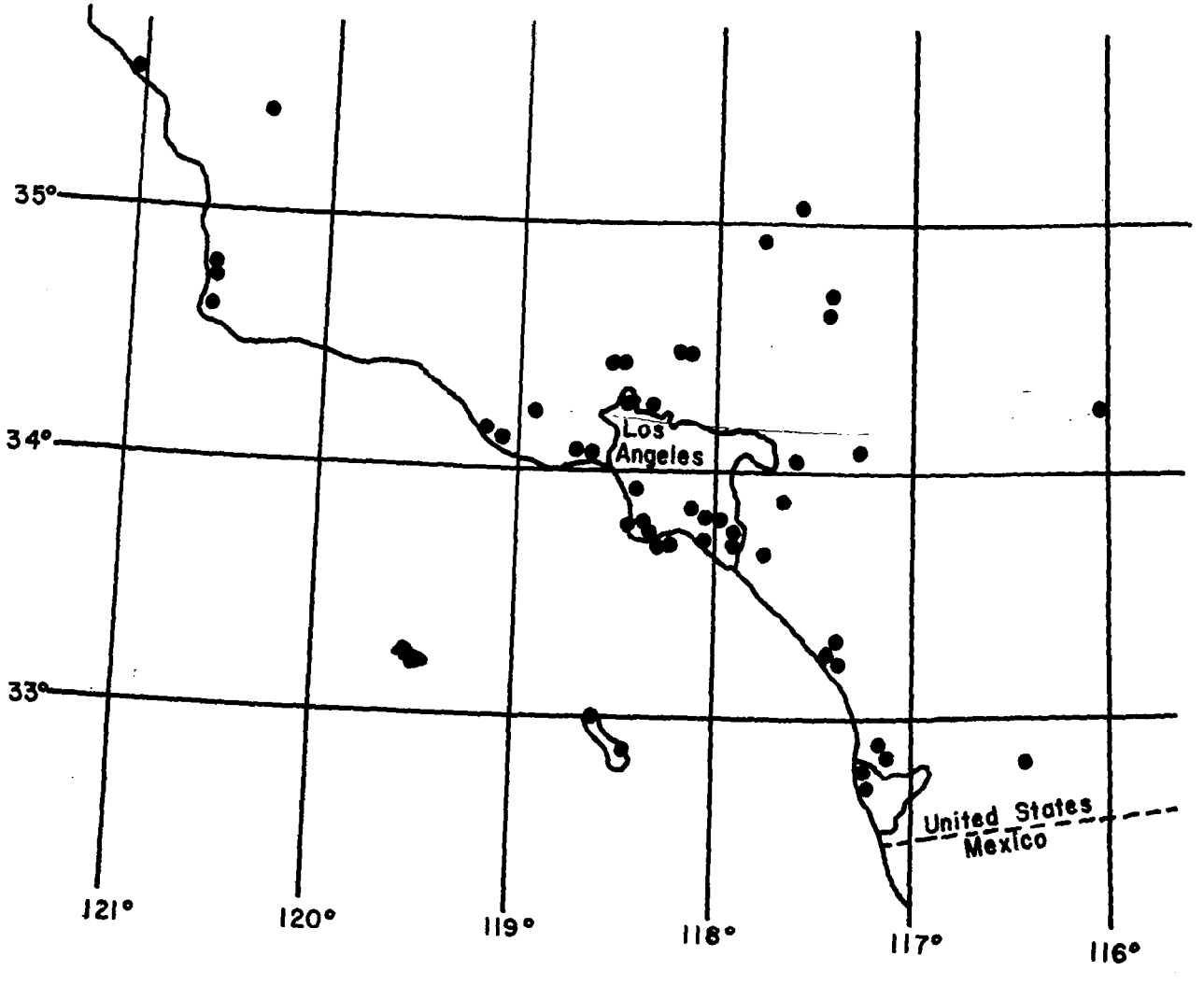

Figure 20 Location of Radar Beacon Ground Stations in the Los Angeles Area

3.2.3.3 Azimuthal Distributions of Microwave Transmitter Main Beams

Typically a common carrier network occupies a modest number of frequencies which are repeated regularly. The main beams of the antennas are narrow and fixed in direction so that the possibility of simultaneously observing two on the same frequency from a given azimuth is considerably reduced.

To assess this problem a common carrier network extending from southern Arizona (see Table 8) to New Mexico and parts of Texas was studied. The frequency of 6063.8 MHz was selected for study since it is often repeated in this network. The 3° beam widths have been added to the assumed satellite beam width of 3° and the main beams of the transmitters plotted in Fig. 21 (0.7° per 1° east of the first transmitter has been subtracted from the stated azimuths to correct for the earth's curvature). The only potential overlap was found in the beams of the tranmitters in White Signal, N.M. and Winkleman, Az which lie about 2° apart in longitude. (See Table 12)

Table 12 Stations in 6 GHz Microwave Network in the Southwest

Location	Azimuth (corrected)
1. Oracle, Az	182°
2. Winkelman, Az	114°
3. Pima, Az	99.3°
4. White Signal, NM	118°
5. Deming, NM	62.3°
6. Rincon, NM	175.3°
7. Rincon, NM	342.3°
8. Organ, NM	80.7°
9. Hueco Mountain, NM	166°

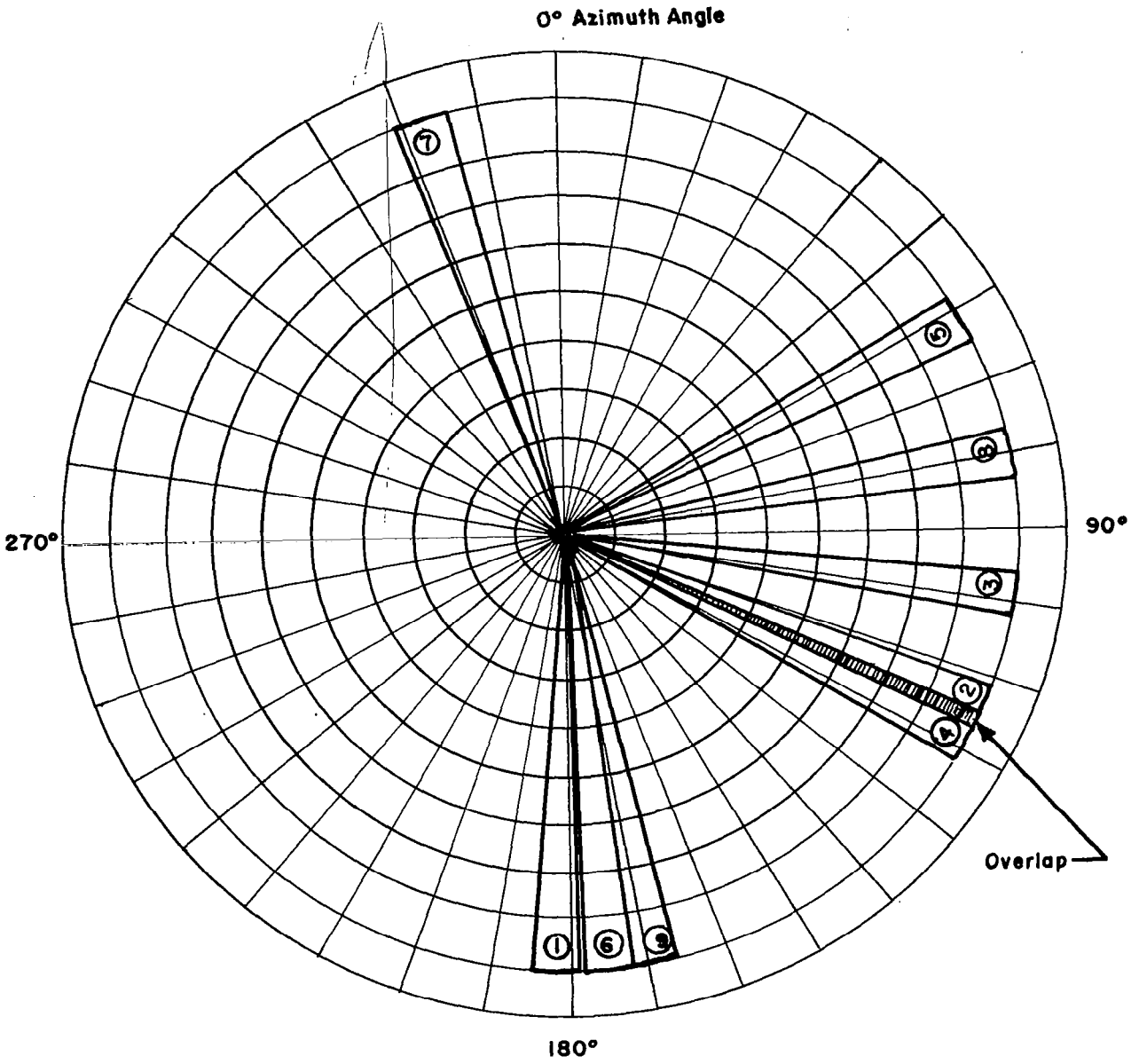

Figure 21 Disposition of Main Beams of Microwave Transmitters Assigned to 6063.8 MHz in the Southwest

In order to establish a clearer picture of the highest signal powers which might impinge on the EEE system, it has been felt desirable to attempt to establish an upper limit to possible effective radiated power on an indirect basis. This has been done by reviewing microwave vacuum tube data and estimating the EIRP's which would result from mating these tubes with efficient high gain antennas.

The informational source for this study was a tabulation of microwave tube data prepared by the National Bureau of Standards (Ref. 38) and covers about 3550 tube types and 44 manufacturers (U.S. and foreign). A list of those tubes and their output powers which deliver the greatest power in some portion of the 0.4 through 40 GHz band has been prepared (see Table 13). From this tabulation a table of maximum output powers as a function of frequency has been constructed (see Table 14). In terms of the tubes included, this is the upper limit of power.

The power levels found in this study are substantially higher than those found in the survey of ground emitters over much of the 0.4 - 40 GHz band. Throughout much of the lower part of the band (0.4 - 36 Hz) emitted powers of 75 or 76 dBW may be found while at higher frequencies this level declines at about 25 dB/decade.

The power received by the EEE system may be calculated using the expression

$$P_r = P_t + G_t - \text{Space Loss in dB} + G_r$$

where:

P_r = power received, dBW

P_t = power transmitted, dBW

G_t = Tranmitting Antenna Gain, dB

G_r = Receiving Antenna Gain, dB

This calculation has been done (see Table 14)for a sampling of tubes at a number of frequencies spanning the 0.4 - 40 GHz band. It has been assumed that efficient high gain transmitting antennas are coupled to these sources, assumed gains being 45 dB except for the two lower frequencies where a 68 ft and a 50 ft paraboloid are assumed for 0.4 GHz and 1.3 GHz, respectively. The receiving antenna has been assumed to be isotropic in all cases.

The results of these calculations for signals received from the subsatellite point (400 km) indicate that, at the lower frequencies, powers in the range of milliwatts or tens of milliwatts could be encountered. Signals received from near the horizon (2000 km) will be at a 14 dB lower level. When the 10 ft diameter paraboloid discussed in the

TABLE 13. MICROWAVE TUBE POWERS

Frequency Band (GHz)	Power (dBW)	Tube Class*	Tube Type
0.4	75	KLA	L3775
0.4 - 0.5	52	KLA	X602K
0.5 - 0.6	63	MAG	QKH517B
0.6	70	AMA	QKS576
0.6 - 0.7	47	KLA	VA894
0.7	63	MAG	QKH517
0.7 - 0.9	47	KLA	VA895
0.8 - 1.0	49	KLA	VA853
1.0 - 1.2	46	KLA	3KM4000LT
1.2 - 1.4	76	KLA	TV2023
1.4 - 1.8	24	BWO	RW712
S(1.5 - 3.9)	73	KLA	TV2016
2.7 - 3.1	75	KLA	TV2028
C(3.9 - 6.2)	68	KLA	SAC4910
X(6.2 - 10.9)	60	AMA	QK506
K(10.9 - 36.0)	45	MAG	QKH1124
15.5 - 17.5	51	MAG	7208B
16.0 - 17.0	56	MAG	VF20
16.2 - 17.2	47	MAG	R9509
23.8 - 24.3	51	MAG	SFD326
24.2 - 24.7	46	MAG	25M10
32.9 - 33.5	47	MAG	SFD332
34.4 - 35.4	46	MAG	L3752
34.5 - 35.2	52	MAG	SDF327
34.5 - 36.5	30	BWO	WJ282
37.0 - 50.0	-10	BWO	F4110/C070
39.5 - 40.3	45	MAG	R9685

* AMA = Amplitron Amplifier
  BWO = Backward Wave Oscillator
  KLA = Klystron Amplifier
  MAG = Magnetron

TABLE 14 EXPECTED RECEIVED POWER FROM SOME STRONG SOURCES

Frequency	Tube Type	Total Power dBW	Assumed Antenna gain (dB)	400 km		2000 km	
				Space Loss (dB)	Power Received (isotrophic) (dBm)	Space Loss (dB)	Power Received (isotropic) (dBm)
0.4	L3775 (KLA)*	75	37	137	5	151	-9
1.3	TV2023 (KLA)	76	40	147	-1	161	-15
3.0	TV2028 (KLA)	75	45	154	-4	168	-18
6.0	SAC4910 (KLA)	68	45	160	-17	174	-31
10.0	QK506 (AMA)	60	45	165	-30	179	-44
16.5	VF20 (MAG)	56	45	169	-38	183	-52
30.0	QKH1124 (MAG)	45	45	174	-54	188	-68
35.0	SDF327 (MAG)	52	45	175	-48	189	-62

* AMA = Amplitron Amplifier
KLA = Klystron Amplifier
MAG = Magnetron

Interim Report (Ref. 39) is assumed for the receiving antenna, the signals received at the lower frequencies would be at a considerably higher level, going to nearly a watt at below 3 GHz for signals from the sub-satellite point and in the tens of milliwatts below 3 GHz for signals from the horizon.

4.0 SYSTEM PARAMETER RELATIONSHIPS

4.1 EEE System Design Parameters

In this section the major system parameters relating to the design of an experiment for measuring emissions from the earth at an orbiting, near-earth satellite are discussed. Its purpose is to show how these parameters are related one to another, and thus to establish the trade-offs between them. For example, large antennas at the satellite would make the equipment more sensitive to emissions from the earth but would require a more detailed examination of the surface of the earth in order to detect all possible emitters.

We begin with the basic relationship between radiated and received powers and antenna effective areas. From Friis' propagation equation

$$P_r = P_t \frac{A_r A_t}{\lambda^2 d^2} \qquad (1)$$

P_r = power received, watts

P_t = power transmitted, watts

A_r = receiver antenna effective area, m^2

A_t = transmitter antenna effective area, m^2

λ = wavelength of radiation, m

d = distance between receiving and transmitting antenna, m

The effective area of the antenna can be related to its effective gain relative to an isotropic radiator in any direction θ, Φ by means of

$$A_{eff}(\theta,\Phi) = \frac{\lambda^2 G(\theta,\Phi)}{4\pi} \qquad (2)$$

Assume that in the case of the receiving antenna one is interested in the maximum gain and that the pattern of the antenna can be defined in terms of a main lobe which has a circular cross-section subtending a total angle α in radians (over which the gain is assumed to be constant). The gain can be approximated, for small angles, by the expression $16/\alpha^2$.

Substituting this result along with (2) into (1), gives

$$P_r = \frac{P_t G_t \lambda^2}{\pi^2 \ell^2} \tag{3}$$

in which the substitution

$$\ell = d\alpha \tag{4}$$

has been made, where:

ℓ = length subtended by the receiver antenna beam along the surface when the beam is directed normally to the earth.

Now, if the minimum detectable signal power at the receiver is defined as that power which is equal to the equivalent noise input power kT_eB where B is the bandwidth, k the Boltzmann's constant, and T_e the effective system temperature, the minimum detectable effective isotropic radiated power $(EIRP)_{min} (=P_t G_t)$ is

$$(EIRP)_{min} = \frac{\pi^2 kT_e B}{\lambda^2} \ell^2, \text{ watts} \tag{5}$$

In concept, the satellite is to scan simultaneously both spatially and in frequency. The maximum rate at which one can scan in frequency past a particular emitter without substantial loss in receiver response is given by [Ref. 40, p.65]

$$F = \frac{B^2 T}{\eta}, \text{ Hz} \tag{6}$$

in which

F = frequency range scanned, Hz

B = bandwidth of the scanning aperture, Hz

T = dwell time on a particular geographical area, s

η = a factor which can be of the order of unity for detection of sinusoids or larger for detection of random type signals.*

For gross calculation purposes a geographic scanning discipline is assumed in which the dwell time on any particular point (emitter) on the surface of the earth is nearly the same as for any other point. This condition is closely achieved in optical scanning techniques using a rotating prism in which a strip of surface of length y is completely scanned in the time it takes the vehicle to advance one strip width.

---

* $\eta = 70$ is found for random noise if the rms fluctuation from reading to reading is to be less than 10% of the true value.

The length y is assumed to be small compared with the prism (vehicle) height and the element of the strip seen at any instant is rectangular in cross section. With a radio frequency antenna the element is not rectangular, nor are the boundaries of the element sharply defined, hence not all points on the surface will be exposed for the same dwell time, and some points may be scanned more than once. Furthermore, the antenna will probably be required to scan left to right and then return right to left causing further loss in scanning efficiency.

In spite of these complications the minimum time (T_t) required to scan an area A can be estimated by multiplying the dwell time T by the area A and dividing by the area subtended by the cross section on the earth's surface ($\pi \ell^2/4$)

$$T_t = \frac{4AT}{\pi \ell^2} \tag{7}$$

Substituting (5) and (6) in (7), with $\eta = 1$ (for detection of sine wave type signals), one obtains (8) which gives the total time to scan a geographical area A over frequency range F:

$$T_t = \frac{4\pi}{\lambda^2 B^2} \frac{kT_e B \, FA}{(EIRP)_{min}}, \text{ sec} \tag{8}$$

To relate this result to the motion of the vehicle, one can express the area scanned in one second in terms of the linear velocity of the spacecraft (v) by the following relation:

$$A = yv \tag{9}$$

where y = the length of the surface path scanned measured in the direction normal to the flight path. Then, taking the total scan time $T_t = 1$ second, (8) becomes

$$Fy = \frac{\lambda^2 B^2}{4\pi v} \frac{(EIRP)_{min}}{kT_e B}, \text{ m Hz} \tag{10}$$

This relation can be simplified by rewriting (5):

$$\ell = \frac{\lambda}{\pi} \sqrt{\frac{(EIRP)_{min}}{kT_e B}} \tag{11}$$

and for (10)

$$Fy = \frac{\pi}{4v} \ell^2 B^2 \tag{12}$$

Note that both of these relations are not explicitly dependent upon the altitude, but to have the same value of ℓ at different altitudes would require antennas with different gains. Equation (11) is plotted on Fig. 22 with frequency as a parameter. It shows the (maximum) value of ℓ for a specified $(EIRP)_{min}$ to kT_eB ratio. Equation (12) is plotted on Fig. 23 for a typical shuttle velocity of 4.75 mi/s with frequency range scanned as a parameter.

As an example, assume measurements are being made in a frequency band near 1 GHz (λ = 0.3m) with a spectrum analyzer with a bandwidth B of 100 kHz, and with a desired detectable $(EIRP)_{min}$ of 100 μW. If the receiver has a sensitivity (kT_eB) of 10^{-14}W, from Fig. 22, $\ell \cong 10^4$m $\approx$ 6 miles, and for a frequency scan width F of 1 GHz, the geographic scan width is (from Fig. 23):

$$y = 10^5 \text{m}$$

or about 60 miles.

For wider bandwidths or higher levels of $(EIRP)_{min}$, wider geographic and frequency scan widths are possible.

Equations (11) and (12) apply strictly only for small percentage frequency scan widths and for antenna scanning angles for which the slant range is not much different from the vehicle height. Where these conditions are not met, Eq. (11) and (12) must be considered approximations which can be used for general system design purposes. With appropriate numerical corrections they can be used for large scan widths. Further, it should be noted that for signals other than CW, such as for radar type signals, a longer dwell time may be required for detection or for signal analysis (η, Eq. 6, greater than unity) and the effective value of Fy would be reduced. The radar case is discussed on page 48 of the Preliminary Report (Ref. 30).

In addition to the above, a practical question is the size of an antenna necessary to achieve a given value of geometric resolution. This is shown on Fig. 24. It is of course a function of the height of the antenna over the surface which it is viewing, as shown.

4.1.1 Slant Range Viewing

All the relationships derived above are based upon the concept of an antenna looking at the nadir point directly under the carrier (satellite or aircraft). The scanning disciplines discussed in section 4.2 include alternative procedures in which the antenna points at some angle with the vertical, for example an angle in which the horizon would be included in the antenna aperture. In this position, the distance from the antenna to various points on the surface of the earth within its aperture vary over quite a large range and the geometrical resolution is not a well-defined quantity. The minimum value of EIRP which can be detected will vary from

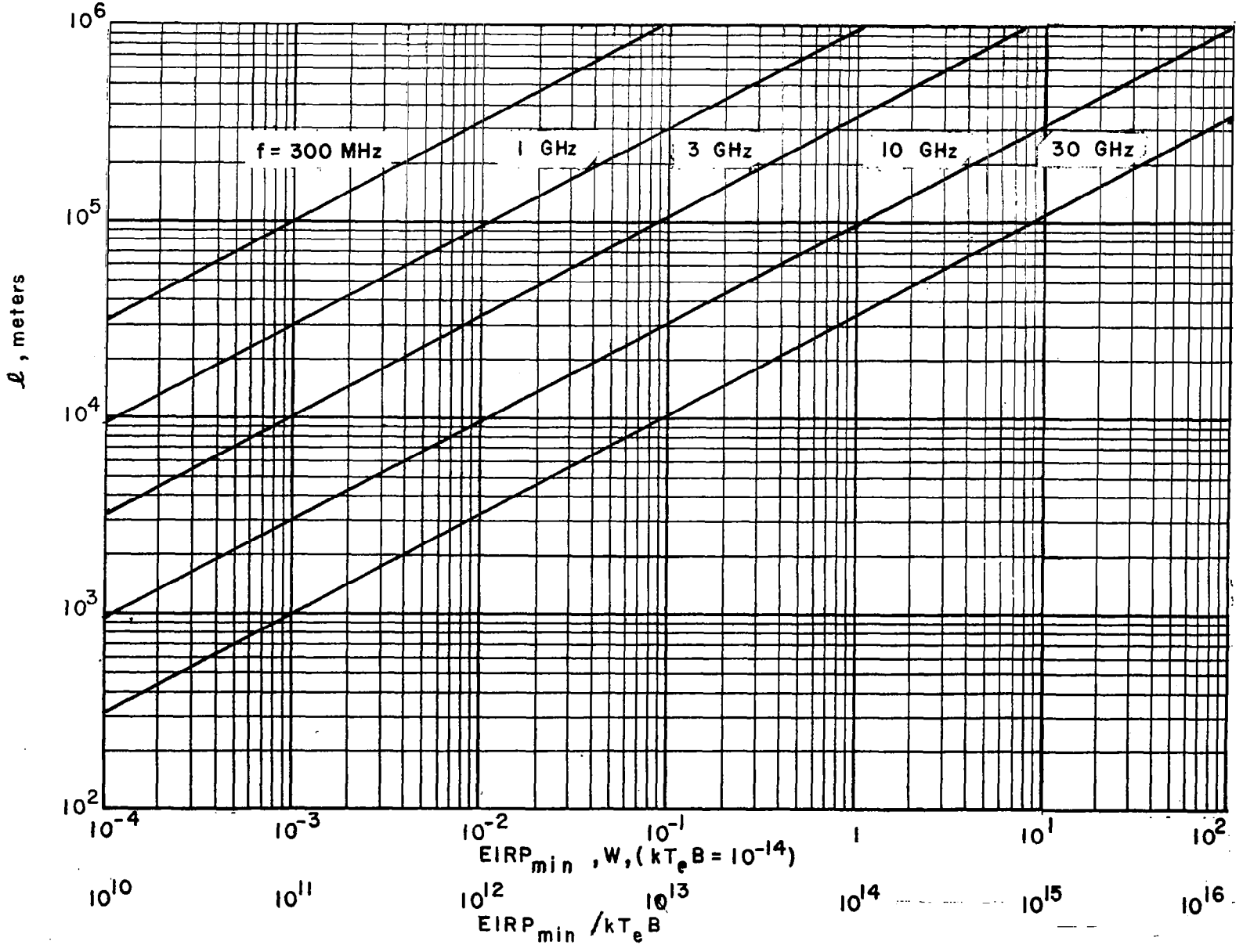

Fig. 22 Spatial Resolution (ℓ) versus Ratio $\frac{EIRP_{min}}{kT_eB}$

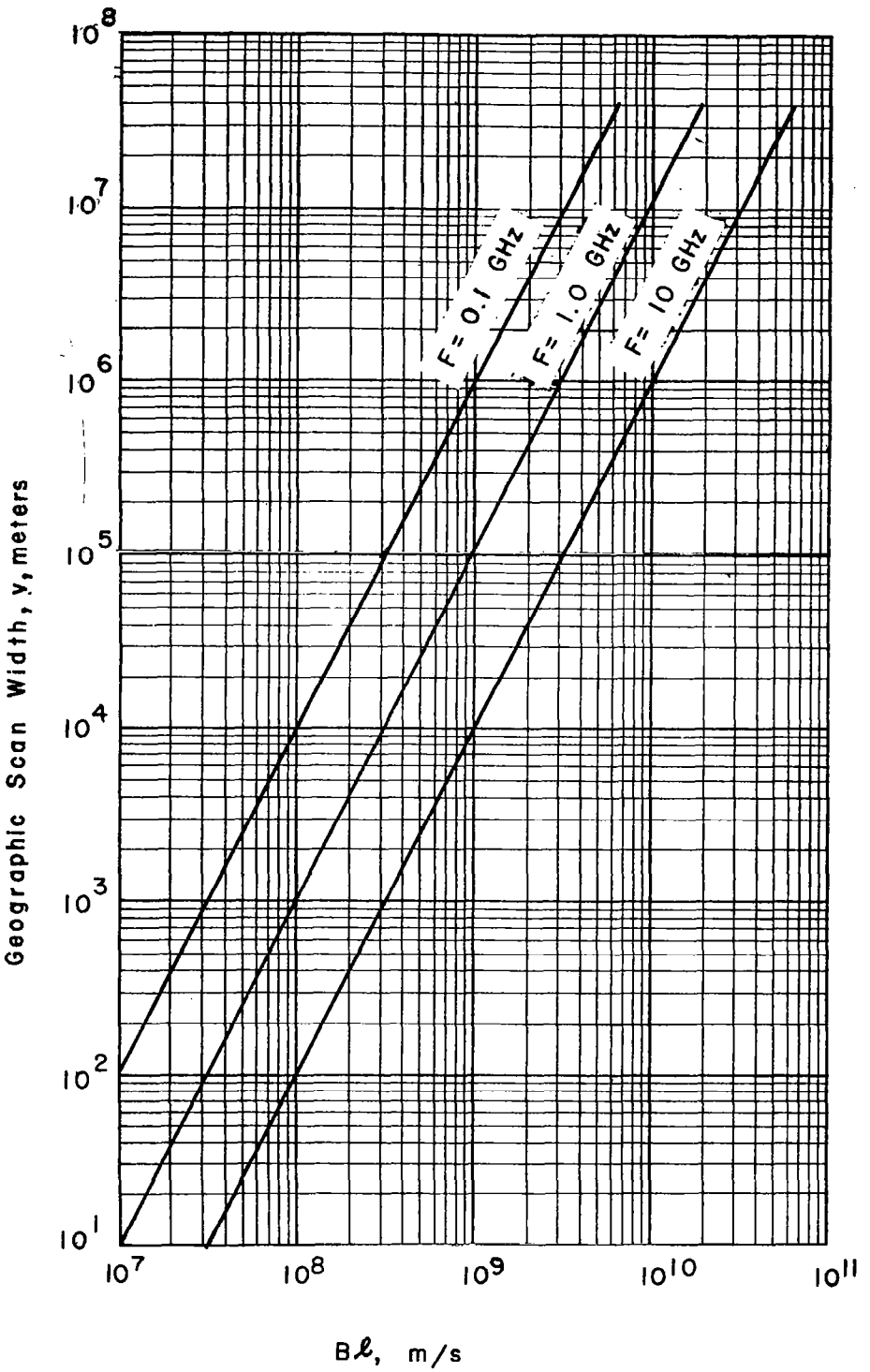

Fig. 23 Geographical Scan Width versus Product of Frequency and Spatial Resolution ($B\ell$) with the Frequency Scan Width as a Parameter. v = 4.75 mi/s. Scan width y small compared to vehicle altitude.

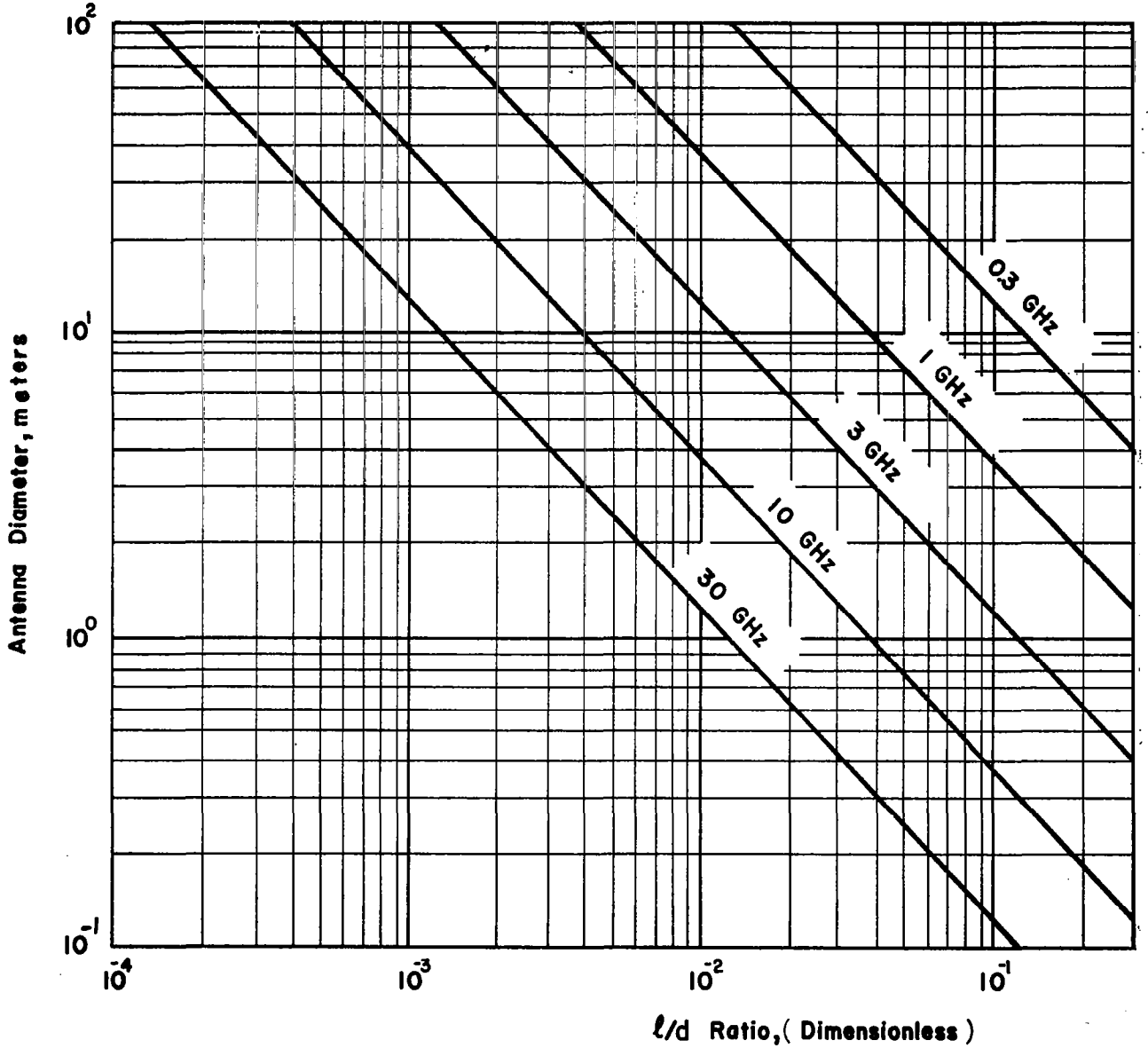

Fig. 24 Beam Angle vs Antenna Diameter with Frequency as a Parameter for a Nadir-looking Antenna. $\ell/d \cong$ half-power beam angle. ℓ = geometric resolution. d = antenna altitude

point to point. The formulas can be used, however, to approximate the characteristics of the configuration by assuming some nominal value of distance such as that which obtains in the direction of the center of the antenna focus. For example, for an antenna pointed close to the direction of the horizon, one might have an effective value of distance r = 1000 miles rather than, say, the nominal 250 mile distance for vertical pointing to nadir. Clearly, for the same geometrical resolution, a larger antenna would have to be used, but note that the EIRP minimum would be the same for the same value of geometrical resolution. Likewise, the effective value of transverse scan, y, would be increased somewhat. For rough approximations, however, the relationships previously derived can all be applied in this case.

4.2 Discussion of Scanning Disciplines

Earlier proposals for electromagnetic environment measurements have recommended both broad beam antennas for wide coverage or narrow beam antennas with wide sweeping angles. A shortcoming of a broad beam antenna is that it sees ground sources from a variety of angles, making it difficult to isolate and to geographically pinpoint specific sources, and its sensitivity is less than that of a narrow beam antenna (unless the latter is used in a tracking mode on specific sources) and thus is more likely to intercept a source which is not emitting continuously, or one which has a rotating directional beam.

The interception probability is a complicated function of the exact geometrical relationship between the location of the transmitters with respect to the flight path, the tranmitter radiated power and antenna pattern, the receiver sensitivity and its antenna pattern, and the scanning discipline in both frequency and geometry. For certain conditions useful approximations can be given; for example, if two antennas are located at two points in a plane, the probability that their beams, if positioned at random, will intersect is:

$$\frac{\theta_1 \theta_2}{4\pi^2}$$

where θ_1 and θ_2 are the angular widths (in radians) of the two respective beams. However, note that if one of the beams rotates with a period equal or less than the dwell time of the other antenna in any specific direction, the probability of intersection can be close to unity.

In examining the ground for distributed (nonintentional) emissions, the wide beam method produces an average of the region examined, possibly washing out the effects of hot spots such as those found in urban areas. A satellite at an altitude of 250 miles has in sight a spherical cap with a radius of about 1400 miles. Such an area may include both rural and urban areas, as well as the sea. The effective average brightness temperature of the entire cap is not expected to be much higher than the nominal temperature of 300 K, while the hot urban areas have been seen to be at temperatures around 30,000 K at VHF.

Using directive antennas pointing toward the horizon has a potential advantage over the vertical pointing arrangement. Since most antennas on the surface of the earth in the frequency range of interest are directive and usually aimed along the surface of the earth, a receiving antenna pointing towards the horizon would be more likely to intercept the main beam of such antennas. But since the distance from the satellite to the nadir, the minimum value of EIRP is also larger with this arrangement. On the other hand, it appears that the satellite receiver will have adequate sensitivity to detect most emitters of consequence. For detecting horizontally directed emissions with an antenna looking vertically, it would be necessary for the satellite to detect a side lobe of the source antenna.

It is clear that the scanning discipline used must depend in large measure on just what one wants to determine. For example, if one is concerned with interference to a specific satellite, one should use an antenna similar to that on the satellite and scan in frequency and geographical regions which are capable of producing interference. In other cases, more general frequency and geographic scans are required.

Without examining specific applications in detail, one can make the following statements:

(a) Intentional or isolated and strong unintentional sources should be measured in such a way that the number seen at one time is small, preferably just one. Frequency assignment policy, having as its purpose the spatial isolation of sources operating at the same or adjacent frequencies, makes it unnecessary to demand high ground resolution for intentional radiators.

(b) Multiple incidental sources may be measured over an area large enough so that many contribute (to give a nearly gaussian receiver input), but not large compared to the area of the cities over which the tests are being made. The latter requirement will make it possible to see the fine structure in variations of noise brightness temperature.

(c) Sweeping methods preferably should be such that sources are examined over a limited range of angles relative to the vertical. This will result in a nearly constant footprint size, nearly constant free-space loss to all sources being observed, and a restricted aspect from which the transmitter antenna pattern is being viewed.

(d) Scanning techniques should account for the effects of directional and rotational properties of both source and receiving antennas in reducing the probability of detecting individual sources.

One can classify any geographic scanning discipline as a variation of two types: (1) nodding, and (2) conical. [An antenna fixed with respect to spacecraft coordinates (such as forward looking) can be considered as a special case of either type.]

In the nodding scan the antenna sweeps back and forth in a direction normal to the direction of spacecraft travel. For a fixed antenna with a circular beamwidth, the area on the ground in the beam of the antenna enlarges and departs more and more from a circle as the angle of inclination departs from the nadir direction. In order to get complete coverage of the width scanned, the angular rate of scan can be varied with inclination angle. Of course, geographic resolution also varies with inclination angle.

In the conical scan the effective geographic resolution remains constant with rotational angle since the angle of inclination remains constant. However, as with nodding scan, at large inclination angles the distortion of the pattern viewed on the ground is considerable as is the variation of dwell time at different points within the pattern.

4.3 CONICAL SCANNING

The area viewed on the ground is suggested by the shaded area shown on Fig. 25. It shows the circular annulus being traced out over a flat surface with the satellite moving in one direction with constant speed. For continuous ground coverage the rate of rotation can be fixed so that the distance advanced in one rotation of the antenna (= distance from A to B on Fig. 25) will be no more than this distance. The distance A to B is

$$d_{AB} = \frac{v}{S} \tag{13}$$

where

v = spacecraft velocity in miles per second

S = antenna rotation rate in rps

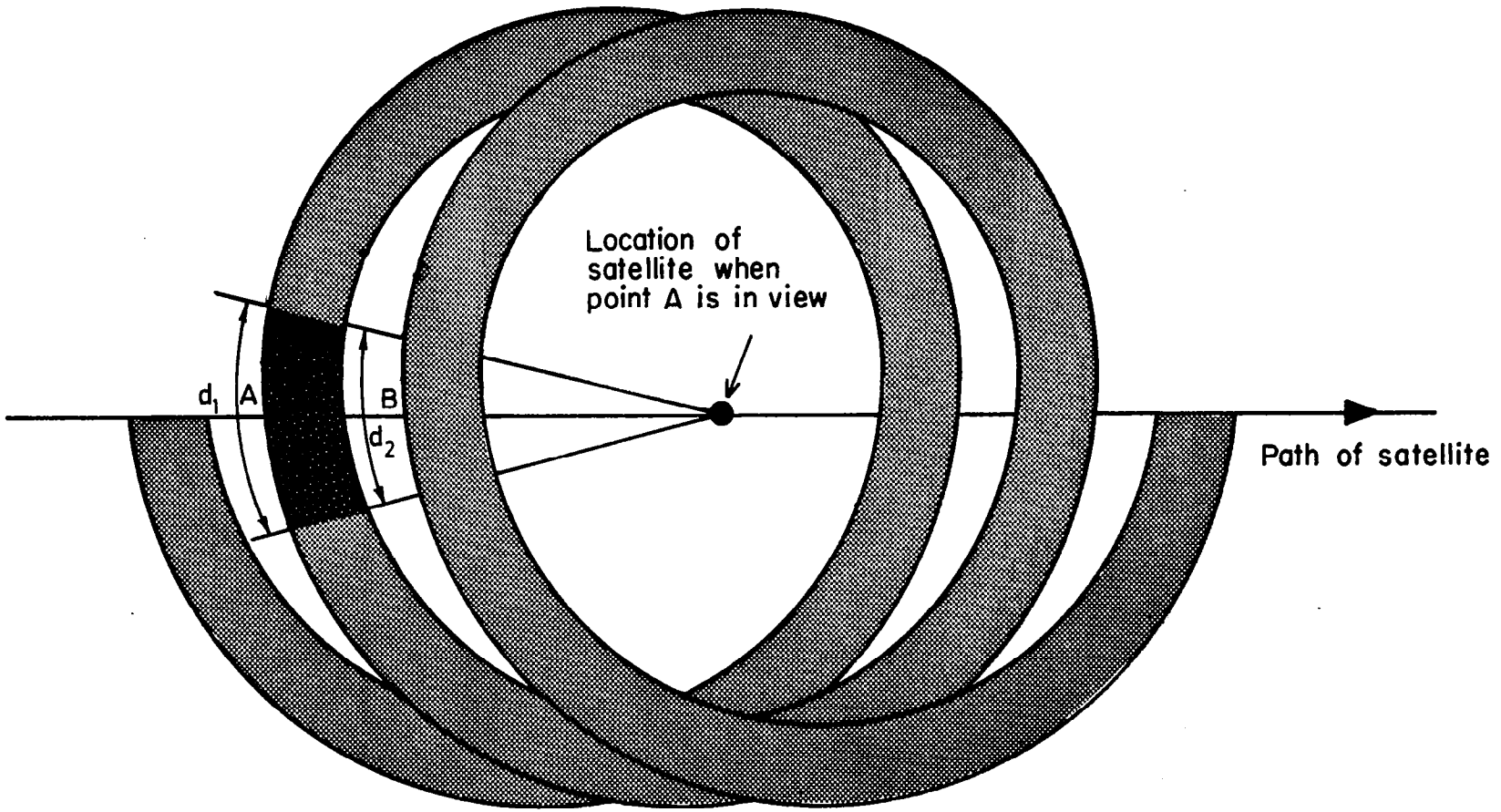

Fig. 25 Surface Area Scanning Pattern

If d_{AB} equals the width of the beam, then successive bands in the spiral are contiguous. Sources which transmit with main lobe axis tangent to the earth will be seen by the spacecraft at various angles of the transmitter main lobe.

4.3.1 Mathematical Analysis

4.3.1.1 Geometrical Considerations

The geometrical conditions as seen in a plane containing the satellite and the earth's center, at the moment when the antenna beam is centered on the plane, are shown in Fig. 26. The figure is an adaptation of Fig. 4-1 in the Interim Report (Ref. 39) with additions to show the antenna beamwidth and the visible ground region. The rays SP and SP_1 are the inner and outer beam edges which, for an actual antenna beam, may be taken to be the rays at which the sensitivity is down 3 dB from the beam center.

Geometric relationships useful in system analysis are:

$$\theta = \cos^{-1} \frac{r}{r+h} \tag{14}$$

$$b + c + \varphi = \pi/2 \tag{15}$$

$$a + c + \theta = \pi/2 \tag{16}$$

From (15) and (16)

$$\varphi = a - b + \theta \tag{17}$$

By the law of sines

$$\frac{\sin \delta}{r+h} = \frac{\sin c}{r} \tag{18}$$

so that using (15) and (16) and the identity $\sin\left(\frac{\pi}{2} + b\right) = \cos b$

$$\cos b = \frac{r+h}{r} \cos(a + \theta) \tag{19}$$

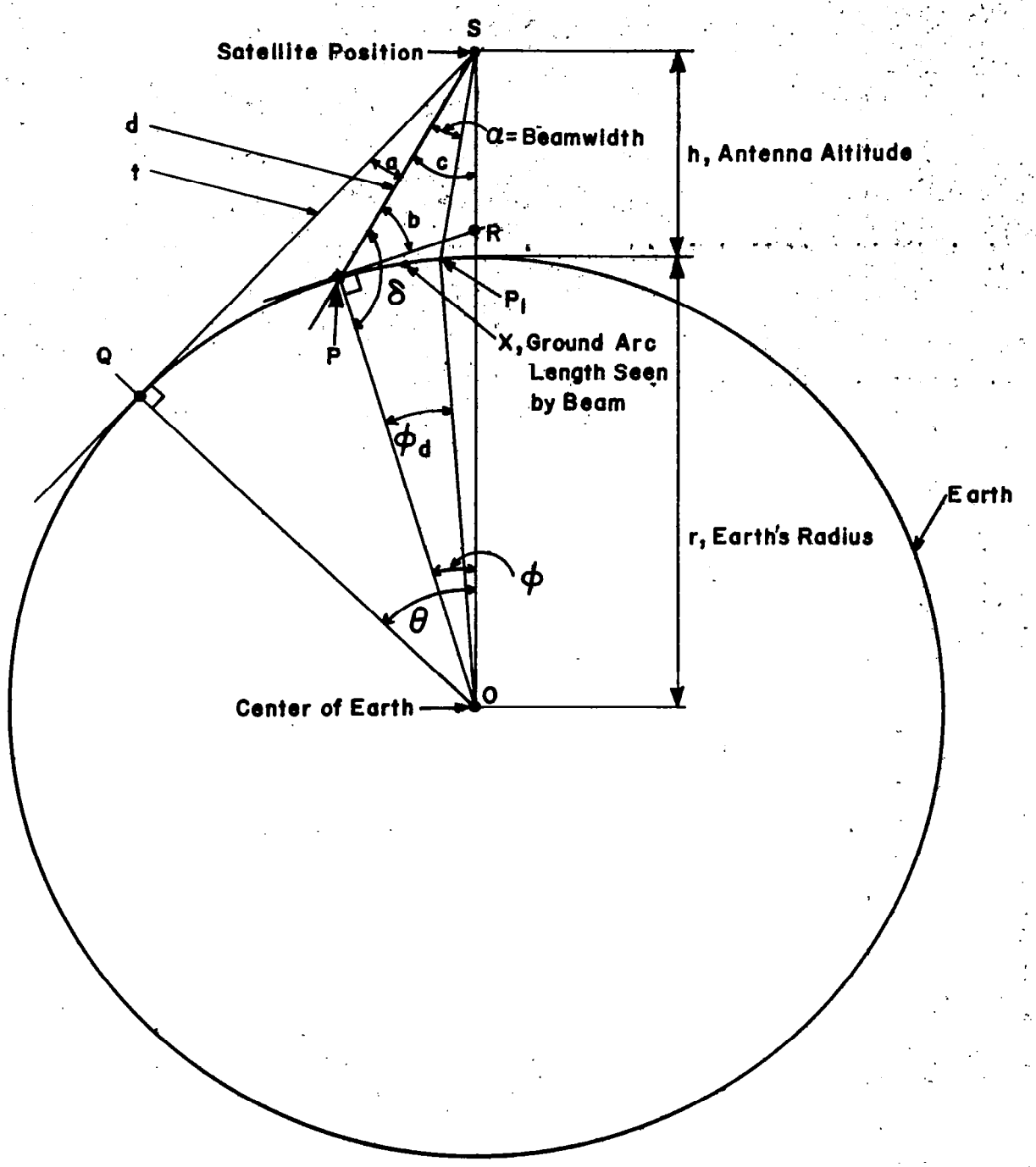

Figure 26 Satellite Above Earth — Geometric Variables Defined

b is the angle of the ray connecting satellite and ground source at P, relative to the horizontal plane at the source. For sources transmitting in a plane tangent to the ground, b is the off-main-beam angle measured in a vertical plane. Furthermore, SP being the outer ray of the cone representing the satellite beam, b is the smallest such angle along the visible arc from P to P_1. b is plotted in Fig. 27 as a function of the angle a by which the satellite antenna is depressed from the horizon line. Figure 27 can be used to determine the range of the angles b for all rays along the visible arc PP_1, given the angle a and the beamwidth α. For example if $a = 40^\circ$ and $\alpha = 10^\circ$, one reads directly for $a = 40^\circ$ a value of $b = 57.6^\circ$ and then reads on the a scale for an angle $a + \alpha = 50^\circ$, $b = 68.4^\circ$. The latter is the angle $(SP_1O - \pi/2)$ on Fig. 26, the angle relative to the horizon plane of the ray from P_1 to S.

For small beamwidths an approximation of the range of angles b (or the angles $\delta = b + \pi/2$) can be developed. From (18), taking derivatives with respect to the angle a

$$\cos \delta \cdot \frac{d\delta}{da} = \frac{r+h}{r} \cos c \cdot \frac{dc}{da} \tag{20}$$

For moderate increments in a, meaning moderate beamwidths, there are moderate increments in δ, denoted $\Delta\delta$ and moderate increments in c denoted Δc so that

$$\Delta\delta \doteq \frac{r+h}{r} \frac{\cos c}{\cos \delta} \Delta c \tag{21}$$

But $(-\Delta c)$ is the beamwidth α, and $\cos c = \cos(\pi/2 - a - \theta) = \sin(a+\theta)$ so that

$$\Delta\delta = \Delta b \doteq - \frac{r+h}{r} \frac{\sin(a+\theta)}{\cos \delta} \alpha \tag{22}$$

This is also the increment in the angle b, which is denoted Δb in (22). For the example cited above ($a = 40^\circ$, $\alpha = 10^\circ$)(22) gives an adequate approximation as ought to be expected from Fig. 27. Observe that over a substantial part of the function shown, the slope is slowly changing, denoting that Δb is proportional to $\Delta a = \alpha$, the beamwidth, over a wide range around any preselected point a. Only near the origin is this not true. Were we to imagine a beam such that $a = 1^\circ$ $\alpha = 9^\circ$, then b would actually range from 6.50° to 22.71°, a difference of 16.21°. From (22) the result would be

$$\Delta b = \frac{4.25}{4} \frac{\sin 20.75^\circ}{\sin 6.50^\circ} \cdot 9^\circ = 29.93^\circ$$

The next variable of importance to be expressed in terms of the angle a is the angle φ defined in Fig. 26. From (17) and (19)

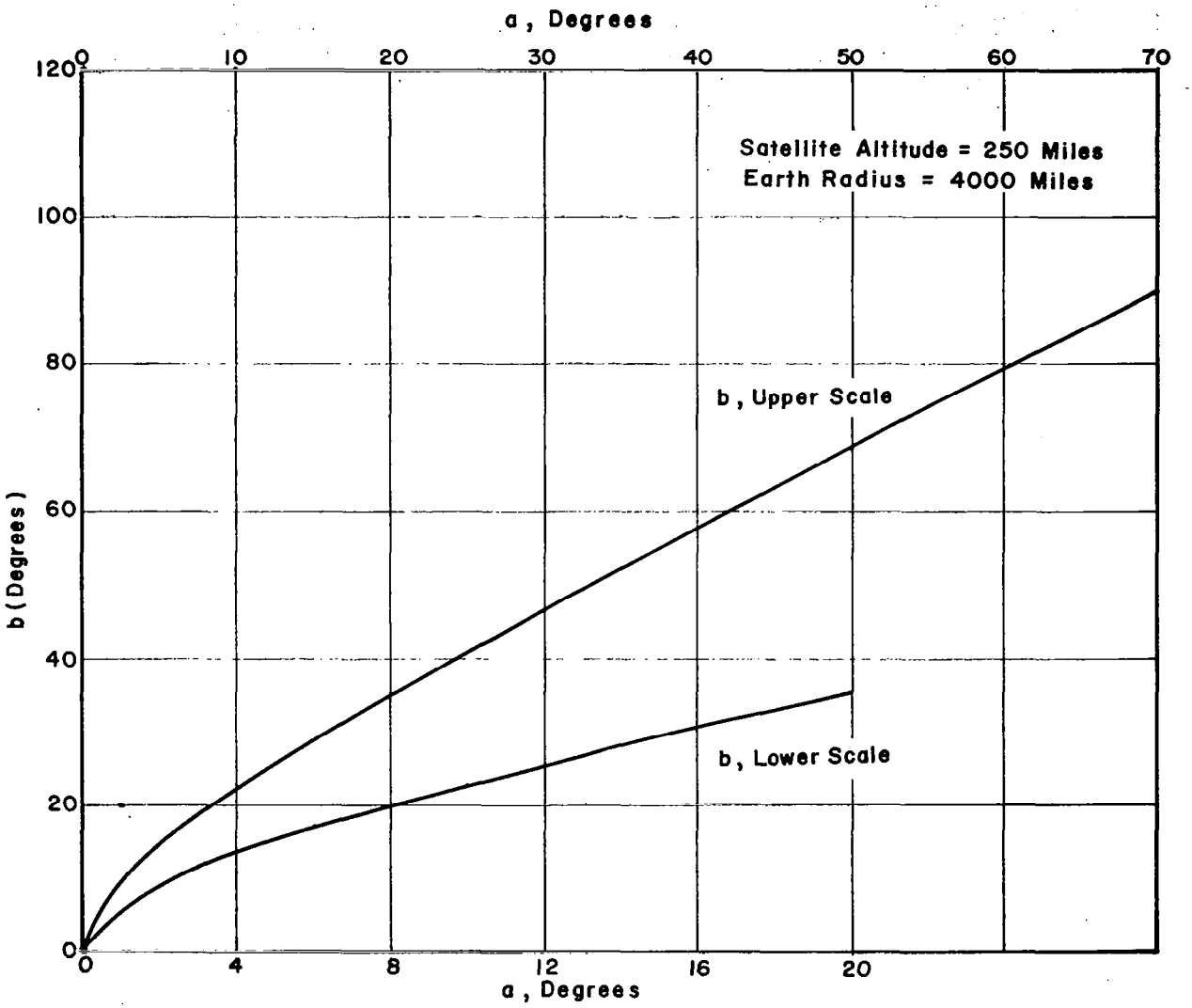

Figure 27 Angle of Ground Source to Satellite Relative to Horizontal Plane, b, as a Function of Angle Relative to Horizon Line, a. (See Figure 26)

$$\varphi(a) = a + \theta - \cos^{-1}\left[\frac{r+h}{r}\cos(a + \theta)\right] \qquad (23)$$

The functional dependence of φ on a is emphasized by writing $\varphi(a)$ in (23). The relationship (23) is plotted in Fig. 28. If the satellite antenna is aimed toward the ground with the ray SP at angle a and ray SP_1 at angle $a + \alpha$, the range of φ, denoted by φ_d in Fig. 26 is

$$\varphi_d = \varphi(a) = \varphi(a + \alpha) \qquad (24)$$

The ground arc length between these two rays is

$$x = r\,\varphi_d = r[\varphi(a) - \varphi(a + \alpha)] \qquad (25)$$

where the φ's are in radians.

Using an earlier example, with $a = 40^\circ$, $\alpha = 10^\circ$, $\varphi(a) = 2.11^\circ$, $\varphi(a + \alpha) = 1.33^\circ$, the ground arc length x is 25.7 miles. With $a = 1^\circ$, $\alpha = 9^\circ$, $\varphi(a) = 14.25^\circ$, $\varphi(a + \alpha) = 7.04^\circ$, x is 502 miles.

As a matter of interest, if a nearly constant ground resolution in the plane shown in Fig. 26 were desired for every value of a chosen, a different beamwidth would have to be used with each value of a. As an example, the entire spherical cap could be covered as shown in Table 15 below. In this example 3 antennas, one with a 2° beamwidth, one with a

Table 15 Coverage of Visible Spherical Cap with Nearly Constant Annular Depth

Beam Range a° to $(a^\circ + \alpha^\circ)$	$\varphi(a) - \varphi(a + \alpha) = \varphi_d$	x, miles
$0^\circ - 2^\circ$	$19.75^\circ - 12.45^\circ = 7.30^\circ$	509.96
$1^\circ - 10^\circ$	$14.25^\circ - 7.04^\circ = 7.19^\circ$	501.96
$9^\circ - 70^\circ$	$7.42^\circ - 0.02^\circ = 7.40^\circ$	516.62

9° beamwidth, and one with about 60° beamwidth, would cover the entire visible spherical cap, with some overlap, in a conical scanning mode.

For small values of beamwidth α, an approximation to φ_d given by (24) can be obtained by taking the derivative of (23). Thus

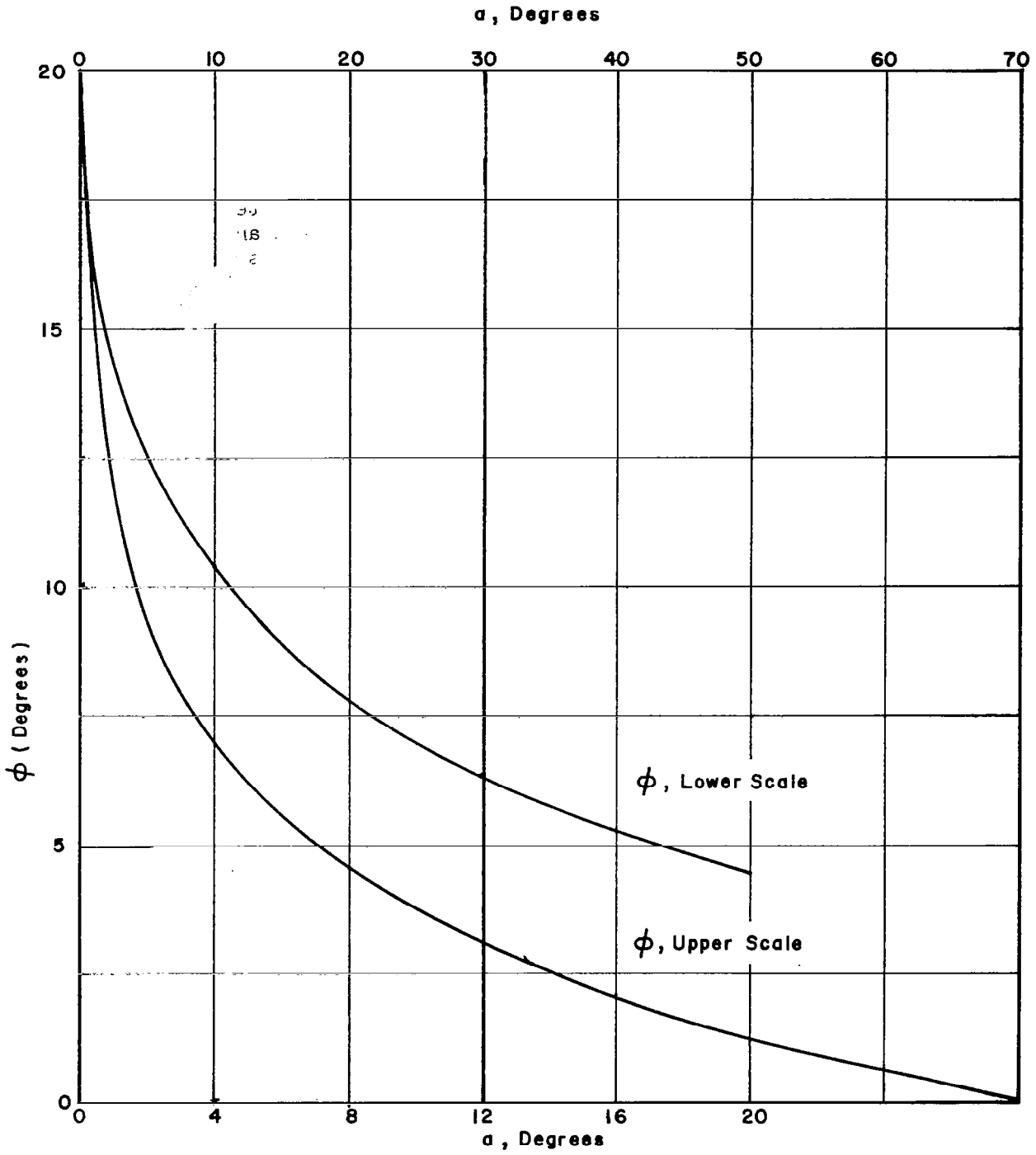

Figure 28 Angular Position of Ground Source, ϕ, as a Function of Angle Relative to Horizon Line, α (See Figure 26)

$$\frac{d\varphi(a)}{da} = 1 - \frac{\frac{r+h}{r}\sin(a+\theta)}{1 - \left[\left(\frac{r+h}{r}\right)^2 \cos^2(a+\theta)\right]^{1/2}} \tag{26}$$

Again, for a small increment in a, Δa, which is the same as the beamwidth α, one gets an increment in $\varphi(a)$ which has been denoted by φ_d,

$$\varphi_d = \left\{ 1 - \frac{\frac{r+h}{r}\sin(a+\theta)}{1 - \left[\left(\frac{r+h}{r}\right)^2 \cos^2(a+\theta)\right]^{1/2}} \right\} \alpha \tag{27}$$

Another variable of importance is the distance d as defined in Fig. 26 from satellite to ground source. d varies from the tangent distance t to the satellite altitude h which is in the ratio of 6 to 1 and is reflected in a free space power loss variation of about 15 dB. From Fig. 26 and relations (16) and (23)

$$d = r\frac{\sin\varphi}{\sin c} = r\frac{\sin\varphi}{\cos(a+\theta)} \tag{28}$$

$$= r\frac{\sin\left\{a + \theta - \cos^{-1}\left[\frac{r+h}{r}\cos(a+\theta)\right]\right\}}{\cos(a+\theta)}$$

Equation 28 is plotted in Fig. 29.

If the beamwidths as indicated in Table 15 are used, the ratios of free space loss at the beam extremities are 3.8 dB for the 0°- 2° beam, 5.4 dB for the 1°- 10° beam, and 7.4 dB for the 9°- 70° beam. These values are obtained by squaring the ratio of the d's at the extremities of each of the 3 beams. The difference in distances at beam extremities therefore adds an uncertainty of up to 7.4 dB to the amplitude measurement for this particular choice of beamwidths. These results suggest that if these uncertainties are to be reduced, the beamwidths will have to be reduced and, with it, the ground coverage. Recognizing that the beamwidth is a function of frequency and that it will vary as the frequency is swept, the uncertainty will, in turn, be a function of frequency.

4.3.1.2 Scan and Dwell Times

The shape of the ground footprint is a complicated function of the shape of the satellite antenna beam and the angle, c, of the beam relative to nadir (or the angle a relative to the tangent ray).

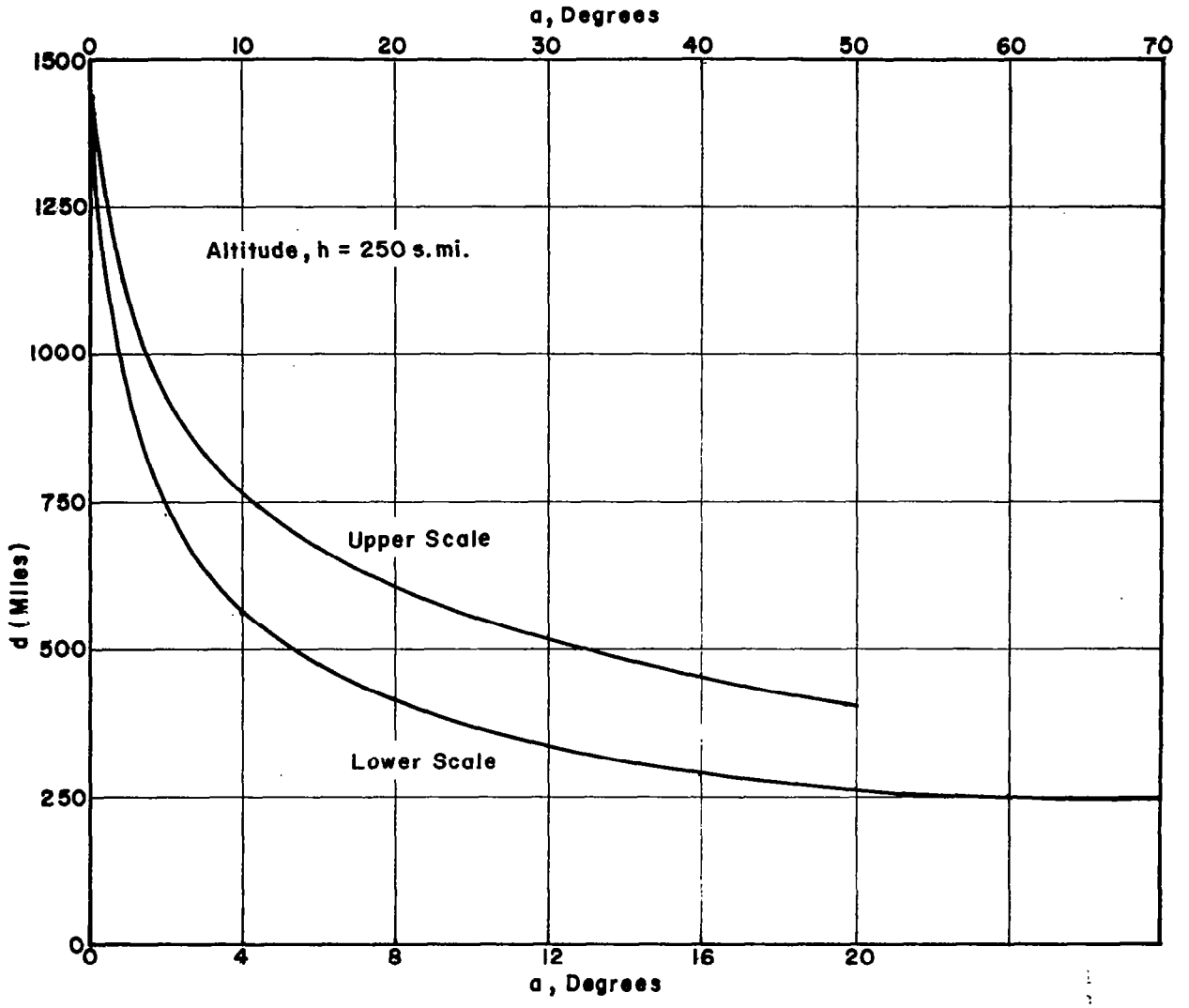

Figure 29 Distance From Satellite to Ground Source, d, as a Function of Angle Relative to Horizon Line, a. (See Figure 26)

The simplifying assumption is made that the region examined on the ground by the beam is approximately elliptical in shape and has a width ℓ_γ (in the sweep direction) given by

$$\ell_\gamma = \alpha\, d_\gamma \tag{29}$$

where α is the beam angle

and d_γ is the distance from the spacecraft to the point on the surface intercepted by the center of the beam defined by the beam pointing angle

$$\gamma = c - \frac{\alpha}{2} \tag{30}$$

relative to the vertical SO in Fig. 26. Values of d_γ are obtained from Fig. 29. Values of ℓ_γ (from Eq. 29) and x (from Eq. 25) are given in Table 16 for α = 1, 3, 10, and 30 degrees and various values of γ.

Table 16. Footprint (Quasi-Elliptical) Dimensions in Miles as a Function of Beamwidth α and Beam Pointing Angle γ

γ	$\alpha \rightarrow$ / d_γ	1°		3°		10°		30°	
		ℓ_γ	x	ℓ_γ	x	ℓ_γ	x	ℓ_γ	x
0	250	4.36	4.36	13.1	13.1	43.6	43.75	131	134.3
10	254.10	4.43	4.51	13.3	13.5	44.3	45.3	133	139
20	267.16	4.66	5.00	14.0	15.0	46.6	50.2	140	156
30	291.75	5.09	6.01	15.3	18.0	50.9	60.5	153	191
40	333.87	5.83	7.98	17.5	24.0	58.3	80.6	175	266
50	408	7.12	12.25	21.4	36.7	71.2	125.4	214	475
60	559	9.75	24.90	29.3	74.7	97.5	269.2	293	
70*	1229	21.45	382.09	64.3	595.0	214.0		643	

* The values in this row are actual values measured from the horizon for a spherical earth.

From the values of ℓ_γ given in Table 16, the corresponding value of $EIRP_{min}$ can be obtained from Fig. 22 using ℓ_γ for ℓ. Figure 30 shows values of $EIRP_{min}$ as a function of the pointing angle γ for antenna apertures of 1^o and 3^o for frequencies of 1 and 10 GHz. Values for other frequencies and angles can be obtained by extrapolation. $EIRP_{min}$ is the value of EIRP which results in an observed signal power equal to a reference noise power of 10^{-14} watts.

Considered now is the coverage obtained using the conical scan. The discussion of tangential scanning in the preliminary report (pp. 45-48, Ref. 30) is pertinent.

For continuous swath coverage at arbitrary angles c relative to the vertical, the required rotation rate is inversely related to the beamwidth x on the ground in the direction of motion of the spacecraft as given by Eq. 13, where $d_{AB} = x$ in Table 16.

The dwell time T is determined by the width ℓ_γ of the beam which is given by (29) and the speed of travel of the sweep on the ground. The latter is found by observing that the radius of the circle described by the central ray of the beam is given by $d_\gamma \sin \gamma$. The speed of travel on the ground for this central ray is therefore $2\pi S d_\gamma \sin \gamma$. The dwell time is therefore

$$T = \frac{\ell_\gamma}{2\pi S d_\gamma \sin \gamma} = \frac{\alpha}{2\pi S \sin \gamma} \qquad (31)$$

Equation 31 is plotted in Fig. 31 for v = 4.75 miles/s, the speed at an altitude of 250 miles, as a function of γ for four values of beam width. The value of rotation rate, S, is plotted in Fig. 32, using (13) and the values of x in Table 16.

4.3.2 Discussion

a) Choice of Beam Pointing Angle

With conical scanning, it is obvious that the largest geographical coverage on a single pass of a satellite is obtained with the largest beam pointing angle γ. If the pointing angle is such that the horizon is included in the antenna aperture, the path width is approximately 2750 s. miles. As seen from Figs. 31 and 32, a 1^o beam would have a rotation rate of 0.014 revolutions per second for continuous coverage, and the dwell time would be approximately 0.21 seconds. This arrangement permits the largest range of frequency scanning, but of course also has the smallest geographical resolution, and the highest value of $EIRP_{min}$. On the other hand, the values of $EIRP_{min}$ and geographical resolution are considered appropriate in view of policies on frequency reassignment and actual levels of EIRP to be expected in accordance with the discussion in section 3 of this report.

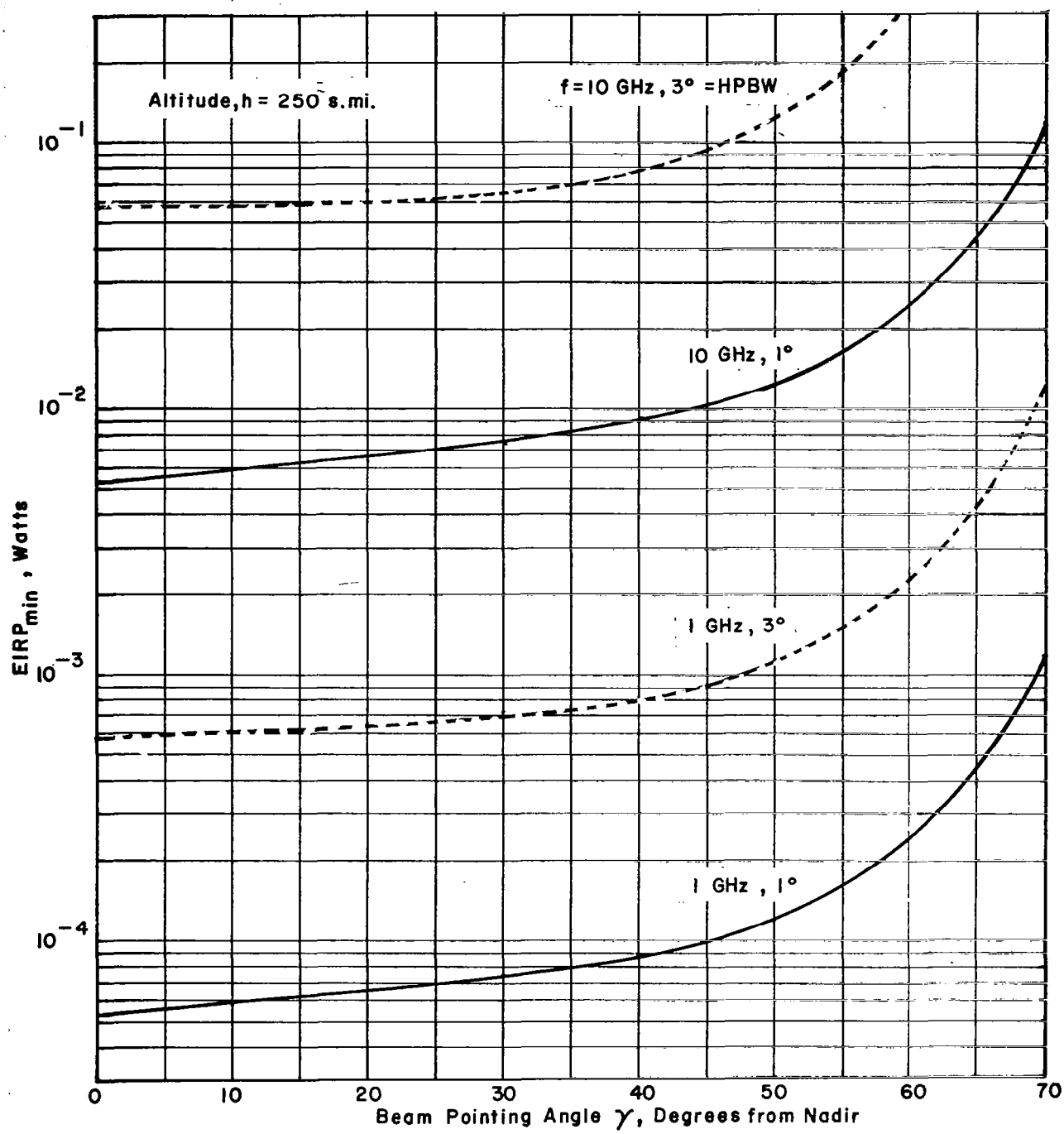

Figure 30 $EIRP_{min}$ as a Function of Antenna Half-Power Beam Width and Pointing Angle

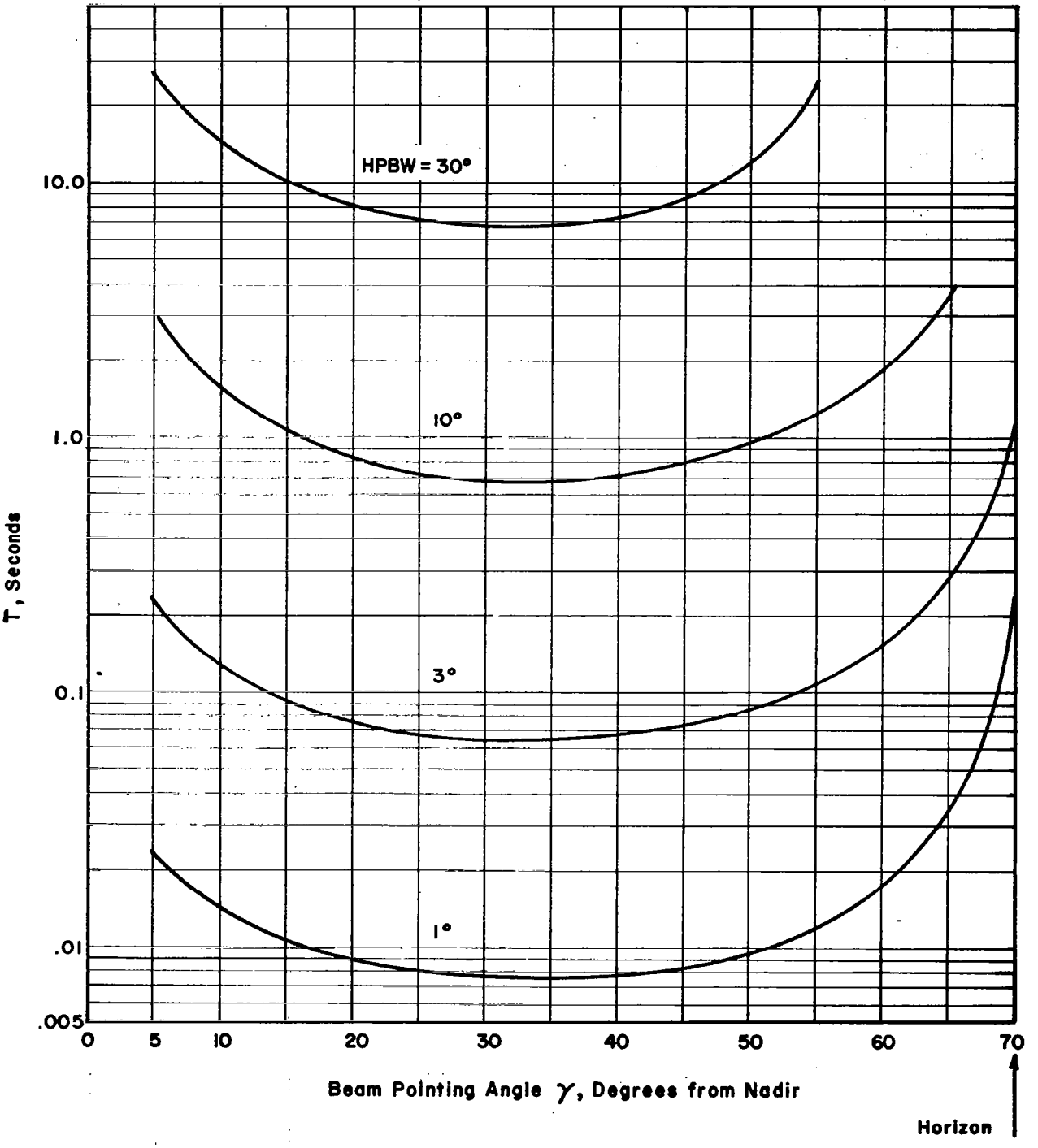

Figure 31 Dwell Time for Conical Scan for Continuous Swath Coverage vs γ for Given Antenna Apertures

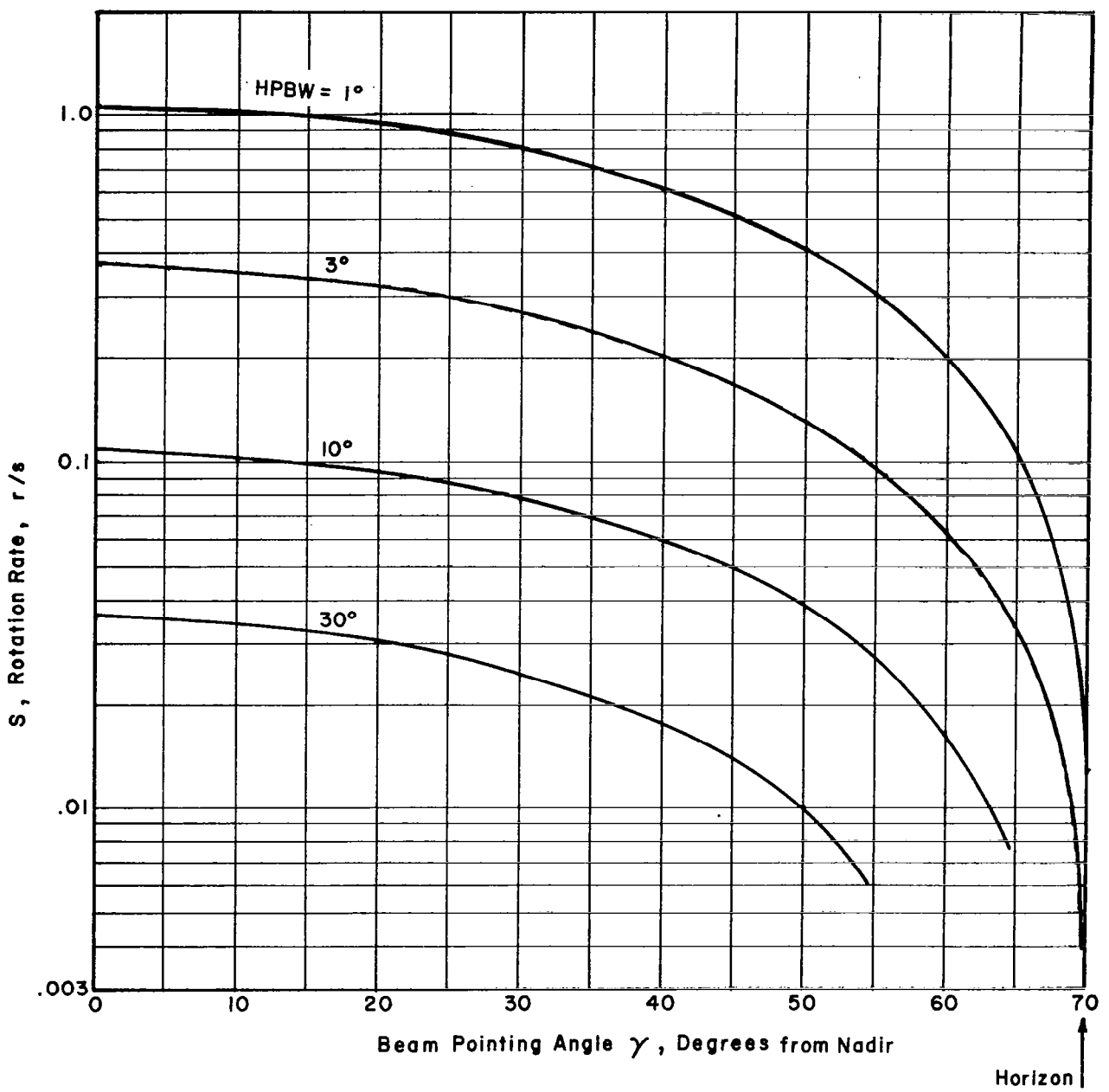

Figure 32 Rotation Rate vs γ for Given Antenna Apertures

Clearly, one has a wide choice of options at his disposal. Slight decreases in the pointing angle from the horizon direction (of the order of 10°) will considerably improve geographic resolution if it is considered necessary. On the other hand, the reduced dwell time permitted for continuous coverage will limit the range of frequency scan by as much as an order of magnitude. The beam width of the antenna could be increased with a corresponding loss in geographical resolution in order to increase the dwell time and permit greater frequency scan width. Thus, for a 1° beamwidth and a 10 kHz bandwidth, the frequency range scannable with continuous geographic coverage at a pointing angle of 33° (most severe case, assuming η (Eq. 6) = 1) is 6.7 MHz. On the other hand, since geographic resolution is better by at least 50 times what it is at the horizon, many fewer targets will be located in the main beam at the same time, and it may be possible to frequency scan at a greater rate by using a wider bandwidth. Increasing the bandwidth by 10 times (to 100 kHz) will compensate for a 100 to 1 decrease in dwell time.

By increasing the antenna beamwidth to say 10° the rate of scan can be reduced by approximately 10 times and the dwell time will be increased by 100 times, giving for a 10 kHz bandwidth a frequency scanning range of 0.67 GHz at a nadir angle of 33°. The geographical resolution then is about 50 miles. Of course, the smaller the angle to nadir, the smaller is the total width of path scanned.

For the most general applications, it is considered that horizon or near horizon scanning will prove to be an appropriate approach, especially in view of the fact that the width of the swath then corresponds approximately to the rate at which the typical satellite orbit progresses around the surface of the earth. Furthermore, this scan, in common with the others, provides for views of many of the targets on successive scans which increases the probability of detection of targets which have directional antennas.

Alternate arrangements may be advisable for other types of investigations. For example, if it is desired to obtain information on interference to satellite antennas which are pointing in an almost vertical direction, then the arrangement with a small pointing angle obviously would be preferred.

b) Refraction and Doppler Effects

The foregoing assumes that rays travel in straight lines without refraction. When observing sources at the horizon, the ray is expected to undergo, in part, the refractive effect which is accounted for in microwave line-of-sight transmission by increasing the earth's radius by a factor of 4/3. Because the ray from source to receiver passes through not only the atmosphere, but also a considerable region beyond,

the refraction is likely to be less than in ground point-to-point transmission. Since this effect depends on the rate of change of index of refraction with altitude, which in turn depends on geographic location and climate, there is some uncertainty in locating the radio horizon. This matter will be given further attention to determine what the refractive effect will be and whether or not it will be necessary to use special means to overcome its variability.

Because of the doppler effect, the center frequency shift when observing a source on the satellite track will be positive and equal to $f\left(1 - \sqrt{\frac{v-c}{v+c}}\right)$ when approaching the source, and negative by an equal amount when leaving it (f = source frequency, v = S/C velocity, c = speed of light). At 3 GHz this amounts to $\pm$ 76 kHz.

c) Frequency Scanning

The basic relation limiting the rate of frequency scan is given by Eq. (6). Although sine wave sources require a value of η in that equation of about unity, some of the sources being measured may resemble gaussian random noise when passed through the satellite receiver bandwidth. For instance, a microwave relay for 600 voice channels using FDM-FM will occupy a band of about 15 MHz. A filter looking at a 1 MHz portion can be expected to see a gaussian process by the central limit theorem. Based on the theory of estimation of gaussian noise parameters (see e.g., Ref. 40, p. 65), η in Eq. (6) should have a value of about 70 to assure that the measurement error is less than 10% of the measured quantity.

Thus for a 1 MHz receiver bandwidth the frequency range scanned in an interval, as found in (31), is

$$F = \frac{B^2 T}{70} \simeq 3.0 \text{ GHz} \qquad (32)$$

Further consideration may show that the high value of η of 70 is not required, permitting up to 10 GHz to be scanned using this discipline.

Many of the signal sources will be pulsed radar with a low duty cycle. Of course, scanning radars may not be pointing in the direction of the spacecraft antenna when the latter is aimed at the radar. The spatial dwell time of 0.21 seconds would have to be increased to guarantee interception of a slowly rotating radar beam. In addition, if the two antennas, radar and satellite are looking at one another and the satellite receiver is sweeping in frequency, it must pass the radar frequency at the time the radar pulse is emitted in order to be detected. For the sweep rate of 2.86 GHz in 0.21 seconds, discussed above, the time any given frequency is in the 1 MHz passband of the receiver is

$$\frac{0.21 \times 1}{3000} = 70 \ \mu s$$

For a pulse repetition rate of 1000 pps, the probability of detection on a single pass is only about 7% with corresponding results for other repetition rates.

To improve the probability of detection, parallel scanning receivers could be used, the bandwidth could be widened or the antenna aperture made larger, permitting longer dwell times.

For example, with the 1° antenna, a bandwidth of 5 MHz, and 5 parallel channels, 1 GHz could be scanned and still one would be certain to receive at least one pulse from a radar with a pulse rate as low as 200 pps (0.2 seconds, dwell time). A scheme for doing this is described in Appendix I.

d) Measurements Normal to the Earth

In this mode the antenna looks down to earth at the nadir. For h = 250 mi each degree of antenna beamwidth will intercept 4.36 miles of the earth's surface so that for beamwidths ranging from 1.6° to 3.2° (which is the range of beamwidths of a 10 foot dish operating in the range of 2-4 GHz), the distance covered on the ground will range from 7 to 14 miles across. The rate of travel of the spacecraft is about 4.75 miles/s, so that a given point on the ground is covered for 1.47-2.94 seconds. The dwell time here is therefore greater than it is for the circular horizon sweep and it will be possible to do the frequency scanning just as it was proposed for the circular sweep. There is sufficient time, in fact, to do a lateral sweep of several beamwidths.

For a spatial dwell time of 0.21 seconds, discussed in connection with the circular sweep, 7 lateral aperture widths can be covered in 1.47 seconds (corresponding to 1.6° beamwidth) resulting in a total width close to 50 miles. At 3.2° beamwidth, 200 miles could be covered. For this small scanning range mechanical scan should be feasible.

e) Sensitivity

Using the parameter values proposed in paragraphs (c) and (d), the sensitivity of each of the proposed techniques can be obtained from Fig. 22. In the case of horizon scan the parameter ℓ is about 25 miles (40 km) for a 1° aperture. For a receiver sensitivity (kT_eB) of 10^{-14} watts this would provide an $EIRP_{min}$ of about 10^{-2} watts at 3 GHz. For the same antenna in vertical scan, the value of ℓ is 4.36 mi (7 km) with an $EIRP_{min}$ of 5×10^{-4} watts at 3 GHz. Lower receiver bandwidths (here assumed to be 1 MHz) would decrease these levels of $EIRP_{min}$.

To put these results in more specific perspective, estimates of received signal-to-noise ratios are made assuming some typical ground based sources. The calculations assume that the main lobes of the ground and space-borne antennas are lined up. Of course, if the space-borne antenna were to look at side or back lobes, the received signal-to-noise ratio would be smaller. Typical antennas will have main lobe to side lobe ratios of 20 to 40 dB.

(1) Microwave Relay Source

Assume a microwave relay transmitter on the ground operating at 2000 MHz, generating 15 watts over a band of 15 MHz. The antenna is a 10 ft dish and is observed from a spacecraft at 250 mile altitude looking at the horizon. The distance between the two is about 1400 miles. The satellite receiver is assumed to have a bandwidth of 600 kHz, a noise figure of 10 dB, and a 10 ft diameter antenna. Thus:

Power transmitted = 42 dBm
Estimated loss in transmitter feeders = 5 dB
Receiver antenna gain = 34 dB
Transmitter antenna gain = 34 dB
Free space loss = 166 dB
Received power = 42 + 34 + 34 - 5 - 166 = -61 dBm

Received power in 600 kHz band = $-61 + \frac{600}{15{,}000}$ dB = -75 dBm
SNR = -75 - (-106) = 31 dB

Thus, the microwave relay main beam will be readily visible at the spacecraft but the relay may not be seen if an aspect well off axis obtains.

(2) Radar Source

Assume an S-band radar at 3 GHz, generating one microsecond pulses with a peak power of 0.5 MW. The antenna is a 15 ft dish. The spacecraft system is as given in (1) above except that the bandwidth is 5 MHz. The parameters here too are typical; the receiver bandwidth has the value chosen in item (c) above for the IF bandwidth used for observing radar emissions. Thus:

Peak power transmitted = 87 dBm
Estimated transmitter feeder loss = 5 dB
Transmitter antenna gain = 40 dB
Receiver antenna gain = 37 dB
Free space loss = 170 dB
Receiver peak power = 87 + 40 + 37 -5 - 170 = -11 dBm
Noise power = kTBF = -174 + 67 + 10 = 197 dBm
SNR (= peak signal power/noise power) = -11 - (-97) = 86 dB

Suppose that the satellite receiver were to look simultaneously at a microwave relay transmitter generating 10 watts in a 15 MHz band. The source antenna is 10 feet. To the observation being made of the received radar signal, this source would look like an additional gaussian random noise and we will treat it as such. The unwanted received signal power is obtained as follows:

Transmitter power = 40 dBm
Estimated feeder loss = 5 dB
Transmitter antenna gain = 37 dB
Receiver antenna gain = 37 dB

Free space loss = 170 dB
Total received power = 40 + 37 + 37 -5 -170 = -61 dBm
Unwanted received power in 5 MHz band = 61 + (1/3) dB = -66 dBm
SNR (= peak signal power/unwanted power) = -11 -(-66) = 55 dB

Even with a microwave source simultaneously present, the radar signal received will be high. Thus, for measuring radar the output of the receiver circuits should be clipped to eliminate the baseline noise associated with internal noise and with unwanted continuous emissions arriving from the ground.

The emissions from radars off the center frequencies are substantial. As we have seen, the spurious emissions may be as high as 100 watts. Assuming this to be a peak power, one would therefore see 20-87 = -67 dB relative to the center frequency peak power. Assuming no substantial change in antenna gains and space loss at the spurious frequency as compared to the center frequency, the received SNR suffers by 76 dB to give an SNR of about 9 dB. This is not very high, but one would expect to be able to see it above the internal noise.

5.0 ANTENNA SYSTEMS

In the frequency interval 400-1000 MHz the antenna size required to achieve a 3° bandwidth is approximately 15 meters on a side. When looking vertically it would see about 13.2 miles at the low end of the band. For observations of noncoherent urban noise it would be more desirable to see a smaller region, from 3 to 6 miles, in which case the antenna would have to be at least twice as large.

In view of the problem of size and cost of making measurements at the low end of the UHF band, a study has been initiated on means for achieving the required antenna properties as efficiently as possible through the use of arrays.

The conventional approach is to arrange elements over an area with linear dimension as given above with regular spacing, at most, equal to one-half wavelength. For the frequency range given, this means an array with 20 elements on a side or a total of at least 400 elements. An array so constructed is called a filled array. The element spacing of one-half wavelength or less is required if the array is not to have multiple beams of equal gain known as grating lobes.

The number of elements caluclated above may be impractical and alternatives are being sought. One possibility is to randomize the element locations. By destroying the periodicity of element placement the multiple lobes can be made to disappear but the effect is actually one of smearing out all but the main lobe; the peak sidelobe level is decreased but the average remains essentially unchanged.

In addition, if the beam steering feature is also desired, the overall system should include equal numbers of programmable phase-shifters and associated controlling circuits. It is therefore logical to look for other means of implementing this task.

A dramatic reduction in the number of elements for a given performance occurs when the radiation source is spatially incoherent. Use can then be made of the radio version of the Van Cittert-Zernike theorem in optics, which states that the mutual coherence function of the field from a spatially incoherent source is the Fourier transform of the intensity distribution of the source. In addition, the spatial coherence function for such sources is stationary in space.

Antenna elements are so located as to make the set of vector spacings between all possible pairs of elements identical to the set of vectors of uniformly distributed points on a planar surface. With no repetitions in vector spacings, N elements of the actual array can represent N(N-1) points on this surface. To realize a two-dimensional equivalent array, the elements should be located on a T or Y base, with most elements clustered around the junction. Only a few elements have to be located at the farthest points. This fact permits realization of equivalent array sizes far in excess of the actual extent of the spacecraft by placing a few elements on arms stretched out of the spacecraft.

Processing involves multiplication and integration of the outputs of every pair of elements in the array. Signal bandwidths are limited to about 1 MHz. Integration should be performed for about 0.1 seconds, after which the procedure is repeated for the next frequency slot. The output of each integrator represents the real part of the mutual coherence function for the vector spacing concerned. The imaginary part may be obtained by shifting the phase of one antenna output and performing the foregoing steps. The outputs of the integrator matrix may be digitized and transmitted to a storage/processing unit on the space shuttle or on the ground. There is an advantage to sending the raw data to ground because, in this form, it has virtually no redundancy. The intensity and angular distribution of sources within each band of frequencies is obtained by inverse Fourier transforming the mutual coherence coefficients in the space domain.

In practice, one may use IF conversion of antenna pickups which facilitates the phase insertion and multiplication process. If unequal lengths of connecting cables are used between the multipliers and antenna elements, allowance should be made for signal phase-shifts in them.

An interesting feature of this system is its capability of successive elimination of strong sources when trying to map more feeble radiations. The technique is analogous to adaptive nulling in adaptive arrays.

The frequency intervals beyond 1 GHz are adequately covered using relatively small parabolic dishes. Table 17 shows the gain and

beamwidth range for parabolic dishes we may expect to use in the frequency intervals of interest here. (See also Fig. 24) At 1 GHz a beamwidth of 3° actually requires a 20 foot diameter parabolic dish. If indeed such a size is to be used, an unfurlable structure would be required.

Table 17 SUGGESTED ANTENNA CHARACTERISTICS

Frequency Range, GHz	Parabolic Antenna Diameter (Ft.)	Beamwidth Range	Gain Range (dB)*
1-2	10	3.2° - 6.4°	27.5 - 33.5
2-4	10	1.6° - 3.2°	33.5 - 39.5
4-8	10	0.8° - 1.6°	39.5 - 45.5
4-8	5	1.6° - 3.2°	33.5 - 39.5
8-16	10	0.4° - 0.8°	45.5 - 51.5
8-16	5	0.8° - 1.6°	39.5 - 45.5
16-40	2.5	0.65° - 1.6°	39.5 - 47.5

* dB above an isotropic radiator with 0.54 efficiency

Current thinking is that the antenna diameter should be limited to 10 feet even in the 1 to 2 GHz interval. The sacrifice in resolution does not appear to be critical. At the low end of this band, one sees the long range radar systems which are widely dispersed geographically. Furthermore, antenna gain is hardly an important consideration for these systems. At the upper end of this band the beamwidth will be close to 3°, giving the desired resolution to the lower powered inhabitants of this region.

The 400-1000 MHz antenna system, if it is indeed to be a processed array, will be fixed in position, and beam positioning would be done as part of the processing operation. For the frequencies above 1 GHz where the parabolic dish is proposed, scanning and positioning may be done

electronically using multiple feeds, or it may be done with fixed feeds positioning the entire antenna. Since one mode of proposed operation involves 360° rotation of the beam, it appears reasonable to recommend a mechanical positioning system in which the entire antenna is moved. As envisioned now most of the data would be collected with the antenna (a) stationary and nadir looking, and (b) with the antenna looking to the horizon and rotating. In order to cover more territory in the nadir position, it is desirable to incorporate a scanning capability perpendicular to the direction of motion, as discussed in par. 4.3.2 (d).

In addition, it would be useful to incorporate a manual pointing facility which will enable the astronaut to focus on a source and follow it as the satellite passes by. In this way, partial radiation patterns of sources would be measured, providing a basis for extrapolating measurements in space to levels observed in aircraft, and perhaps on the ground as well.

Polarization of the sources being measured has been mentioned in earlier experimental proposals as information worth obtaining. The justification has not yet been explored, but it is reasonable at this stage to ask that the antenna be designed to respond to orthogonal linearly polarized waves and to incorporate combiners which will make the antenna circularly polarized in either sense.

6.0 PROBABILITY OF DETECTING AN EARTHBOUND EMITTER

The following sections consider a rotating receiver similar to the one proposed in our preliminary report. The probability that a satellite receiver will detect a transmitter on earth depends upon properties of the satellite's orbit and the antenna characteristics of both satellite and transmitter. We will first determine how often the receiver looks at a particular point on the earth's surface and then determine the probability that is actually will detect a tranmitter at which it is looking.

6.1 Coverage

6.1.1 As a Function of Latitude and Orbital Inclination

Consider a satellite circling the earth in an orbit inclined to the equator. At any particular time the satellite can see any point

on the earth's surface between its nadir point and the horizon. If the earth did not turn, the swath covered on a single orbit of the satellite would be the set of points on the earth's surface which lie between two planes equidistant from and parallel to the plane in which the satellite rotates. Thus, if the satellite followed the equator, the swath would be the area between two corresponding lines of latitude to the north and south.

Now let the earth rotate under the satellite at a rate of one revolution/24 hrs., or 15 degrees/hr. = 0.00416 degrees/s. If the satellite has a period of 90 minutes, each point on the swath of a second orbit will be displaced 22.5° of longitude from the corresponding point on the swath of the first orbit. But at higher latitudes, a degree of longitude represents a smaller distance than at low latitudes. Since the width of swath is constant and the displacement decreases with latitude at higher latitudes successive orbits overlap one another more and more.

In general, the satellite will see a given point n times on any set of successive passes, where n is a function of the latitude of the point and the angle of inclination of the orbit. The following calculations determine that function explicitly.

The swath width in degrees of longitude (angle $\overline{A_N P B_S}$ in Fig. 33) can be expressed as a function of latitude (arc $A_N E$). The location of point A_N is determined when the satellite is at point A and the location of B_S is determined when the satellite is at point B. We need relationships giving LONG $(A_N) = \angle \overline{OPA_N}$ in terms of LAT(A_N) = arc $\overline{A_N E}$ and LONG$(B_S) = \angle OPB_S$ in terms of LAT(B_S) = arc $B_S E$.

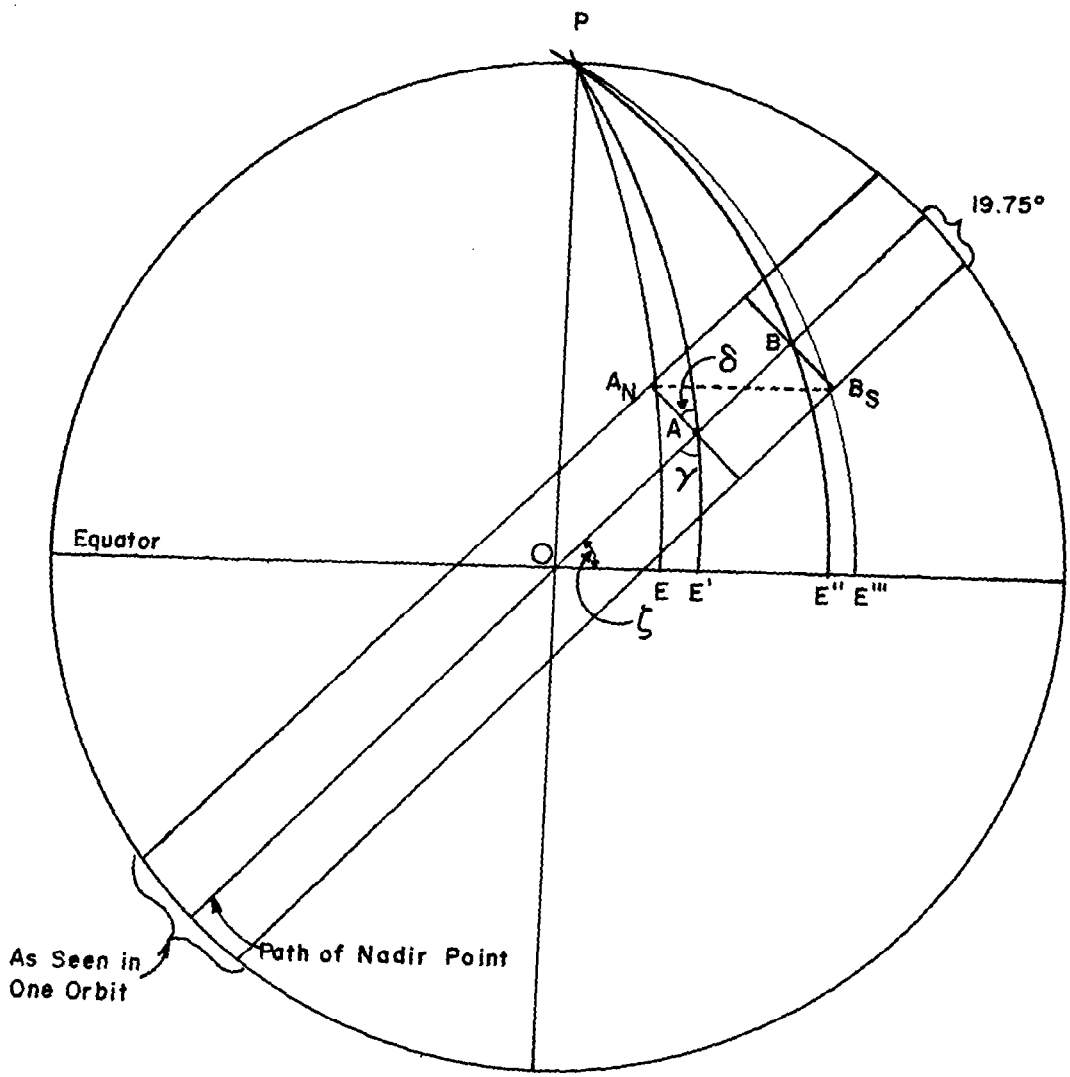

Figure 33 Longitudinal Width of the Swath as a Function of Latitude

Assume temporarily that the earth is not rotating. Let the satellite follow an orbit of inclination ζ, and let ν equal the constant arc $\overline{A_N A}$. In Fig. 33, P is the earth's pole and the line $O\overline{EE'}$... is the equator. Let the constants

$$k_1 = \cos \nu \qquad k_3 = \cos \zeta$$

$$k_2 = \sin \nu \qquad k_4 = \sin \zeta$$

By spherical trigonometry,

$$\text{LAT}(A) = \arctan \left[\frac{k_4}{k_3} \sin [\text{LONG}(A)] \right] \tag{33}$$

and conversely

$$\text{LONG}(A) = \arcsin \left[\frac{k_3}{k_4} \tan [\text{LAT}(A)] \right] \tag{34}$$

The included angle

$$\gamma = \angle OAE' = \arcsin \left[k_4 \left(\frac{\sin (\text{LONG}(A))}{\sin (\text{LAT}(A)} \right) \right]$$

$$= \arcsin \left[\frac{k_3}{\cos[\text{LAT}(A)]} \right].$$

$$\delta = \angle \overline{A_n AP} = 90^\circ - \gamma$$

$$\cos (\delta) = \frac{k_3}{\cos[\text{LAT}(A)]} \tag{35}$$

and

$$\sin (\delta) = \cos \left(\arcsin \left[\frac{k_3}{\cos(\text{LAT}(A))} \right] \right) \tag{36}$$

Since

$$\text{LAT}(A_N) = 90^\circ - \text{arc } A_N P = 90^\circ - \arccos [k_1 \sin[\text{LAT}(A)] + k_2 k_3]$$

therefore

$$\text{LAT}(A) = \arcsin \left\{ \frac{1}{k_1} \left(\sin \left[\text{LAT}(A_N) \right] - k_2 k_3 \right) \right\} \tag{37}$$

Expression (37) gives the latitude of point A as a function of the latitude of point A_N. To determine the longitude of point A_N in terms of its latitude, note that

$$\text{LONG}(A_N) = \text{LONG}(A) - \angle \overline{A_N PA}$$

Substituting (34) for the first term and using a trigonometric identity to determine the second gives,

$$\text{LONG}(A_N) = \arcsin\left[\frac{k_3}{k_4} \tan\left[\text{LAT}(A)\right]\right]$$

$$- \text{arc cot}\left[\frac{\frac{k_1}{k_2} \sin\left(90^\circ - \text{LAT}(A)\right) - \frac{k_3 \cos\left(90^\circ - \text{LAT}(A)\right)}{\cos(\text{LAT}(A))}}{\sin(\delta)}\right]$$

Substituting (37) for LAT(A) and defining the new variable

$$V_N = \frac{1}{k_1}\left[\sin\left(\text{LAT}(A_N)\right) - k_2 k_3\right]$$

gives

$$\text{LONG}(A_N) = \frac{k_3}{k_4} \frac{V_N}{\cos(\arcsin(V_N))}$$

$$- \arctan\left[\frac{k_2 \cos\left(\arcsin\left[\frac{k_3}{\cos(\arcsin[V_N])}\right]\right)}{k_1 \arcsin(V_N) - \frac{k_2 k_3 V_N}{\cos(\arcsin(V_N))}}\right] \qquad (38)$$

A similar line of reasoning gives for B_s,

$$\text{LONG}\,[B_s] = \arcsin\left[\frac{k_3}{k_4}\,\frac{V_s}{\cos(\arcsin V_s)}\right]$$

$$+\arctan\left[\frac{k_2 \cos \text{ arc sin } \left[\dfrac{k_3}{\cos(\arcsin (V_s))}\right]}{k_1 \cos\,(\arcsin(V_s)) + \dfrac{k_2 k_3 V_s}{\cos\,[\arcsin\,(V_s)]}}\right] \qquad (39)$$

where

$$V_s = \frac{1}{k_1}\,[\sin\,(\text{LAT}(B_s)) + k_2 k_3]$$

Now it is necessary to take into account the earth's rotation. Since the rate of the earth's rotation and the speed of the satellite are both constant, the longitudinal displacement of a point A_N is proportional to the length of the arc OA; similarly, the displacement of B_s is proportional to OB.

$$\text{The displacement of } A_N = \frac{OA}{360^\circ} \quad X \quad \frac{360^\circ}{\text{day}} \quad X \text{ period (in days)}$$

But from spherical trigonometry

$$OA = \arcsin\,\frac{\sin AE'}{\sin \zeta}$$

In terms of the latitude of A_N this is

$$OA = \arcsin\,\frac{V_N}{k_4} \qquad (40)$$

and in terms of the latitude of B_s it is

$$OA = \arcsin\,\frac{V_s}{k_4} \qquad (41)$$

Thus

$$\text{LONG}\,(A_N) = (38) \;-\; (40)$$

and

$$\text{LONG}\,(B_s) = (39) \;-\; (41).$$

Subtracting (40) from (41) gives the difference in longitude,

$$\text{width} = \arcsin\left[\frac{k_3}{k_4}\ \frac{V_s}{\arccos V_s}\right]$$

$$+ \arctan\left[\frac{k_2 \cos\left(\arcsin\left[\frac{k_3}{\cos \arcsin (V_s)}\right]\right)}{k_1 \cos[\arcsin (V_s)] + k_2 k_3 \left(\frac{V_s}{\cos[\arcsin(V_s)]}\right)}\right]$$

$$- \text{period} \cdot \arcsin\left[\frac{V_s}{k_4}\right]$$

$$- \arcsin\left[\frac{k_3 V_N}{k_4 \cos[\arcsin(V_N)]}\right]$$

$$+ \arctan\left[\frac{k_2 \cos\left(\arcsin\left[\frac{k_3}{\cos[\arcsin (V_N)]}\right]\right)}{k_1 \cos[\arcsin(V_N)] + k_2 k_2\left(\frac{V_N}{\cos[\arcsin(V_N)]}\right)}\right]$$

$$+ \text{period} \cdot \arcsin\left[\frac{V_N}{k_4}\right] \qquad (42)$$

Computer calculations of width as a function of latitude for various orbital inclinations led to the data plotted in Fig. 34. Note that maximum swath width occurs at a latitude equal in degrees to the orbital inclination angle ζ minus the coverage angle ν.

6.1.2 Number of Times Seen--Successive Swaths

We can now calculate the number of times a point at a given latitude is likely to be seen in a consecutive set of orbits.

Consider a line segment of length w which is continually displaced along the X-axis in steps of length d (Fig. 35). If $d \geq w$, the probability P[1] that a point on the axis is covered exactly once by the line segment is $\frac{w}{d}$. The probability P[1+] that it is covered more than once is 0. If $d \leq w < 2d$, the probability that a point on X will not be covered at all is zero and the probability that it will be covered more than twice is zero. The probability P[2] that it will be covered exactly

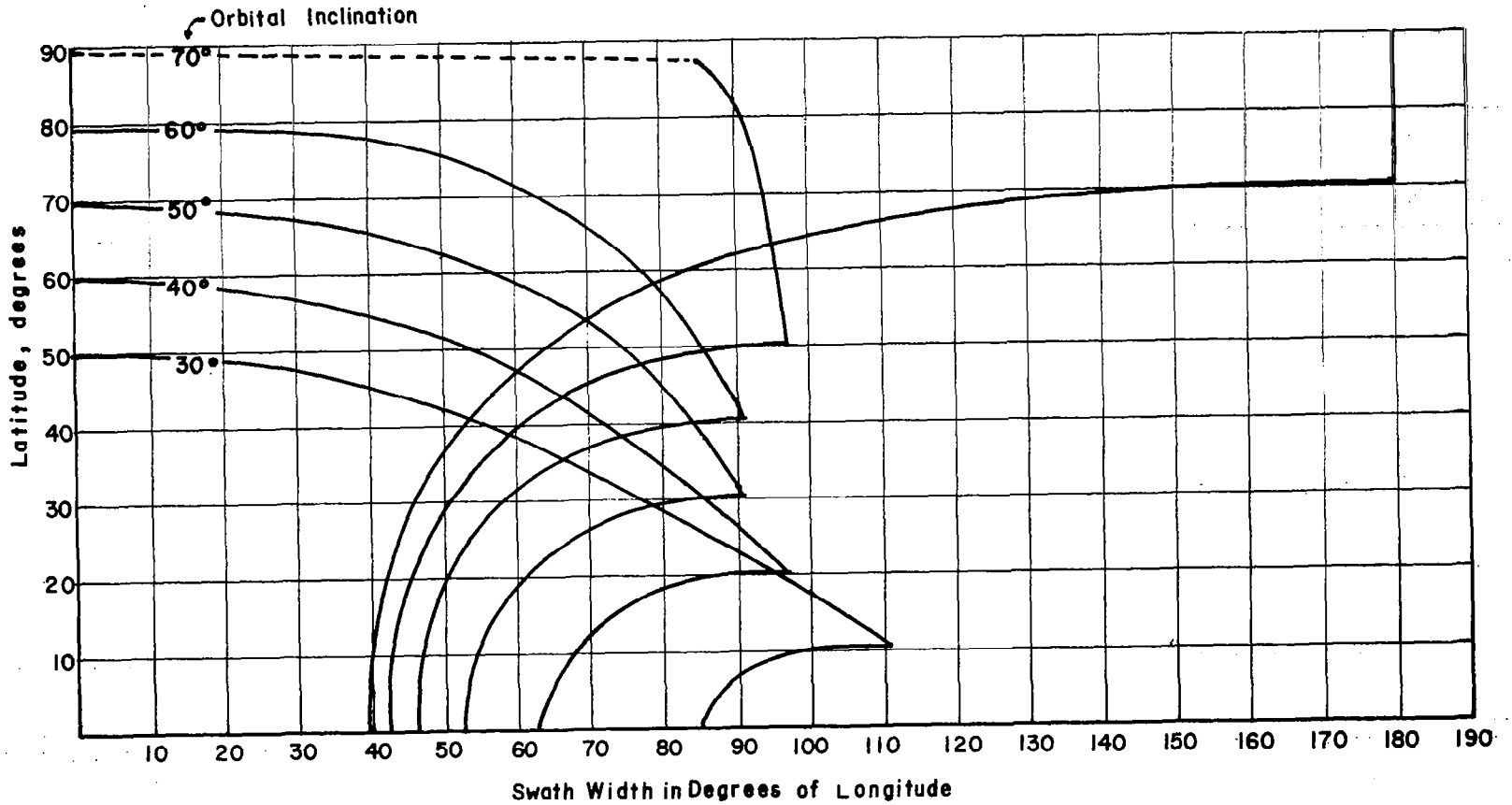

Figure 34 Swath Width as a Function of Latitude for Various Orbital Inclinations

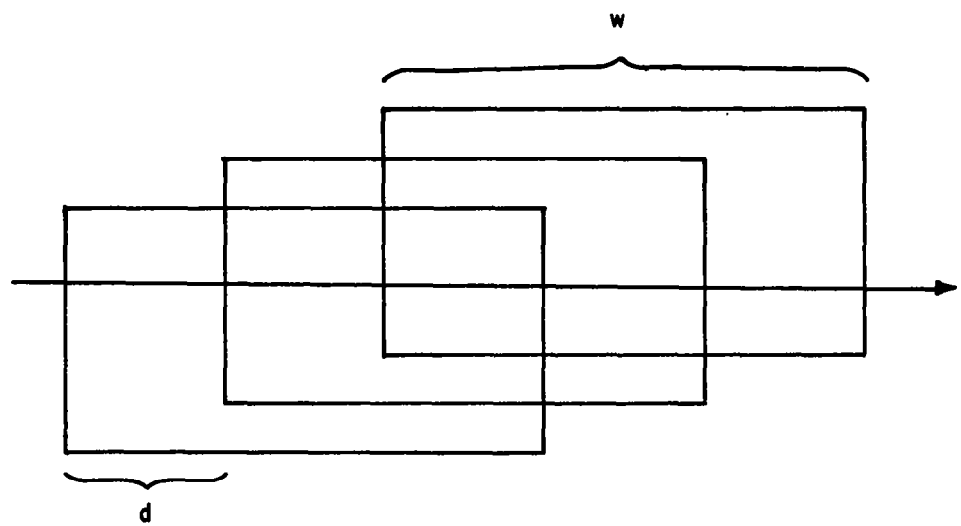

Figure 35 An Area of Width w Continually Being Displaced Along an Axis in Steps of Length d

twice is $\frac{w-d}{d}$, and the probability P[1] that it will be seen exactly once is therefore $1 - \frac{w-d}{d} = \frac{2d-w}{d}$.

Generalizing,

$$\begin{aligned} &\text{If} \quad |w - nd| > 1 && P[n] = 0 \\ &\text{If} \quad -1 \leqslant (w - nd) < 0 && P[n] = \frac{w - (n-1)d}{d} \\ &\qquad 0 \leqslant (w - nd) \leqslant 1 && P[n] = \frac{(n+1)\,d - w}{d} \end{aligned} \tag{43}$$

or

$$\begin{aligned} &\text{If} \quad n < \text{Int}\left[\frac{w}{d}\right] && \text{then} \quad P[n \leqslant] = 1 \\ &\qquad n = \text{Int}\left[\frac{w}{d}\right] + 1 && P[n \leqslant] = \frac{w - (n-1)d}{d} \\ &\qquad n > \text{Int}\left[\frac{w}{d}\right] + 1 && P[n \leqslant] = 0 \end{aligned} \tag{44}$$

where $P[n \leqslant]$ is the probability that a point will be covered at least n times.

These results can be applied to the data presented in figure 34. Let $d = \frac{\text{period}}{24 \text{ hr.}} \times 360^{\circ} \approx 23.25^{\circ}$ (for a 93 min orbit) and

w = Width (LAT)

Figure 36 shows the probability that a point at latitude L will be covered at least n times by successive swaths of a satellite in a 250 mile, 50° orbit.

6.1.3 Number of Times Seen - Single Orbit

If the satellite antenna rotates as the satellite progresses in its orbit, we can once more apply (44) to approximately determine the probability that a point within the swath of the satellite will be seen by the main beam of the receiver at least n times in a single pass of the satellite. We will approximate the cycloidal path swept out by the main beam by a series of annuli. The displacement d of each annulus from the preceding one is equal to the thickness of the annulus. The width w of the annulus in a direction parallel to the direction of motion at a distance x from the path of the nadir point is

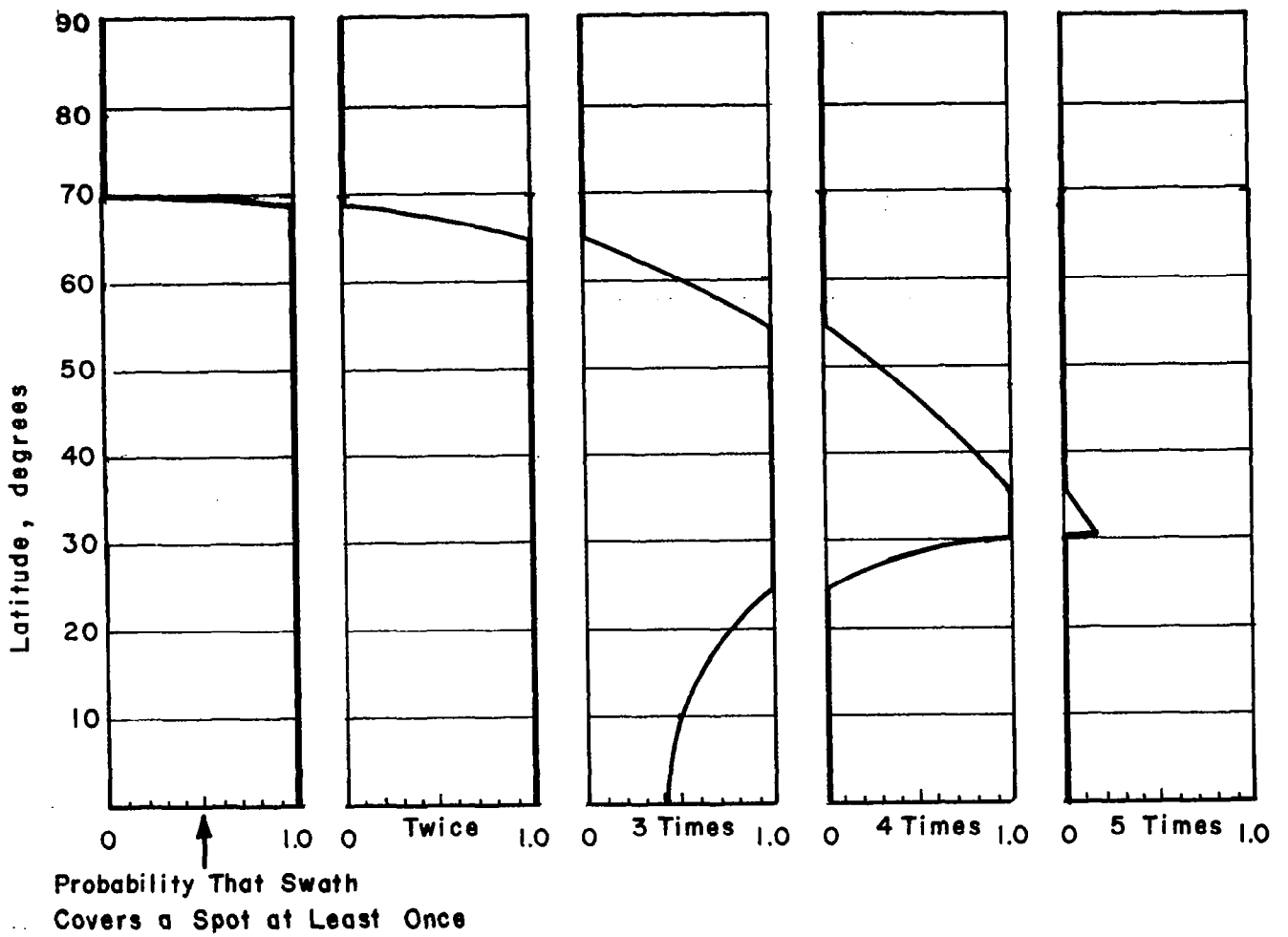

Figure 36 Probability of Multiple Sucessive Coverings by the Swath of a Satellite in a 250 mi 50° Orbit (Example: A point on the Earth's surface will never be covered three times by the satellite's swath if the point lies above the 65th parallel, and it will always be covered at least three times if it lies between the 24th and 54th parallels. There is a 50% chance that a point at a latitude of 10° (N or S) would be seen at least three times.)

$$w = 2\left(\sqrt{r^2 - x^2} - \sqrt{(r - d)^2 - x^2}\right) \quad \text{when } x < (r-d)$$

$$w = 2\sqrt{r^2 - x^2} \quad \text{when } (r-d) < x \leq r$$

$$w = 0 \quad \text{when } x > r$$

where r is the radius of the outside edge of the annulus. Fig 37 shows w as a function of x for the case where r = 2600 km and d = 816 km. This corresponds to a satellite in a 400 km (250 mi) orbit using an antenna with a 2^{o} vertical beamwidth.

As the figure shows, most (about 95%) of the swath is seen at least twice on each orbit. And recalling figure 34, note that all points except those at very high latitudes are covered at least twice by successive swaths.

Finally, note that these successive sets of swaths cover a given point twice a day: once when the satellite is ascending, and once when the satellite is descending. Thus, such a satellite would look at most of the points covered by its path at least eight times a day, and it would see points in the mid-latitude many more times.

6.2 Probability to Detect a Transmitter in the Main Beam

Let us now determine the probability that a receiver looking directly at a directional transmitter will see its main beam.

Assume initially that both the transmitter and receiver have no sidelobes or backlobes, and that there is a sharp cut-off at the edge of the main beam. There are two cases of interest: a fixed transmitter and a rotating transmitter.

Case I: Fixed Orientation
Example: common carrier transmitter

Assumptions:

1. The transmitter is within the beam of the satellite.
2. The transmitter has no sidelobes or backlobes.
3. The orientations of the transmitters are randomly distributed.
4. The center of the transmitter's mainbeam is directed along the tangent to the earth's surface.
5. Vertical and horizontal beamwidth of the transmitter are the same.

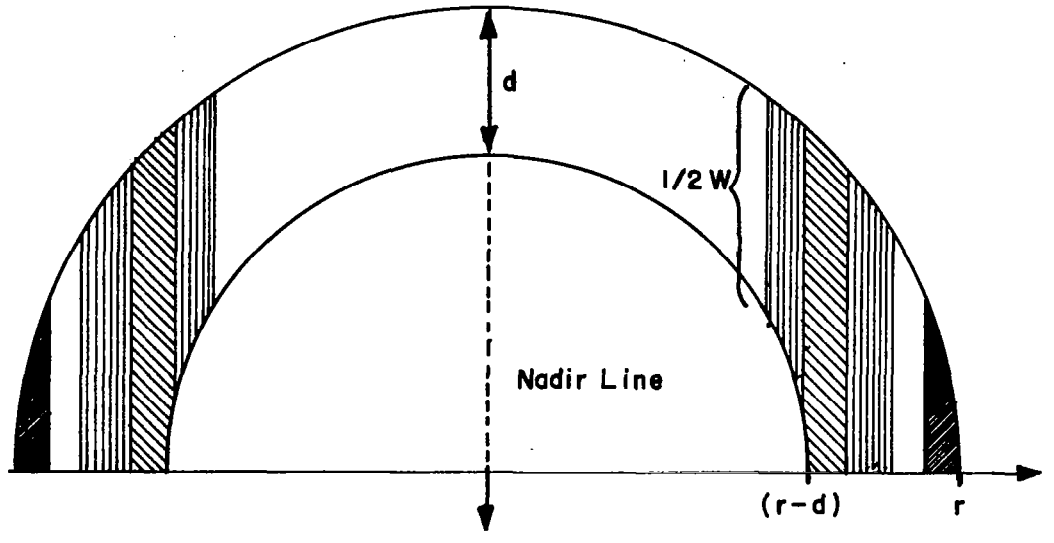

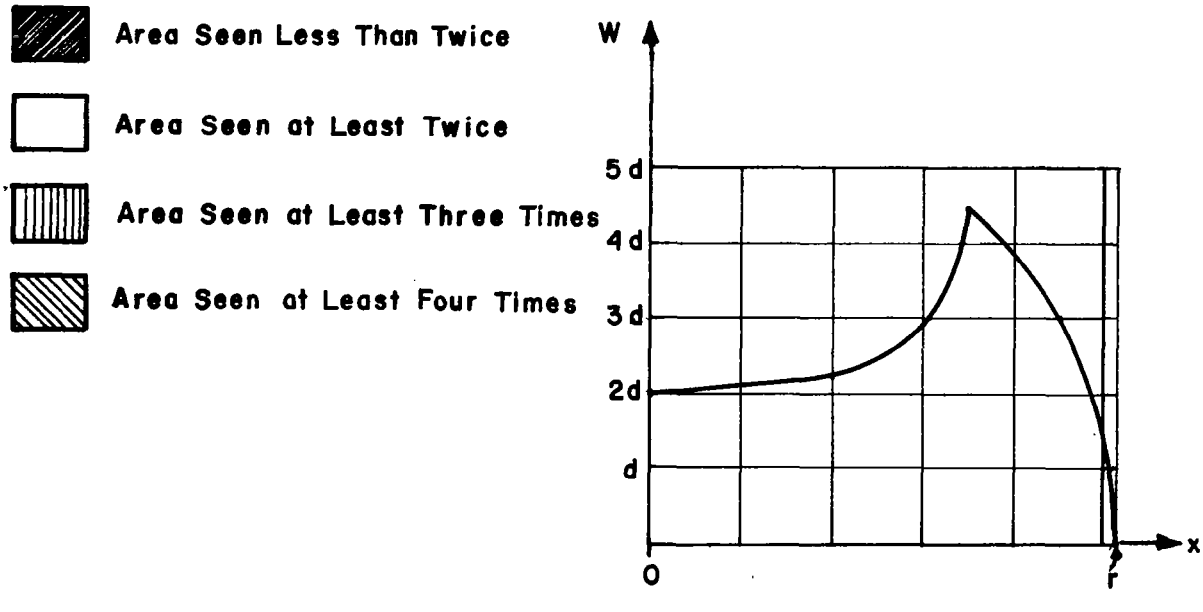

Figure 37 Coverage Within a Swath as a Function of Displacement, x, from the Nadir Line. d is the distance between successive annuli, and W is the width of the annulus along a line parallel to the direction of motion.

Calculations: The probability that the satellite will see an emitter within its footprint is equal to the probability that the beam of the emitter will hit the satellite. Since the beam must point in the proper direction in both the vertical and horizontal planes,

$$P_t = P_v \times P_h$$

where

P_t is the total probability of detecting the transmitter

P_h is the probability that the transmitter points at the receiver in the horizontal plane, and

P_v is the probability that it points at the receiver in the vertical plane

Let φ_h = the horizontal beamwidth of the emitter [if a given tower can transmit in two directions we can multiply P_h by 2].

Then,

$$P_h = \frac{\varphi_h}{360^\circ} \qquad (45)$$

Values of P_h are given in Table 18.

Table 18. Probability of Seeing a Transmitter Randomly Oriented in the Horizontal Plane as a Function of Horizontal Beamwidth.

φ_h	P_h	φ_h	P_h	φ_h	P_h
1°	0.00277	3°	0.008333	6°	0.01666
2°	0.00555	4°	0.01111	8°	0.02222
				10°	0.02777

As Fig. 38(a) shows, it is possible for the receiver to be out of the main beam of the transmitter in the vertical plane even though the transmitter is in the main beam of the receiver and the receiver is in the transmitter's main beam in the horizontal plane. If, in Fig. 38(b) the trapezoid acdf is the total area seen by the receiver at a given instant and abed is the area over which the transmitter's main beam will hit the receiver,

$$P_v = \frac{abef}{acdf} = \frac{[A + B + 2\,(x-y)\tan(\frac{\alpha}{2})\,y}{[A + B]\,x} \approx \frac{y}{x} \qquad (46)$$

where

$$y = \frac{\beta}{360^\circ\ 8000\ \pi}\ (\text{Miles}) = \frac{\beta}{360^\circ\ 12{,}800\ \pi}\ (\text{km}) \qquad (47)$$

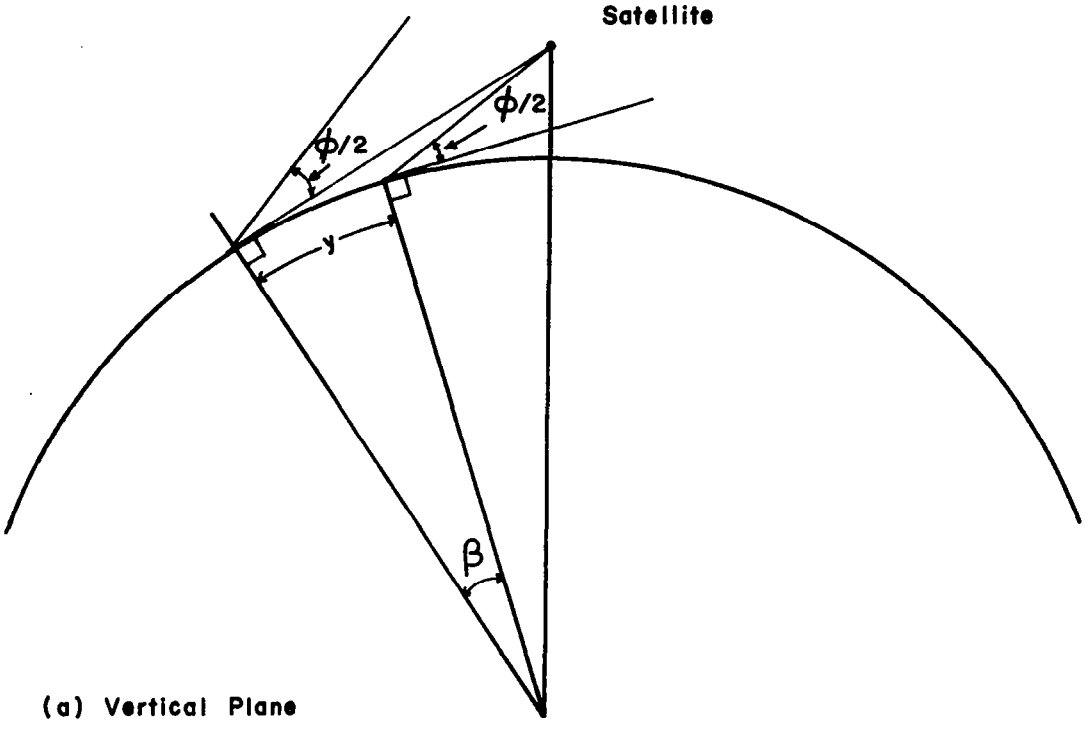

(a) Vertical Plane

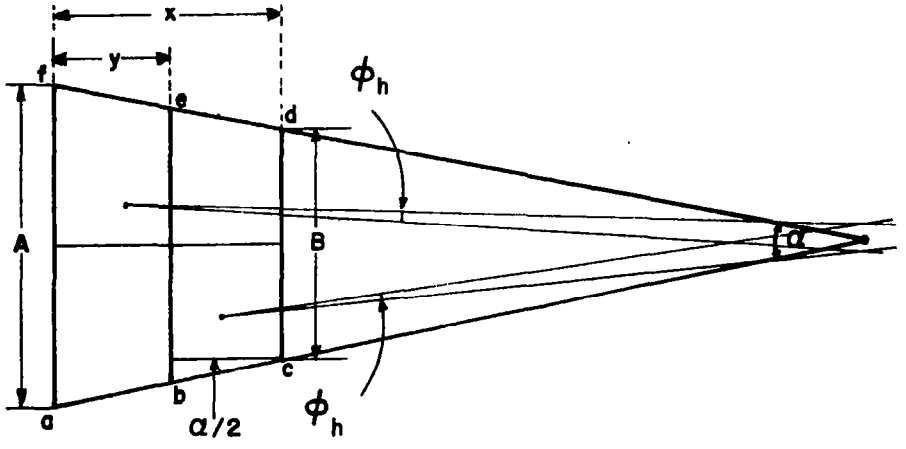

(b) Horizontal Plane

acdf = Area Within Beam of Satellite [A Function of α]

abef = Area Where $(\delta - \frac{\pi}{2}) < \frac{\phi}{2}$ [A Function of ϕ and α]

Figure 38 Ways in Which the Main Beam of a Transmitter Within the Footprint of the Receiver Might Intercept the Receiver

and

$$\beta = -70.25 + \frac{\varphi_v}{2} + \arcsin\left[\frac{r}{r+h}\sin(90^\circ + \varphi_v/2)\right] \qquad (48)$$

For various values of $\varphi_v/2$, relations (47) and (48) yield the values in Table 19.

Table 19. Depth of Area in which the Transmitter Can Be Seen as a Function of Transmitter Vertical Beamwidth.

$\frac{\varphi}{2}$	β	y	
1°	0.97	68 mi	= 109 km
2°	1.916	134 mi	= 215 km
3°	2.766	193 mi	= 310 km
4°	3.616	252 mi	= 405 km
5°	4.383	306 mi	= 492 km

The total probablility of detecting a transmitter within the footprint of the receiver's main beam is

$$P_t = P_h \times P_v \qquad (49)$$

This is a function of φ_h and φ_v, the horizontal and vertical beamwidths of the emitter. If $\varphi_h = \varphi_v = \varphi$ and the satellite has a footprint 480 km (300 miles) long, the following probabilities shown in Table 20 result.

Table 20. Probability of Detecting a Fixed Transmitter as a Function of Transmitter Beamwidth.

φ	P_h	P_v	P_t
1°	0.0277		
2°	0.00555	0.2266	0.00126
4°	0.01111	0.4466	0.00496
6°	0.01666	0.6433	0.01072
8°	0.0222	0.8400	0.01866
10°	0.02777	1	0.02777

Case II: Rotating Transmitter
Example: Beacon Radar

Beamwidth: Horizontal 4°; vertical 30°.
Rotation Rate: 14 rpm = .233 rps = $83.88^\circ/s$
prf: 350 pps or one pulse every 2.8 ms

Calculations: Assume that the radar is within the beam of the satellite. Since most radars have broad vertical beamwidths, we w assume that a pulse emitted anywhere within the footprint of the s can hit the receiver. To see the radar, the receiver must be look at the proper frequency while the radar is looking at the satellite and emitting a pulse. Thus,

$$P_t = P[\text{radar looks at satellite w/in freq.window}] \times P\begin{bmatrix}\text{radar emits a pulse} \\ \text{w/in freq. window}\end{bmatrix}$$

$$= \frac{\#\text{ of degrees swept by radar in freq. dwell time}}{360^\circ} \cdot \frac{\text{freq. dwell time}}{\text{time between successive pulses}}$$

If the frequency dwell time is greater than the time between successive pulses, set the second factor equal to one. Thus,for a frequency dwell time of 5 ms

$$P_t = \frac{(83.88 \times .005) + 4^\circ}{360^\circ}$$

$$= 0.01227$$

Example 2: Long Range Radar

Beamwidth: Horizontal 1.5°; vertical $5\text{-}30^\circ$
Rotation Rate: 5 rpm = $30^\circ/s$
prf: 350-370 pps = one pulse every 2.8 ms
Pulse duration: 2 us

$$P_t = \frac{(.005 \times 30) + 1.5}{360^\circ} \times 1 = 0.0046$$

6.3 The Effect of Sidelobes

As these examples show, the probability of the mainbeam of a transmitter encountering the mainbeam of a receiver is rather low, even if we take into account the fact that the receiver may look at the same transmitter eight or more times per day.

But the treatment above is a gross simplification. For real antennas, the gain rolls off gradually, as the off-axis angle increase instead of falling off to zero immediately outside the main beam. The

so-called main beam is just the angle within which the gain is within 3 dB [sometimes 10 dB] of the gain along the axis of the antenna, and a receiver may see a signal from the transmitter even though neither is in the main beam of the other. Now, for the receiver to see the transmitter, we must have

$$S_r > P_t + G_t + G_R - \text{free space loss} - k.$$

S_r is the receiver sensitivity in dBm,

P_t is the transmitter power in dBm

G_r and G_t are the gains in dB of the receiving and transmitting antenna respectively and k is a constant lumping together such things as feed losses and desired signal-to-noise ratio.

Thus, for a given transmitter and receiver at a fixed distance, the receiver will detect the transmitter if and only if $G_t + G_r >$ some constant k_2, where G_t and G_r are both functions of the off-axis angles φ_t and φ_r respectively.

Figure 39 shows the gain patterns of two typical parabolic dish antennas and Fig. 40 shows a plot of φ_t vs φ_r at various values of of the gain product $[G_t + G_r]$ for the same pair of antennas. If the transmitter and receiver are oriented at random, for a given value of k_2 the probability P_D that the receiver will detect the transmitter is equal to the probability that a point $(\varphi_t \varphi_r)$ chosen at random lies to the left of the appropriate contour line. This is equal to the ratio

$$P_D = \frac{A_c}{A_{180}}$$

where A_c is the area under the contour and A_{180} is the total area of the rectangle bounded by the lines $\varphi_t = 0$, $\varphi_t = 180^o$, $\varphi_r = 0$, and $\varphi_r = 180^o$.

If the receiver does detect the transmitter, the probability P_ψ that the transmitter is within an angle ψ of the axis of the receiver is

$$P_\psi = \frac{A_{\psi c}}{A_c}$$

where $A_{\psi c}$ is the area under the contour C and to the left of the line $\varphi_T = \psi$.

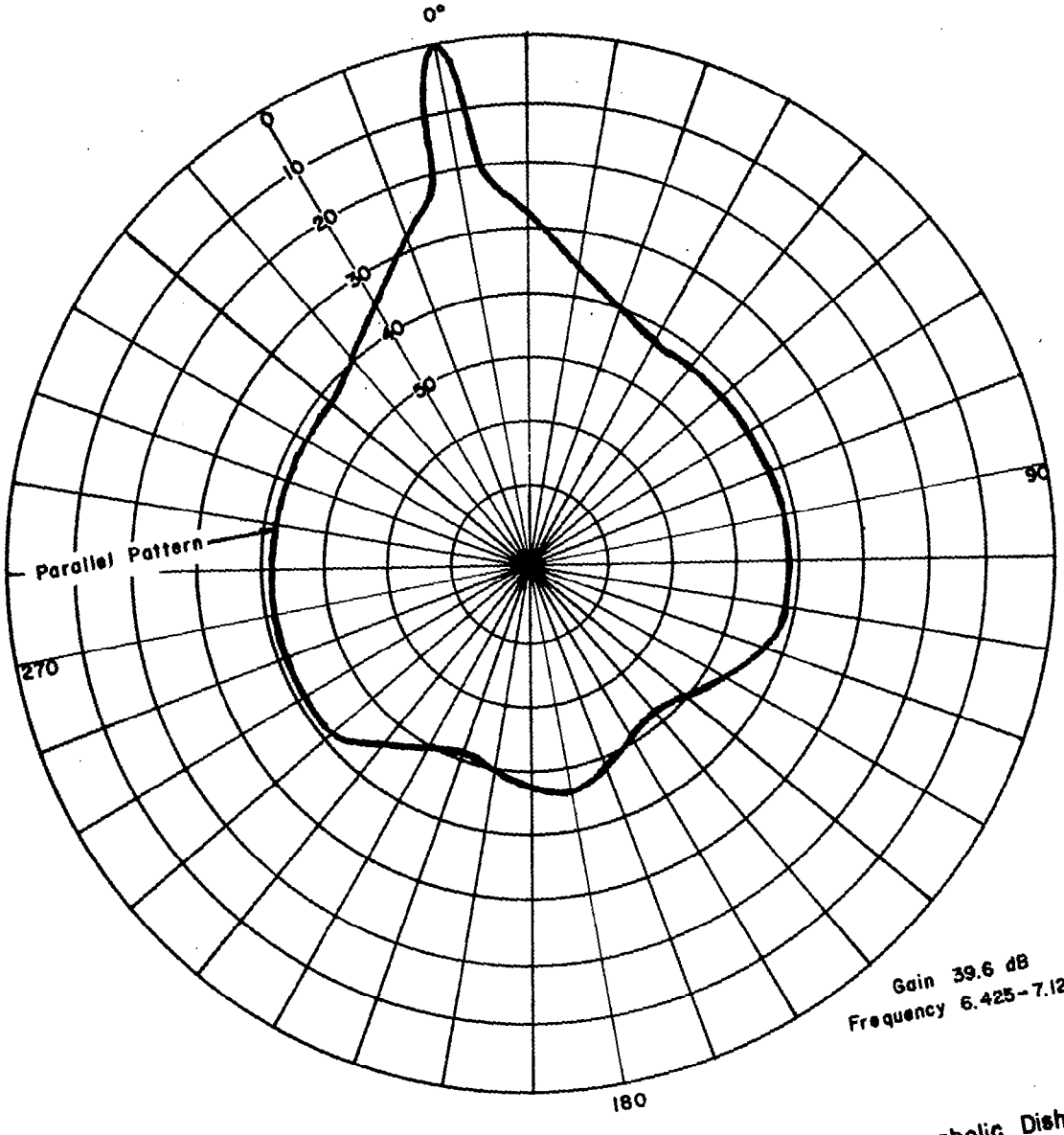

Figure 39(a) Smoothed Out Gain Pattern of a Typical Parabolic Dish: 6-ft. Prodelin Model 163-740

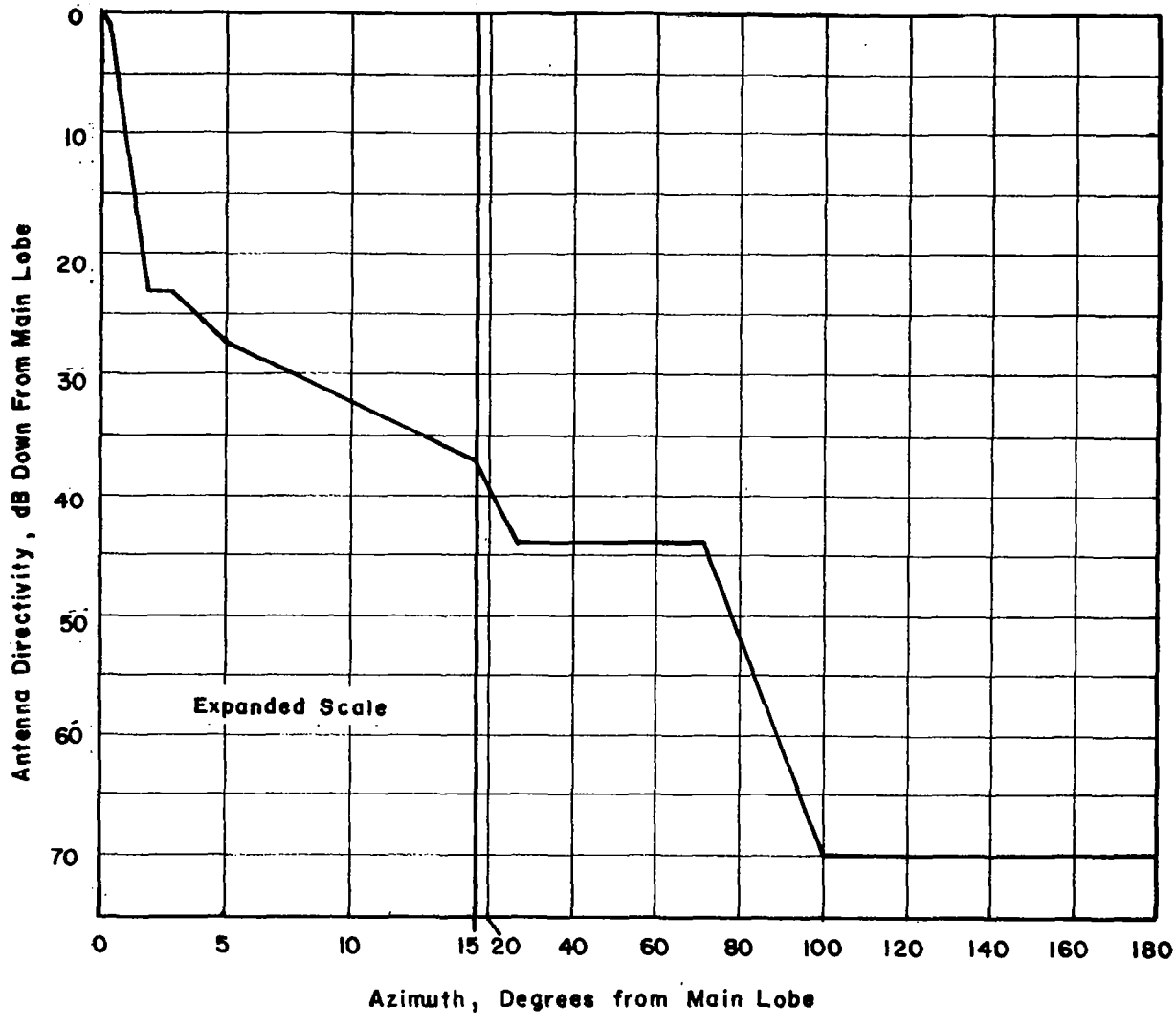

Gain = 44.1 dBi at 6.775 GHz

Figure 39 (b) Smoothed Out Gain Pattern of a Typical Parabolic Dish: 10-ft. Prodelin Model 165-700

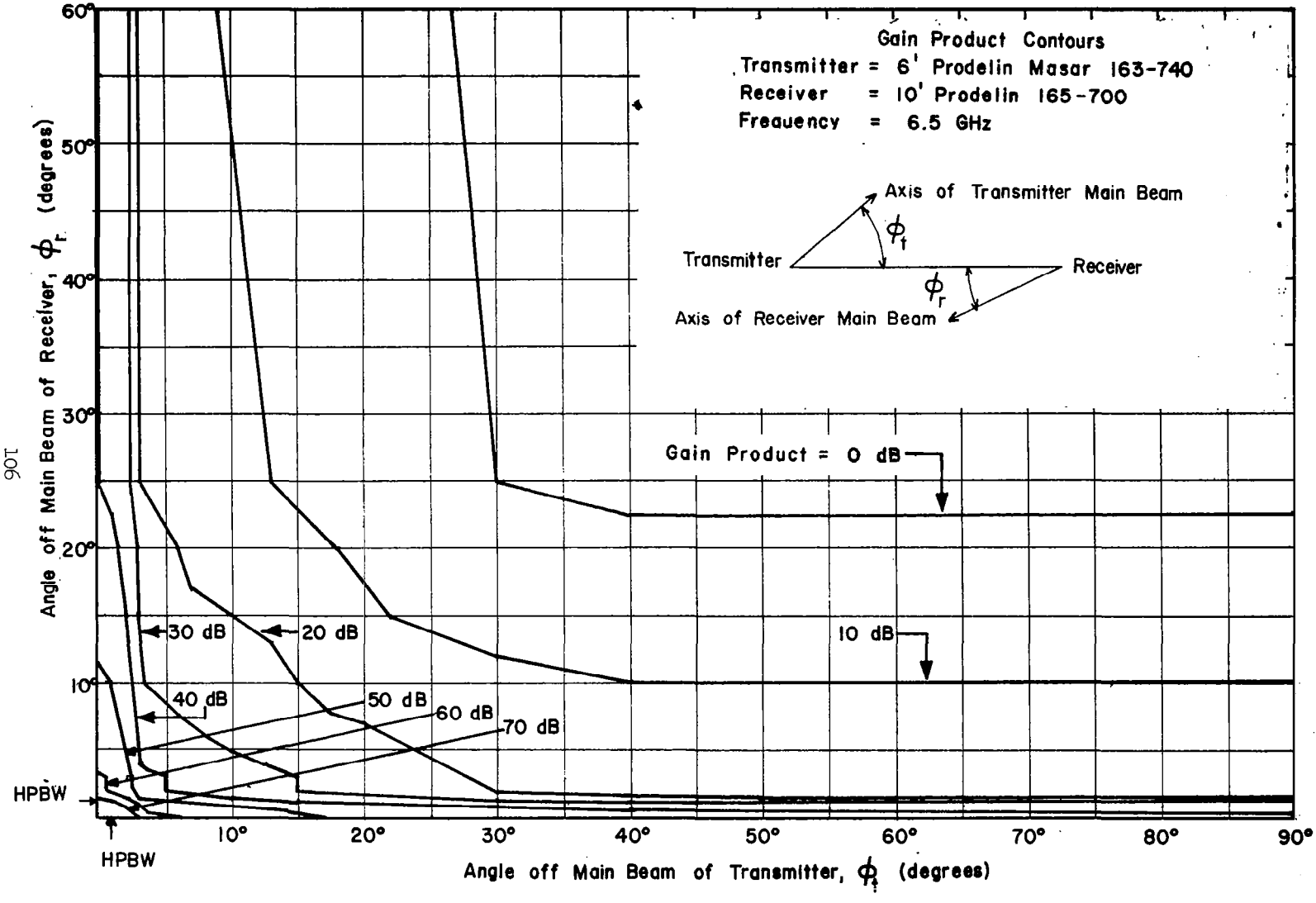

Figure 40 ϕ_t Versus ϕ_r at Various Values of the Gain Product $[G_t + G_r]$

Signals can be received by an antenna from an object not in the main beam at any given time because of the antenna's finite response in other directions. Indeed, the antenna will respond at least as well to a source out of the beam as it will to one in the beam if the ratio of their EIRP's is greater than the inverse ratio of the antenna's gains in the direction of the two sources. Thus, a sufficiently strong source may be detected regardless of pointing direction of the antenna.

6.3.1 Quantitative Estimate

In Appendix II an analysis is presented of the probability density function of the received signal power assuming a source located at random in the visible area under the satellite and assuming various conditions of antenna main-lobe and side-lobe gain. In addition, the groundwork is laid for accounting for multiple sources on the ground. In order to demonstrate the significance of the side-lobe leakage problem more clearly, the targets of a given type are assumed to be randomly located over the earth's surface with average densities as given in Table 21. Similarly, since antenna gain patterns are somewhat irregular, they also may be treated in a statistical sense. To simplify the analysis, a 360° planar pattern is assumed rather than a 4π radian (spherical) pattern. The approximation is not considered too serious because: (1) if a 4π radian pattern were used, perhaps as much as 2/3 of the total solid angle of the satellite antenna contains no targets since that portion looks into space, and (2) with a one degree beamwidth pointed at the horizon almost half of the area on the ground is covered in one rotation of the main beam. For the purpose of obtaining order of magnitude estimates, this accuracy is considered to be usable.

Typical gain distribution data are given in Fig. 41 for antennas having maximum gains of 10, 20, 30, and 45 dB. These are smoothed curves representing typical antenna pattern data such as given in Ref. 41. Actual antenna patterns will be less smooth, but the curves shown are considered to be reasonably representative. Using these curves and average density data, the curves shown on Fig. 42 can be derived. The curves show the expected number of targets detected by the spacecraft as a function of effective satellite receiver system sensitivity, $EIRP_{eff}$. These curves are derived as follows.

Let the maximum gains of satellite and target antennas be respectively $G_{S\ max}$ and $G_{T\ max}$. Likewise the minimum gains are $G_{S\ min}$ and $G_{T\ min}$. The maximum effective value of the EIRP is then

$$EIRP_{max} = P_o + G_{T\ max} \qquad (50)$$

where P_o is the power output of the target.

$EIRP_{max}$ specifies the sensitivity of the satellite receiver (when corrected for space loss and maximum receiver antenna gain) in order to detect any such targets.

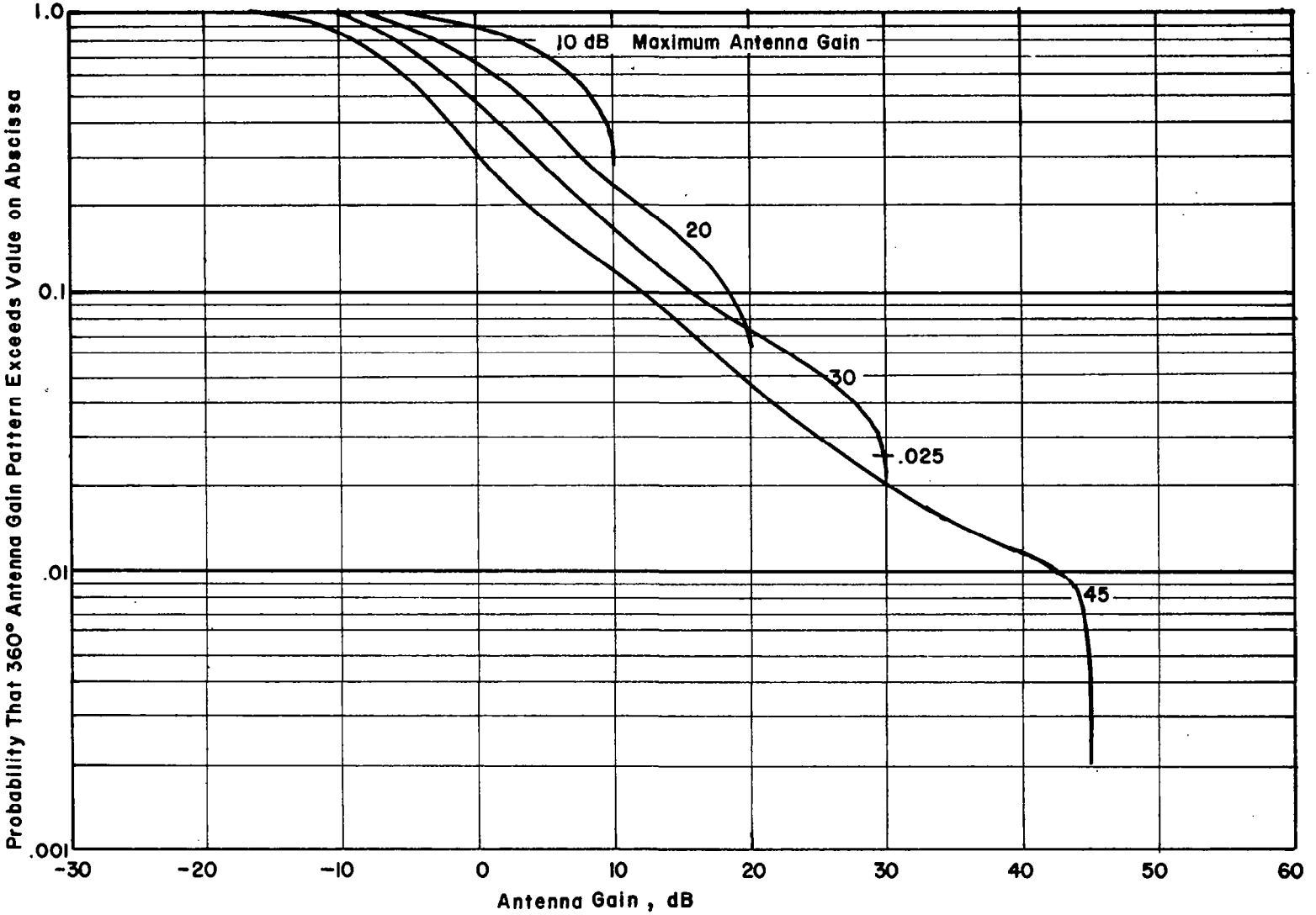

Figure 41 Gain Distribution Function for Various Sized Antennas

The apparent minimum value of EIRP seen by the satellite receiver when both target and satellite antennas are pointed for least power transfer is

$$\begin{aligned} EIRP_{A\ min} &= EIRP_{max} - (G_{T\ max} - G_{T\ min}) - (G_{S\ max} - G_{S\ min}) \\ &= P_o + G_{T\ min} - G_{S\ max} + G_{S\ min} \end{aligned} \tag{51}$$

$EIRP_{A\ min}$ specifies the sensitivity of the receiver (when corrected for space loss and minimum receiver antenna gain) required to detect all such targets, regardless of pointing direction of either antenna. The total number of targets in view of the satellite at any time is the density of targets multiplied by the area in view, assumed to be 5×10^6 sq. miles for a satellite 250 miles high. [The area of the United States (48 States) is approximately 3×10^6 sq. miles.]

Table 21 shows data used in plotting the curves on Fig. 42. For item 7 (land mobile), it is assumed only 1% of the actual number of transmitters is transmitting at a given time. The horizontal asymptote for this item is drawn at 3460 targets and extends to the right to -11 dBW ($EIRP_{A\ min}$). At the other end of the curve the vertical asymptote is drawn at 33 dBW ($EIRP_{max}$) and extends to 3460 reduced by the probability at maximum gain (0.025 for a 30 dB gain antenna, from Fig. 41) or 86 targets.

To get the expected number of targets seen at a given $EIRP_{eff}$ requires that suitable account be taken of the two antenna patterns. In this case, because of the uniform shape of the pattern distribution functions, the two extreme points are simply connected by straight lines (with appropriate rounding at the ends).

The value of $EIRP_{eff}$ shown on the abscissa of Fig. 42 can be adjusted upward by inserting an attenuator in the input of the receiver. The lowest value obtainable is, of course, determined by the satellite antenna gain and the receiver sensitivity.

Table 22 gives the minimum value of $EIRP_{eff}$ for various frequencies and for values of receiver bandwidth and antenna gain consistent with the recommendations made for the system in the Preliminary Report [30]. The values are based on the following formulas:

$$EIRP_{eff} = FKTB_r - G_S - L_f$$

L_f = free space loss = $\left[\frac{\lambda^2}{(4\pi t)^2}\right]_{dB}$ at the target distance, t, = 1436 mi for h = 250 s. mi altitude.

Table 21 Calculations of Number of Targets in View

Ref. Item in Table 4	No. of Emitters in $5 \times 10^6 mi^2$ (from Col. 4 of Table 4) **	Typical Power Output (dBW) P_o	Typical Target Gain G_{Tmax} (dB)	G_{Tmin} (from Fig. 41) (dB)	Gain of 3 m. Satellite Antenna‡ G_{Smax}(dB)	$G_{S\ min}$ (dB)	$EIRP_{max}$ (dBW)	$EIRP_{Amin}$ (dBW)	Range of Probability (from Fig. 41)
7	3460*	23	10	- 5	21	- 8	33	-11	0.025
15	1420*	30	22	- 9	30	-11	52	-20	0.0015
22	170*	66	34	-12	31	-11	100	12	0.0005
39	9300*	0	35	-12	42	-14	35	-68	0.0003

* Only 1% of transmitters assumed active at one time.

‡ From Fig. 24 and $G = 16/\left(\frac{\ell}{d}\right)^2$.

** 5×10^6 is approximate number of mi^2 in view for a satellite 250 mi high.

Reference Items:
7) Land Mobile, mobile base (450-470 MHz).
15) Air Traffic Control Radar Beacon, Ground site 1030 MHz (960-1215 MHz).
22) Long Range Radar (1250-1350 MHz).
39) Microwave Point to Point Common Carrier (3700-4200 MHz).

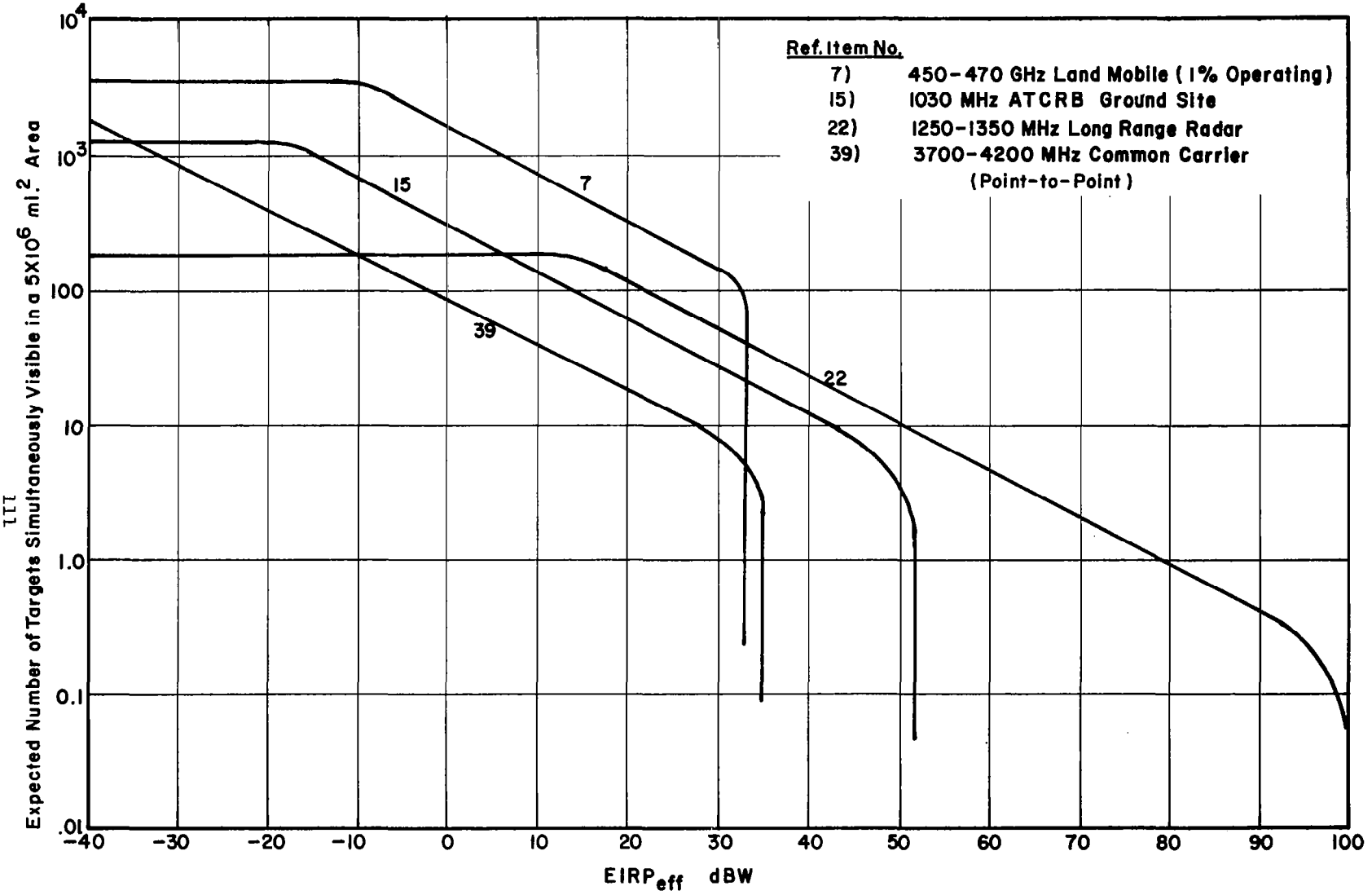

Figure 42 Expected Number of Targets vs Receiver System Sensitivity, $EIRP_{eff}$

Table 22 EIRP of Ground Source which Results in a Signal Power at the Satellite Equal to Satellite Receiver Noise

Frequency f(GHz)	Receiver Bandwidth B_S(MHz)	$FKTB_S$(dBW)	L_f(dB)	G_S(dB)	$EIRP_{eff}$(dBW)
0.5	0.5	- 137	- 153.7	21.5	- 4.8
1.0	0.5	- 137	- 159.7	27.5	- 4.8
2.0	1.0	- 134	- 165.7	33.5	- 6.6
3.0	1.0	- 134	- 169.3	37.0	- 1.7
4.0	1.0	- 134	- 171.8	33.5	4.3
5.0	1.0	- 134	- 173.7	35.5	8.5
10.0	2.0	- 131	- 179.7	41.5	15.7
20.0	3.0	- 125	- 185.7	41.5	19.2
30.0	3.0	- 125	- 189.3	45.0	19.3
40.0	3.0	- 125	- 191.8	47.5	19.3

$FKTB_S$ = satellite receiver noise power. F = 10, assumed noise figure.

B_S = satellite receiver noise bandwidth.

G_S = satellite antenna main beam gain. Assumed to correspond to the gains of parabolic dishes 10 feet in diameter from 0.5 to 3.0 MHz, 5 feet in diameter from 4 to 10 MHz, and 2.5 feet in diameter from 20 to 40 MHz.

Table 22 applies if the satellite bandwidth B_S exceeds the target bandwidth B_t. If $B_S/B_t < 1$, the received power is decreased and the tabulated value $EIRP_{eff}$ should be increased by $[B_S/B_t]_{dB}$.

It should be noted that what is plotted is the total number of targets visible in the identified band. Because the targets are actually distributed in frequency assignments over each band the total number of

targets received at the same time will be reduced from the values shown in Fig. 42 by the ratio of the bandwidth of either (1) the transmitter or (2) the receiver (depending on which is greater) to the total width of the band (assuming targets are assigned to frequencies uniformly distributed over the band). Thus, if the long-range radar requires 1.0 MHz of bandwidth and the analyzer bandwidth is less than this (say 100 kHz), the ordinate values for this system should be divided by 100 to get the number of targets seen at any one time.

The cases treated assumed similar services operating at a given frequency. Some bands accommodate mixed services, some operating with high power and some with low power. The 470-512 MHz band, for instance, is used for the land mobile service in some places and for UHF TV in others. Using arguments similar to those used to derive the preceding results, it is found that when a mobile source of 50 watts transmitter power is in view of the satellite main beam, it is likely to be swamped by the TV sources entering via side lobes. The latter will be stronger by 10 to 20 dB.

Although many approximations have been made in this analysis, it is thought to correctly indicate the magnitude of the problem of separating targets in the satellite antenna main beam from those outside it, especially since the target antenna will likely not be pointing in the direction of the satellite. It seems clear that some means of selectively identifying specific targets geographically will have to be developed, including adjustment of $EIRP_{min}$ levels and maintaining a history of targets detected along with correlation from one period of time to another. Other means of target identification can be developed.

7.0 HARDWARE IMPLEMENTATION

7.1 Introduction

The proposed space shuttle electromagnetic environment experiment [30, 39] can provide at least the following information for each terrestrial radio source it sees:

a. Signal amplitude (as measured from orbit)

b. Frequency

c. Approximate location (latitude and longitude)

d. Time of sighting

e. Azimuth angle from which the receiver looks at the transmitter.

Table 23 lists some of the types of documents that could be produced from this information.

TABLE 23 TYPES OF DOCUMENTS THE EEE COULD PRODUCE

EIRP, location, and emission patterns of sources by frequency
Frequency and emission pattern of sources by location
Activity at a given location as a function of time:
daily (per hr or per 1/10 of a day)
weekly (per week day)
seasonally (per season)
Percentage on-time
of specific transmitters
within bands
Usage as a function of frequency (No. of emitters above a given EIRP)
Signals received from known transmitters
Isopleths for a given area and frequency
Location and orientation of unsuspected sources
Number and power of transmitters at a given frequency within a given area
Fading as a function of location and time, weather
Apparent horizon as a function of time
Locations of potential interferers to a given site.
Extrapolations of signal levels to a given altitude and position
Probability of emissions from a given location
Prf's of pulsed emitters
Type of modulation of various emitters
Rotation rates of certain transmitters
Polarization
Moments of frequency distribution.

7.2 Data Flow

The block diagram in Fig. 43 summarizes the proposed data flow system.

7.2.1 On-Board Elements

7.2.1.1 Receiver

Basically, no significant difficulty is anticipated in the development of a suitable sweeping receiver. A receiver developed by the National Scientific Laboratory [4] is designed to cover the frequency range 0.4 to 12.4 GHz. The dynamic (amplitude) range achieved is stated to be 65 dB minimum. The amplitude range requirement has not yet been fully considered but indications are that the range of amplitudes could exceed 100 dB, suggesting that the present capability may need to be extended. The receiver uses a YIG tuned preselector filter over part of its range and achieves a 6 dB noise figure in the range 0.4 to 1 GHz and 10 dB in the range 1 to 12.4 GHz. This should be adequate. With a 6 dB noise figure the effective input temperature is about 1200 K. When measuring urban incidental noise, brightness temperatures of several thousand Kelvins are typically observed.

Though no thorough search has been made of off-the-shelf hardware, spectrum analyzer manufacturers can supply equipment for the frequency range of interest, with dynamic range quoted as high as 100 dB and with the noise figure at the low end of the frequency range of 5 dB.

The receiver should scan a given frequency band sequentially and produce one 6-bit amplitude record for each frequency slot. The amplitude steps need not be equally spaced: it might be desirable to have finely spaced steps at low amplitudes and widely spaced steps at high amplitudes.

The frequencies in a given band need not be contiguous; indeed, security considerations will require that the receiver skip certain blocks of frequencies in any given band. In addition, it would be convenient for the receiver to be able to selectively omit or include coverage of either specific frequencies or frequency ranges during the course of the experiment, following instructions from either ground or on-board personnel.

For horizon scanning, data rates which will be useful for reference purposes can be established. For surveying continuous transmissions, the dwell time in each frequency slot is to range from 153 to 42 μs depending on the frequency band in use. Assuming $2^6 = 64$ amplitude steps for each measurement, the highest rate needed is

$$6 \frac{\text{bits}}{\text{sample}} \Big/ 42 \frac{\mu\text{s}}{\text{sample}} = 140 \text{ k bits/s}$$

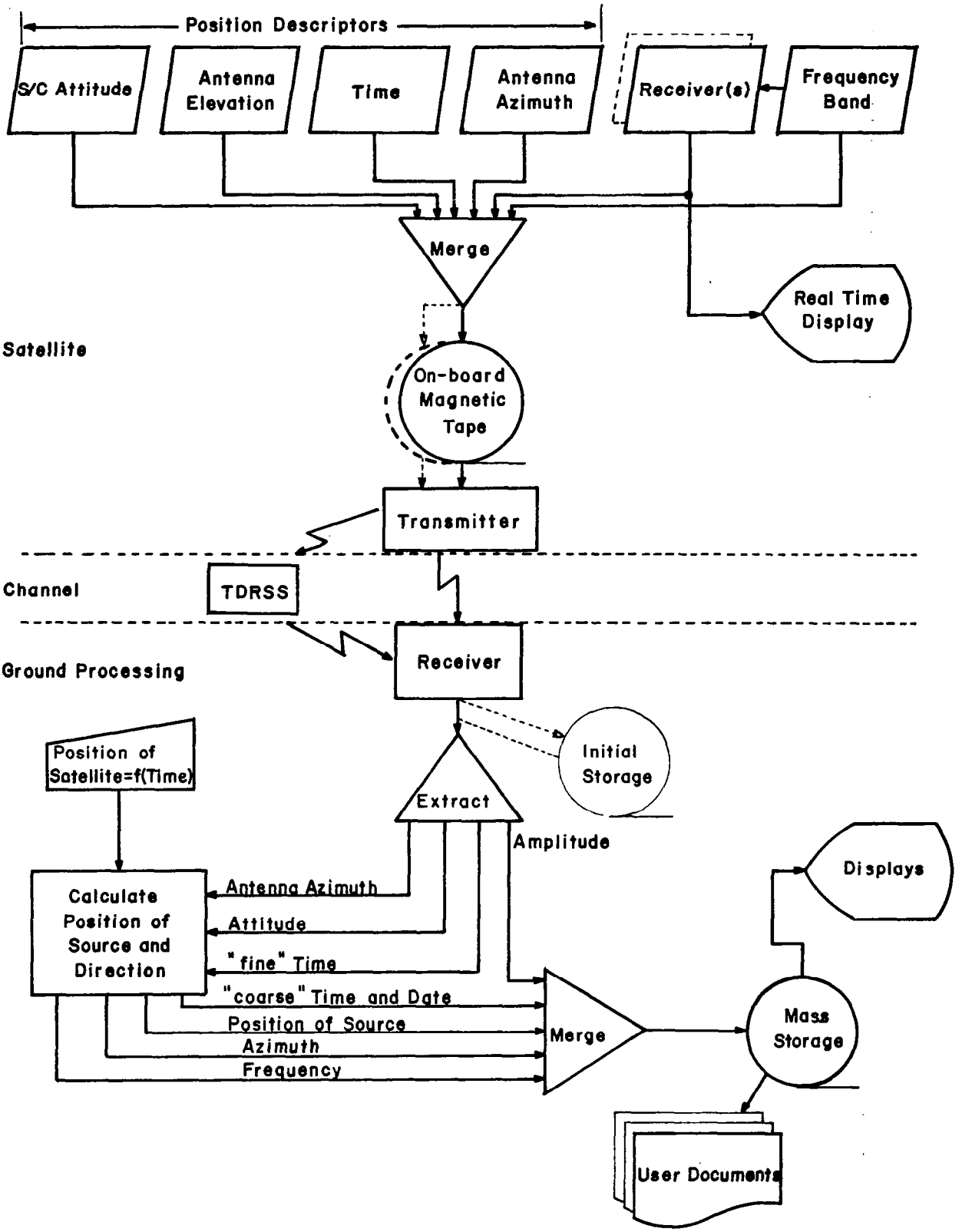

Figure 43 Data Flow

For pulsed radar observations, the scheme devised makes five measurements in five contiguous bands in 5 ms. Assuming data are found in each band (it is likely that no more than two bands will contain information, but estimates are made on the basis of all five) and that peak amplitude, pulse repetition rate, and pulse width are each recorded in 6 bits, and the data requirement is 18 k bits/s, the radar measurement needs are rather small. Both estimates assume there are data in every frequency slot, and every frequency slot will be given a corresponding allocation of transmission time.

7.2.1.2 Position Indicators

A person looking at a segment of a satellite-produced photographic or radar map of the earth's physical features would have little difficulty in pinpointing the location. But he would have a great deal of difficulty with a map of the earth's radio environment because such a map is unlikely to bear much relationship to a topographic map. Thus, the system mapping the earth's electromagnetic environment must record, along with each datum from the receiver, some index that will indicate where the receiver was looking when that datum was recorded.

Computing the position of an emitter requires knowledge of eight parameters: the location of the spacecraft relative to the earth (three degrees of freedom), the attitude of the spacecraft relative to the earth (three degrees of freedom) and the orientation of the antenna relative to the spacecraft (two degrees of freedom). Nonetheless, it is not necessary to transmit all eight parameters for every reading. The position of the spacecraft as a function of time can be accurately computed on the ground, either during or after the flight; the attitude of the spacecraft will vary slowly, and the elevation of the antenna will be changed infrequently. Only the antenna azimuth angle is likely to change significantly between one reading of a frequency slot and the next. Thus, to fully describe the location of a given target it is sufficient to record the time and antenna azimuth angle for each reading. Records of the spacecraft attitude and the antenna elevation can be updated much less frequently. Figure 44 shows a possible format for the data stream produced by the experiment.

The precision with which the position and time must be specified depends on both the accuracy with which the satellite's position is known and the shape of the antenna main beam. The antenna azimuth angle should be specified with a precision commensurate with the horizontal beam width of the antenna; e.g., the azimuth of an antenna with a 2° horizontal beam width ought to be specified within at least one degree. Since propagation effects on earth will make the range and elevation of an emitter much less certain than the azimuth, elevation angle can be specified with less precision than azimuth.

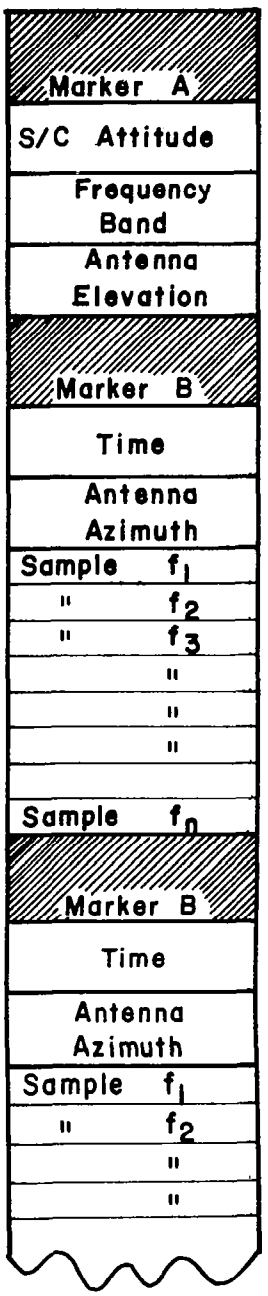

Marker A Identifies Beginning of Transmission of Attitude, Frequency Band, Antenna Elevation Data

Marker B Identifies Beginning of Time, Azimuth and Sequential Sweep Through Frequencies in Band

Figure 44 Possible Data Stream Format

7.2.1.3 Real-Time Display

While not strictly necessary, an on-board real-time display might be useful because it could:

a. Give immediate assurance that the experiment is working properly.

b. Provide clues to proper corrective adjustments.

c. Allow an on-board operator to immediately note areas of interest so he can insure that the receiver is in operation during subsequent passes over that area.

d. Allow the operator to manually change the receiver attenuation, antenna elevation, or frequency scan rate for strong or weak signals.

The objective of any display system should be to show variation of five parameters: time, amplitude, frequency and geographic location (x and y or latitude and longitude). Three-dimensional displays are possible using the conventional two-dimensional presentation of an oscillograph by intensity modulating the beam, but a human operator can distinguish no more than four distinct intensity levels. A fourth dimension can be added by using color or with special superimposed marking either alpha-numeric or graphical.

Pseudo-third dimensions can be accomplished by using particular scan and deflection patterns; an example is shown on Fig. 45 (Ref. 47). With such a display, geographic location information could be obtained by an auxiliary PPI (plan position indicator) showing the antenna pointing direction.

Obviously various combinations of these arrangements are possible, and the more complex will require operator training. The use of two separate displays probably is easiest to mechanize and to interpret.

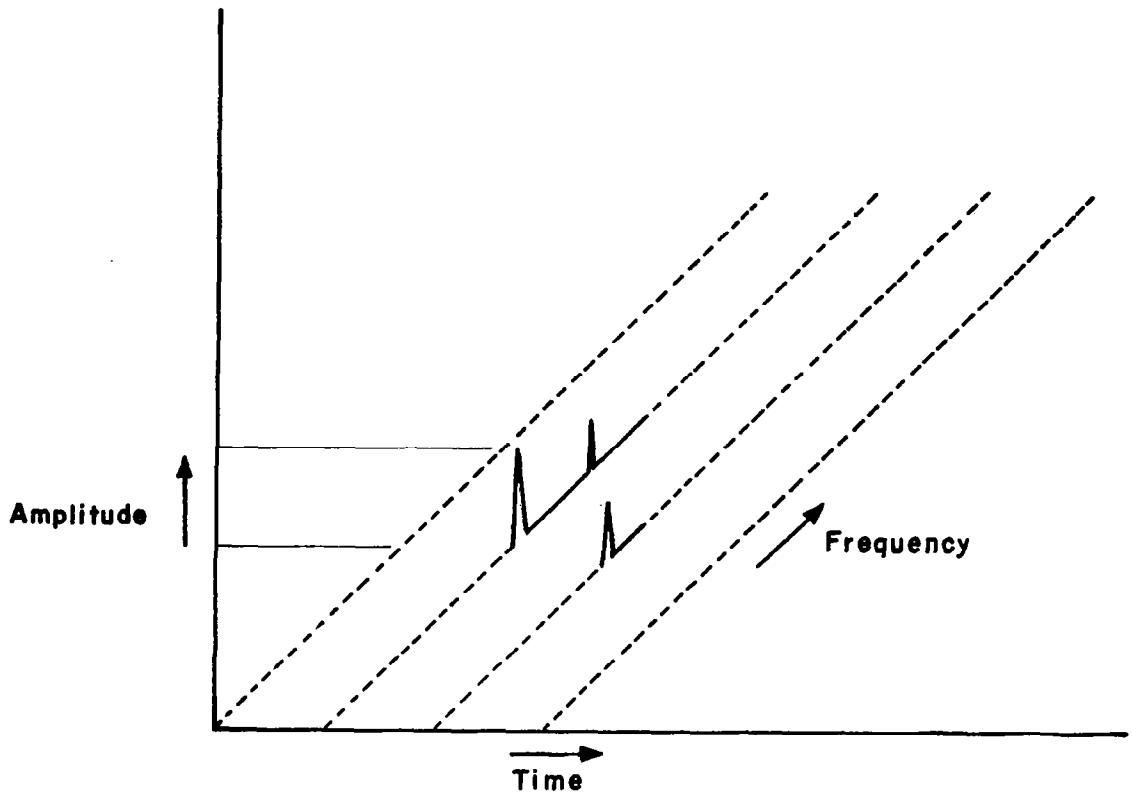

Figure 45 Pseudo 3-Dimensional Display

7.2.1.4 On-Board Data Storage and Processing

If data are sparse, it is advantageous to transmit them with proper identification as to time of occurrence, location, and frequency, and to eliminate the slots containing no useful information. Whether or not this is done will depend on an analysis of the expected amount of data and an assessment of the overhead costs in attaching identifiers to the data as compared to the cost of retaining vacant slots. Moreover, it is necessary to decide what is meant by "sparse data." For some purposes, such as the determination of percentage on time, it would be necessary to record the fact that a given area was examined at a given time, and no emission was detected.

If the TDRS is used as a data relay to ground the requirements of information storage would be determined by the queuing discipline for the relay satellite. If data are relayed to ground stations en route, the storage requirements are determined by the time to travel between ground stations, time over the ground station, data rate capability of the satellite-to-ground link, etc.

In either case, on-board storage need only be sufficient to store one orbit's worth of a 150 k bit/s/octave signal. This is well within the capability of currently available space-qualified recorders.

7.2.2 Ground Processing

Before discussing data handling techniques at greater length, it is appropriate to make some rough estimates of the total amount of data that may be produced. There are several approaches that can be used.

7.2.2.1 Method I: Data Available to Be Measured

Assume that the satellite makes measurements of every 50 km × 50 km plot on the globe between 70° North and South latitudes. The total surface area ($A = 4\pi R^2 \sin\theta$) is 3.9×10^8 km^2, and there are 195,288 (18 bits) such 2500 km^2 plots. Using the bandwidths of Table 24 there are 13,576 frequency bands. Thus, there are (195,288) × (13,576) = 2.65×10^9 spatial-frequency slots. Each reading in each of these slots ought to record the information shown in Table 25.

Clearly, these are overestimates. The receiver will doubtless operate only a few hours a day and may not cover all bands. If the receiver operates only 6 hours a day and covers only two octaves, the second estimate will be too high by a factor of 10. Nonetheless, comparison with Table 26, a list of the storage capacities of some of the largest currently available mass memory systems, indicates that the amount of data produced by the satellite is large by current standards. Thus, ground storage and processing is a nontrivial problem.

TABLE 24 NUMBER OF BITS NEEDED TO REPRESENT MEASURABLE PARAMETERS, FIRST METHOD

Frequency

dwell	Bandwidth	Freq. Range	Total Range	# of Bands
153 μs	0.458 MHz	400-1000 MHz	600 MHz	1310
118 μs	0.591 MHz	1000-2000 MHz	1000 MHz	1692
84 μs	0.832 MHz	2000-4000 MHz	2000 MHz	2403
59 μs	1.182 MHz	4000-8000 MHz	4000 MHz	3384
42 μs	1.671 MHz	8000-16,000 MHz	8000 MHz	4787
				13,576 freq. slots ≈ 14 bits

Amplitude 64 levels 6 bits

Location

$1^\circ \times 1^\circ$ squares = 180 × 360 = 64,800 cells ≈ 16 bits

elim lat $\geq 70^\circ$ = 140 × 360 = 50,400 " ≈ 16 bits

Azimuth $360^\circ \div 1.4^\circ$ = 256 units 8 bits

Time

16ths of a day	4 bits
Day	3 bits
Month	4 bits
or Date	9 bits

TABLE 25 NUMBER OF BITS NEEDED TO REPRESENT MEASURABLE PARAMETERS, SECOND METHOD

Amplitude	64 levels	6 bits
Azimuth	to within 1.5^{o}	8 bits
Elevation		4 bits
Time:		
	hour ≈ 16th of a day	4 bits
	day	3 bits
	month	4 bits
		29 bits

TABLE 26 AVAILABLE MASS MEMORY SYSTEMS

International Video Corp. [43], IVC-1000 (a device, not a system)

Read/write speed, 8×10^{6} bits/s

Reel capacity, 9×10^{10} bits

Unicon [42] 690-212; Precision Instruments Inc., Palo Alto, Cal.

Medium: (laser burns holes in metallic strips on rotating drums)

Read spread: 3.4 M bits/s

Capacity: 0.7×10^{12} bits

Terabit Memory System [44], Ampex

Medium: 2 in. mag. video tape

Read/write rates: 6×10^{6} bits/s

Maximum System capacity: 2.9×10^{12} bits

RCA TCR-100 [45]

Medium: Video tape cartridges

Read/write speed: 15×10^{6} bits/s

Equipment Capacity: 8.8×10^{12} bits

If the experiment were to run continuously, each spatial frequency block might be covered 10 times a day for one week. If all these data were to be recorded the amount of storage space necessary for such a mission could therefore be as great as

$$2.6 \times 10^9 \times 28 \times 70 \approx 5 \times 10^{12} \text{ bits}$$

7.2.2.2 Method II: Amount of Information Transmitted

The assumption that the satellite receiver produces 150 k bits/s for each octave bandwidth is consistent with the data in Table 25. If operated continuously for 7 days, the experiment would require

$$150 \times 10^3 \text{ bits/s} \times 60 \text{ s/min} \times 60 \text{ min/hr} \times 24 \text{ hr/da} \times 7 \text{ da}$$

$$= 9 \times 10^{10} \text{ bits/octave} \times 5 \text{ octaves} = 4.5 \times 10^{11} \text{ bits}$$

7.2.3 Equipment

7.2.3.1 Real Time Display

A ground-based real-time display would be similar to the satellite-based real-time display discussed above.

7.2.3.2 Storage

Given the large size of the data base and the potential wide variety of usage patterns, a storage system based on conventional computer tape and tape drives might be unnecessarily large, slow or expensive. As Table 26 indicates, other storage media are currently being developed, and these systems should be evaluated at greater length for the EEE data storage.

7.2.3.3 Computing

The ground computing system must:

a) Calculate positions of emitters, given the time and attitude data and the equation of motion of the satellite.

b) Format incoming data for storage.

c) Manage the data base.

d) Find and retrieve data from storage and print required frequency listings, maps, and charts.

e) Perform any other processing (possibilities described in Section 7.2.5).

7.2.4 Formats

In general, the best storage format for large data bases cannot be determined without some idea of the relative frequency with which the user community will request different types of data. If, for example, many users are interested in listings of transmitter locations as a function of frequency, and few are interested in frequency listings as a function of location, the structure of the data base ought to make it easy to list data as a function of frequency, even if doing so would make it more difficult to locate files by geographic location.

In spite of the dependence of the storage format on intended usage patterns, several comments are appropriate:

1. At the very minimum, the user must be able to request data either by frequency or geographic location.

2. The storage scheme must be flexible and should not restrict access modes unnecessarily.

3. The data base should not set an arbitrary limit on the number of readings from a given emitter or geographic location. While establishing a fixed file length might simplify the writing of software and abbreviate memory requirements, it ultimately means that potentially useful data must be thrown away. Looking at one source from a number of different angles and at many different times of day can provide valuable information about a source's emission patterns or diurnal activity cycle.

7.2.5 Processing

In addition to locating, retrieving, and formating data, other data-procuring activities may be either required or desirable. These activities could include:

1. Array Processing: If an antenna array rather than a single dish is used at the lower frequencies, array processing will be required. If a narrow beam and an omnidirectional antenna are used simultaneously to differentiate between on-axis and off-axis signals, somewhere--either in the receiver on-board, or on the ground--one signal must be subtracted from the other.

2. Gain Compensation: The experiment may use a number of different antennas, and the gain of each antenna will vary somewhat as a function of frequency. Processing, either on the ground or on board, can remove gain variations due to the antennas and convert all data recorded to a single unified scale. Thus, a single emitter seen through both a low gain and a high gain antenna will not appear to have two different amplitude levels, and a source at the high end of an antenna's frequency range will not appear to be more powerful than a source of equal amplitude at the low end.

8.0 CONCLUSIONS

This report gives the results of a study aimed at developing a concept for measuring electromagnetic fields emanating from earth using the space shuttle as a measuring system platform. The following are the conclusions drawn:

a. Current spectrum use is such that the range of main beam EIRP values to be expected from licensed sources over the range 0.4-40 GHz is in the order of 100 dB. At specific frequencies utilized by one type of service, the range of EIRP is smaller. However, with frequency sharing among services using widely different power levels EIRP differences of 40-50 dB will occur at certain frequencies. The received amplitudes for a given ground source using a high gain antenna may, in addition, vary over a range of about 50 dB depending on the pointing direction of the ground source.

b. A spatial scanning procedure which sweeps the antenna beam circularly exposing a helical annulus on the ground as the satellite progresses in its orbit is feasible. If the region viewed is at or near the horizon, there is the possibility of measuring the main beam emission of directive sources transmitting to receivers on the ground. For a 1^{o} beamwidth satellite antenna looking at the horizon the region in the aperture is about 20 miles wide by about 400 miles deep. A frequency sweeping regimen was developed which makes it feasible to sweep, at least over an octave range, during the time the satellite antenna is over a source. The frequency sweep is based on using a scanning band window of width 0.5 MHz at lower frequencies to about 3 MHz at higher frequencies. A mechanism for insuring capture of a low duty cycle radar was also worked out.

c. For a 250 mile altitude orbit, at an inclination of 50^{o}, points within the latitude $\pm 65^{o}$ will be in the satellite antenna aperture at least 8 times a day. At latitudes of 30^{o}-40^{o} most sources will be in the aperture at least 16 times per day. Assuming a flight duration of two weeks is dedicated to a single one of the octave frequency ranges, most of the sources at mid latitudes would be seen in that range $16 \times 14 = 224$ times, and seen from various directions. Sufficient data may be available to give an adequate ground source radiation pattern.

d. Signals entering via satellite antenna sidelobes will obscure the measurements. First, a source in view of the satellite but not on the main beam may give rise to an output reading greater than a source of equal power in the satellite antenna's main beam. Second, at frequencies where both high and low power sources are used (e.g., UHF TV and mobile services) the high power sources may make it virtually impossible to measure the low power ones. Finally, the accumulated small contributions from many sources operating at the same frequency entering via sidelobes may be considered as having the effect of raising the noise level of the system.

e. The satellite can produce prodigious amounts of data--at least 10^{10} bits. The amount of data and its format, and uncertainty in the range and direction of an observed source, dictate that developing software to efficiently process, store, and retrieve the data will require a major effort. Developing the software demands some knowledge of the relative frequency with which the user community will request different types of information. Users should be able to request data by frequency or by geographic location; other access modes might prove convenient as well. A fixed file length, although it would simplify data processing, would throw away much valuable data. The data produced by the satellite are potentially capable of yielding information on location, frequency, amplitude, emission pattern, duty cycle and diurnal, weakly, and seasonal variations in output for every transmitter it sees. Which of these characteristics are to be produced depends on the value of the information to the user community and the cost of extracting it from the stored records.

The work done to date suggests the following problems be given further attention:

a) Atmospheric propagation effects should be analyzed, particularly for the horizon looking mode where refraction and scattering may be significant, and at the higher frequencies where absorption is important.

b) Some means of discriminating sources in the main antenna beam from those entering the receiver via the side lobes will be necessary, such as use of multiple antennas or computer source identification based on the multiple measurements made at the same frequency.

c) Data compression and efficient storage and retrieval schemes, appropriate to the uses of the data, require attention. Programs for generating data output formats typically required by users, ought to be developed.

d) Because of the tremendously flexible operational procedures available in geographic and frequency scanning, and because frequency uses are so variable from one band to another, a careful examination of the uses of the data collected should be made and the system operation optimized in each case. Full advantage should be taken of use of manual control to alter scanning modes adaptively during flight. This should be a continuing study.

9.0 REFERENCES

1. V. F. Henry and J. J. Kelleher, "Radio Frequency Interference Experiment Design for the Applications Technology Satellite," NASA TN D-5041, May 1969.

2. K. H. Hurlbut and C. J. Zamites, "Electronics Program: Radio Frequency Interference at Orbital Altitudes," Report No. TDR-269 (4250-44)-2, October 1964.

3. H. K. Mertel, "Feasibility Study of Man-Made Radio Frequency Radiation Measurement," NASW-1437, Convair Div., General Dynamics Corp., Aug. 1, 1966.

4. "Study of Existing and Planned Radio Interference and Propagation Program (RIPP) Experiments," NAS 5-11835, Modification 27, National Scientific Laboratories, Inc., March 1972.

5. "A Report on a Study for the Inclusion of a Radio Frequency Interference Experiment on an ITOS-D Series Spacecraft," AED-R-3906F, RCA Corporation, January 1973.

6. "Feasibility Study of Man-Made Radio Frequency Radiation Measurements from a 200-Mile Orbit," General Dynamics, Convair Div., Feb. 1967.

7. W. W. Ward et al., "The Result of the LES-5 and LES-6 RFI Experiments," TN-1970-3, Lincoln Laboratory, MIT, Lexington, Mass., Feb. 1970, AD 703 738.

8. W. W. Ward, et al., "The Results of the LES-5 and LES-6 RFI Experiments," TN-1970-3, suppl-1, Lincoln Laboratory, MIT, Lexington, Mass., July 1970, AD 709 766.

9. K. H. Hurlbut and C. J. Zamites, "UHF Radio Frequency Interference Measurements at Synchronous Altitudes," TR-0066 (5230-01)-1, Aerospace Corp., El Segundo, Cal., Jan. 1970, AD 703 712.

10. J. R. Herman and J. A. Caruso, "Radio Astronomy Explorer (RAE)1 Observations of Terrestrial Radio Noise," NASA-CR-122401, Analytical Systems Corp., Burlington, Mass., Oct. 1971, N72-24165.

11. Bergman, Rice, and Miles, "Mathematical Computer Model and Predictions for ATS-F Radio Interference Experiment at 6 GHz," COM-72-11409, Office of Telecommunications, Boulder, Colo., Aug. 1972.

12. R. E. Taylor, R. E. Prince, and D. N. McGregor, "A Shuttle/Spacelab RF Environment Survey Facility," Paper 14B, Natl. Telecommunications Conf. (NTC-74), Dec. 2-4, 1974, San Diego, Ca.

13. S. E. Scrupski, "Users Starting to Hop Aboard U.S. Communications Satellites," Electronics 95, 3 October 1974.

14. "Space Shuttle RFI Experiment Study," Interim Report, Operations Research, Inc., Silver Spring, Md., 22 July 1974.

15. H. K. Mertel, "Feasibility Study of Man-Made Radio Frequency Radiation Measurements from a 200-Mile Orbit," Report No. ZZK 67-007, Convair Div., General Dynamics, San Diego, Cal., Feb. 1967.

16. G. Ploussios, "Noise Temperature of Airborne Antennas at UHF," Technical Note 1966-59, Lincoln Laboratory, MIT, Lexington, Mass., 6 Dec. 1966.

17. A. H. Mills, "Measurement and Analysis of Radio Frequency Noise in Urban, Suburban, and Rural Areas," NASA-CR-72490; GDC-AWV68-001, Convair, San Diego, Cal., Feb. 1969, N69-18667.

18. A. H. Mills, "Measurement of Radio Frequency Noise in Urban, Suburban and Rural Areas," NASA-CR-72802; GDC-AWV70-001, Convair, San Diego, Cal., Dec. 1970, N71-14754.

19. G. Anzic and C. May, "Results and Analysis of a Combined Aerial and Ground Ultrahigh Frequency Noise Survey in an Urban Area," NASA-TM-X-2244; E-6002, Lewis Research Center, Cleveland, Ohio, April 1971, N71-22623.

20. G. Anzic, "Radio-Frequency Noise Measurements in Urban Areas at 480 and 950 Megahertz," NASA-TM-X-1972, Lewis Research Center, Cleveland, Ohio, March 1970, N70-20688.

21. G. Anzic, "Aerial RF Noise Measurement in Urban Areas at UHF Frequencies," NASA-TM-X-52751, Lewis Research Center, Cleveland, Ohio, April 1970, N70-32673.

22. G. Anzic, "Measurement and Analysis of Radio-Frequency Indigenous Noise," 1970 IEEE International Symposium on Electromagnetic Compatibility Record.

23. C.R.W. Barnard, "VHF Noise Levels over Large Towns," Royal Aircraft Establishment, Tech. Report 67213, August 1967, AD 827-640.

24. W. E. Buehler, C. H. King, and C. D. Lunden, "VHF City Noise," 1968 Record of IEEE EMC Symposium, pp. 41-51, January 1968.

25. E. N. Skomal, "Analysis of Airborne VHF/UHF Incidental Noise over Metropolitan Areas," IEEE Trans. on EMC, May 1969, p. 76.

26. E. N. Skomal, "The Range and Frequency Dependence of VHF-UHF Man-Made Radio Noise in and above Metropolitan Areas," IEEE Trans. on Vehicular Technology, May 1970.

27. C. J. Zamites and K. H. Hurlbut, "Measurements of Interference Levels in the UHF Band from Aircraft Altitudes," IEEE Trans. on EMC, Aug. 1970.

28. D. Madison, L. Kuehn, T. Bode, "Airborne European RF Measurements in the 100-500 MHz Band," ESD-TR-72-293, IIT Research Institute, Chicago, Ill., Nov. 1972, AD 758 772.

29. "RFI Experiment Definition Project Report," Report No. 74-N-003, National Scientific Laboratories, Inc., McLean, Va., June 1974.

30. F. Haber, R. M. Showers, et al., Preliminary Report, "Space Shuttle Electromagnetic Environment Experiment," University of Pennsylvania, Dec. 3, 1974, Contract NAS5-20707, Moore School Report 75-04.

31. International Frequency List, International Telecommunication Union, Geneva, Switzerland, 1 Feb. 1965.

32. List of Radars furnished by the Frequency Assignments Branch, Federal Aviation Agency, Washington, D.C., April 1975.

33. Spectrum Engineering--Key to Progress, Joint Technical Advisory Committee, Institute of Electrical & Electronic Engineers, Inc., 1968.

34. Henry Jasik, ANTENNA ENGINEERING HANDBOOK, McGraw-Hill, 1961.

35. D. Madison, et al.,"Airborne European RF Measurements in the 100-500 MHz Band," ESD-TR-72-293, IIT Research Institute, Chicago, Ill., Nov. 1972, AD 758 772.

36. Statistical Abstracts of the United States, 1974, U.S. Department of Commerce, Washington, D.C.

37. Charles A. Gettier,"ATCRBS Performance Analysis for Los Angeles ARTCC," Report FAA-RD-72-36, IIT Research Institute, Chicago, Ill., August 1972, AD 754 266.

38. J. K. Moffitt, Tabulation of Data on Microwave Tubes, National Bureau of Standards Handbook 104, National Bureau of Standards, Washington, D.C. 1967.

39. F. Haber, R. M. Showers, et al., "Space Shuttle Electromagnetic Environment Experiment: Phase A: Definition Study," Interim Report, Moore School Report 76-01, Univ. of Pa., May 3, 1975.

40. R. F. Ficchi, Ed., PRACTICAL DESIGN FOR ELECTROMAGNETIC COMPATIBILITY, Hayden Book Co., New York, 1971.

41. "Interference Notebook," Rome Air Development Center, RADC-TR-66-1, June 1966.

42. N. Schneidewend, G. Symes, T. Grainger, R. Carden, "High-Density Mass Memories," EE Systems Engineering Today, Aug. 1973.

43. Ibid, September 1973.

44. Ibid, October 1973.

45. L. Dobbins, C. Horton, "User-Oriented Data Cartridge Recording Systems," RCA Reprint RE 20-6-19.

46. J. M. Hayes, C. R. Thompson, "High Data Rate S/C Tape Recorders," IEEE National Telecommunications Conference, Houston, Texas, Dec. 1972.

47. W. R. Vincent, "RF Noise Radiated by a Rapid Transit System," 1974 IEEE Electromagnetic Compatibility Symposium Record, San Francisco, Cal., July 16-18, 1975, 74CH0803-7 EMC.

48. R. C. Johnson, "Radar Search Antennas and RFI," IEEE Trans. on EMC, Vol. EMC-6, July 1964, pp. 1-8.

49. J. J. Bussgang and T. L. Fine, "Interpulse Interval Distribution in the Environment of N Periodic Radars," IEEE Trans. on RFI, Vol. RFI-5, pp. 7-10, June 1963; also, B. H. Metzger, "Interpulse Interval Distribution in the Environment of N Periodic Radars," IEEE Trans. on EMC, Vol. EMC-6, July 1964, p. 45.

50. P. F. Panter, COMMUNICATION SYSTEMS DESIGN, McGraw-Hill Book Co., 1972.

51. H. E. Curtis, "Interference Between Satellite Communication Systems and Common Carrier Surface Systems," BSTJ, May 1962, pp. 921-943.

52. D. T. Thomas, "A Half Blinder for Reducing Certain Sidelobes in Large Horn Reflector Antennas," IEEE Trans. on Antennas and Propagation, Nov. 1971, pp. 774-776.

53. R. R. Grady, "Sidelobe Control in the Horn Reflector Antenna," Nat. Electronics Conf. Proceedings, Dec. 7-9, 1970, pp. 360-363.

54. F. J. Freil, "Spectrum Sharing Criteria for Space and Terrestrial Systems," IEEE Symposium on EMC Record, 1971.

55. Safety Guide for the Prevention of Radio Frequency Radiation Hazards in the Use of Blasting Caps, Safety Library, publication no. 20, Institute of Makers of Explosives, March 1971.

56. Nomenclature des Stations Fixes, International Telecommunications Union, Vol. 2, 1959.

57. R. W. Moss, et al., Study to Access Future Role and Requirements for a Fixed-Base Monitoring System, Volume 1 - Introduction and Background, Contract RC-10208, FCC, prepared by Georgia Institute of Technology, Atlanta, Ga. 1973.

58. Rules and Regulations, FCC.

59. Myron Kayton and Walter R. Fried, Avionics Navigation Systems, John Wiley and Sons, Inc., New York, 1969.

60. J. E. Adams, G. G. Ax, R. D. Jennings, "Compatibility of Systems in the 1600 MHz Region," IEEE International Electromagnetic Compatibility Symposium Record, July 1972, IEEE, 1972, p. 32.

61. Frank A. Gunther, "Troposcatter Communications, Past, Present and Future," IEEE Spectrum, Institute of Electrical and Electronic Engineers, Inc., Sept. 1966.

62. Official Registry of Public Safety Radio Systems, Milton B. Sleeper, North Adams, Mass.,Oct. 1961.

Appendix I

A SCANNING RECEIVER FOR PULSED SOURCES

Detecting pulsed RF sources such as radars demands special consideration. If the two antennas, radar and spacecraft, are looking at one another and the spacecraft receiver is sweeping in frequency, it must pass the radar frequency when a pulse is being emitted in order to detect it.

We can view the scanning process as taking place in steps, with the receiver filter center frequency being stepped periodically by an amount equal to the receiver IF amplifier bandwidth. When the pulse occurs it encounters one of the receiver filters which may or may not be centered on or near the pulse radio frequency. Assume, for instance, that we are searching the 1-2 GHz band where many radars will be found. If we are to search the entire band in 0.2 seconds, Eq. (32) shows that we will need a bandwidth of at least 591 kHz. Using this bandwidth, each bandwidth increment would be observed for about 118 microseconds. If the pulse repetition rate is 1000 pps, pulses occur at intervals of 1 millisecond and the probability of a pulse falling exactly into the filter corresponding to its center frequency is about 10%. At higher frequencies where the bandwidth prescribed by Eq. (32) is larger, the frequency dwell time is smaller, and the probability of encountering a pulse is even smaller. To insure interception, the technique of ubiquitous spectrum analysis may be used in conjunction with conventional scanning. Most radars are found in the range of 1-4 GHz and repetition rates are generally higher than 200 pps, or have pulses at most 5 ms apart. If we allow T_a to be at least 5 ms, at least one pulse will be encountered. In a spatial dwell time of 200 ms there are forty 5 ms intervals and in each we will examine 1/40 of the total range. For the 1-2 GHz range this means examining 25 MHz at a time. To get an acceptable frequency resolution, the 25 MHz band may be examined in a bank of five contiguous filters, each of a bandwidth of about 5 MHz. Each of these sub-bands of 5 MHz would be examined for 5 ms and sometime during this interval one or more pulses would occur if the sub-band corresponds to a frequency at which the pulse has significant energy. For the 2-4 GHz. range, 50 MHz would be examined at one time. Five sub-bands, each of 10 MHz bandwidth, would cover this range, yet keep the sub-band filters to a reasonable number.

A block diagram of the receiver for the 1-2 GHz band is shown in Fig. I-1. It is arranged to do a conventional scan in discrete steps in a band of about 600 kHz looking in each band for 118 μs. At the same time it will examine forty 25 MHz bands, observing each 5 MHz sub-band for 5 ms. While the entire 25 MHz IF filter output could be examined without going to the sub-bands, using the technique shown will reduce the noise level.

Receiver for 1-2 GHz band

FIGURE I-1

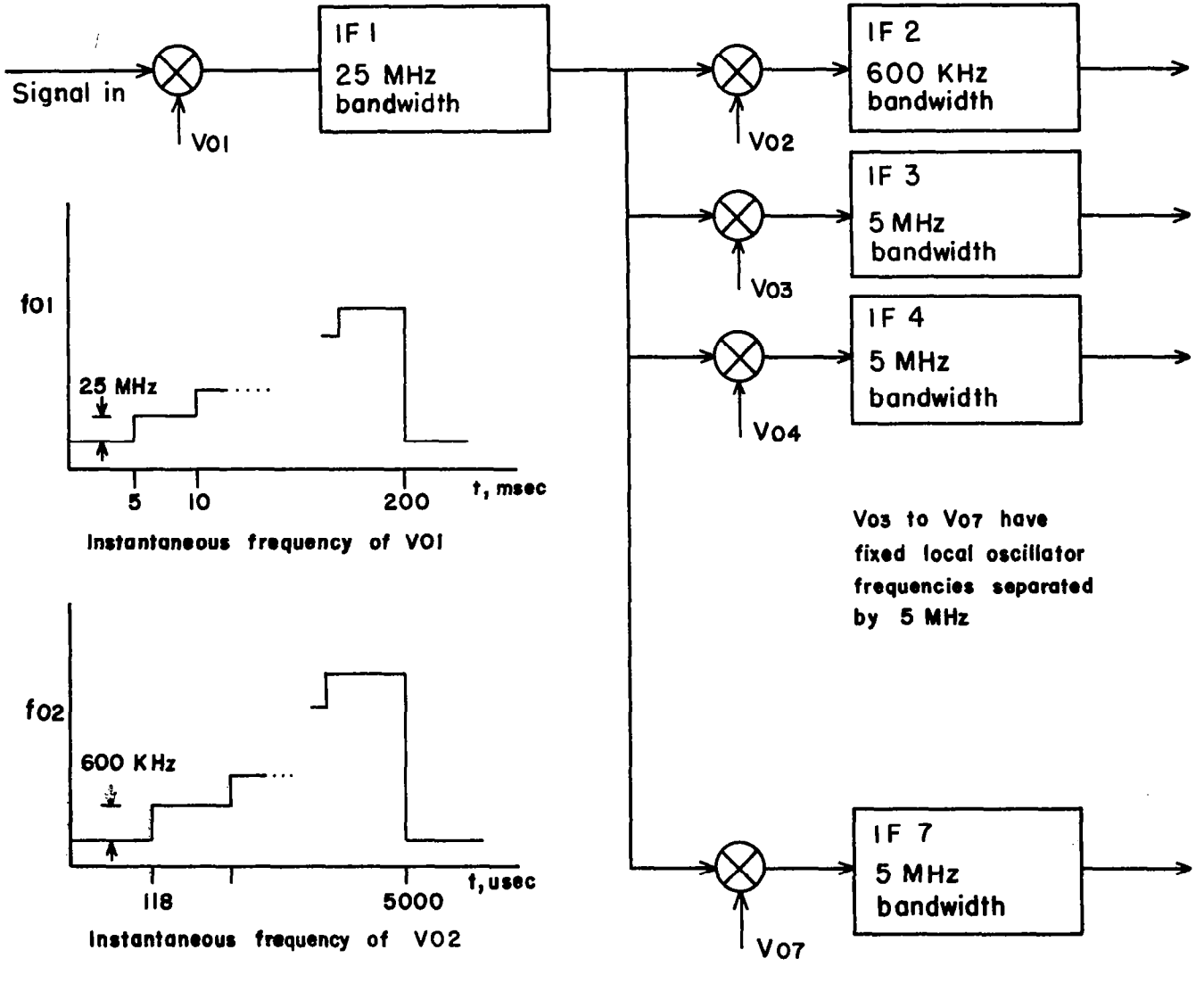

The 5 MHz filters have sufficient bandwidth to accept most radar pulses without distortion and the observation interval is enough to allow two or more pulses to show up. This assertion is based on the observation that the predominant L-band radars used for air traffic control have pulse widths of 2 μs at a repetition rate of 350 pps and the predominant S-band radars have a pulse width of 0.8 μs at a repetition rate of 1200 pps. The 5 MHz filter described here can accept pulses as short as 0.2 μs at repetition rates as low as 200 pps. This suggests that each interval can be used to give peak received pulse power and time between pulses or repetition rate. As a rule only one of the 5 MHz filters will pass the pulses, though two adjacent filters may sometimes share the spectral energy of the arriving pulses. In rare cases, nonadjacent 5 MHz filters may contain output information suggesting that more than one source is in view of the receiving antenna. Depending on the results of a survey of frequency assignment, we may ultimately recommend that data from only one of the five filters be passed on to the recording apparatus.

The 5 MHz filters may also see non-radar sources which, if they occur, will usually give rise to a low level noise-like background. Since these channels are being included specifically for recording pulsed radar, it is advisable to design the measuring circuit so that it requires a minimal level in order to respond.

Appendix II

MATHEMATICAL MODEL FOR SATELLITE ANTENNA SIDELOBE EFFECTS

II.1 Analysis and Modeling of Sidelobe Leakage

A problem of major importance is the non-zero sensitivity of the satellite antenna to sources off the antenna main beam. As shown in Fig. 18 and pp. 42-44 of the preliminary report(Ref. 30.) and Fig. II.1 below, the angle θ, which is half the visible region from the satellite, is 19.75° (= 0.3447 radians) for a satellite altitude of 402 km (250 miles) and corresponds to a surface distance of 2174 km (1379 miles). The total arc length visible on earth is therefore 4437 km (= 2757 mi) and the total area visible is over 1.5×10^9 hectares (5.9×10^6 sq. mi). A satellite over the middle of the U.S. would therefore see essentially all of the U.S. Accounting for refraction, the satellite actually sees beyond the east and west coast lines. The antenna main beam will be pointing in some one direction at any given moment but the sidelobes will be exposed to all that is visible below. The survey study reported in section 2 of this report shows that a substantial number of emitters may be operating simultaneously in different parts of the country on the same frequency. One must therefore expect that in some circumstances, sources off the main beam of the satellite antenna will be large enough to give readings which, with no further examination, would be interpreted as coming from the direction of the main beam. It is, in fact, conceivable that the number of sources off the main beam, operating at the same frequency, number in the tens for some high power services and in the hundreds for some low power services.

The effects of off-axis sensitivity are considered from several viewpoints as follows.

(a) No source on main beam. The reading obtained above the receiver noise level is due to sources visible to the side lobes. Methods must be found for recognizing this condition and for rejecting such measurements as spurious.

(b) Large source on the main beam. The reading obtained is to some extent due to off-axis sources. A method for correcting reading to eliminate sidelobe sources would be desirable.

(c) Small source on the main beam. The reading obtained is largely due to the sidelobe sources obscuring the source to be measured. This appears to be a major problem. The off-axis sensitivity has the effect of adding to the random noise, essentially reducing the sensitivity of the system.

The problem is examined along two lines. First, the effect is quantified by modeling the sources on the ground and the satellite antenna characteristics, and determining the properties of the signals

arriving from undesired directions. In this regard it should be noted that continuous wave transmitter sources will all look more or less like Gaussian random noise to the receiver described in the preliminary report. This is so because the typical sources are broad-band information bearing, and the measuring system looks at a small part of the emission bandwidth. For such sources the independent unwanted signals will each contribute additively to the total received power and the sum signal will look like Gaussian noise. The preliminary report recommends measuring pulsed signals (i.e., radar outputs) in circuits of sufficient bandwidth to conserve their shape. Such signals, emanating from a number of independent transmitters, will be asynchronous, resulting in a quasi-random succession of pulses with random amplitudes at the point of measurement in the receiver. The two outputs types, noiselike and random pulselike, will require different measures for their representation.

The second line along which the problem is treated is to seek ways of recognizing and correcting the effects of sidelobe sensitivity. The recognition aspect can be handled either by using multiple antennas and receivers or by processing the successive readings obtained with a single antenna. The methods investigated thus far are described below. The correction aspect is similar to other problems of detecting signals in noise and this too is discussed below.

Fig. II-1 shows a cross-sectional view of the earth, the cross-sectional plane containing the satellite location S, the center of the earth O, and a point on the earth's surface P at which a source is located. The region of earth in view from the satellite is a spherical cap which subtends an angle 2θ at the center of the earth. The point Q on the surface of the earth is also in the cross-sectional plane and is the satellite's horizon point in this plane. Power from the ground source at P is transmitted to the satellite at S along the line PS which is at angles $\underline{b}$ and $\underline{a}$ relative to tangent planes at P and Q, respectively. The main beams of the antennas of P and S are generally not oriented along the connecting line PS. The assumption is made that the ground antenna main beam is oriented somewhere in the plane tangent to P at an angle b_1 relative to the cross-sectional plane as shown in Fig. II-2. b_1 is therefore the angle between the main beam of the ground antenna and the line denoted PR in Fig. II-1; this angle is assumed uniformly distributed in 2π radians. The orientation of the satellite antenna main beam depends on the scanning mode. In this analysis the power received by the satellite off its main beam is of interest. Since the main beam occupies a small angle compared to the total angle of view of the satellite, the angle occupied is ignored and it is assumed that sources on the ground see only the off-main beam sensitivity.

A source located on the cap is assumed uniformly distributed over the visible area. The probability of a finding the source on the surface in the angular interval $(\varphi, \varphi + d\varphi)$ is

$$f_{\varphi}(\varphi)d\varphi = k \cdot 2\pi r^2 \sin\varphi \, \alpha \, \varphi \qquad \text{(II-1)}$$

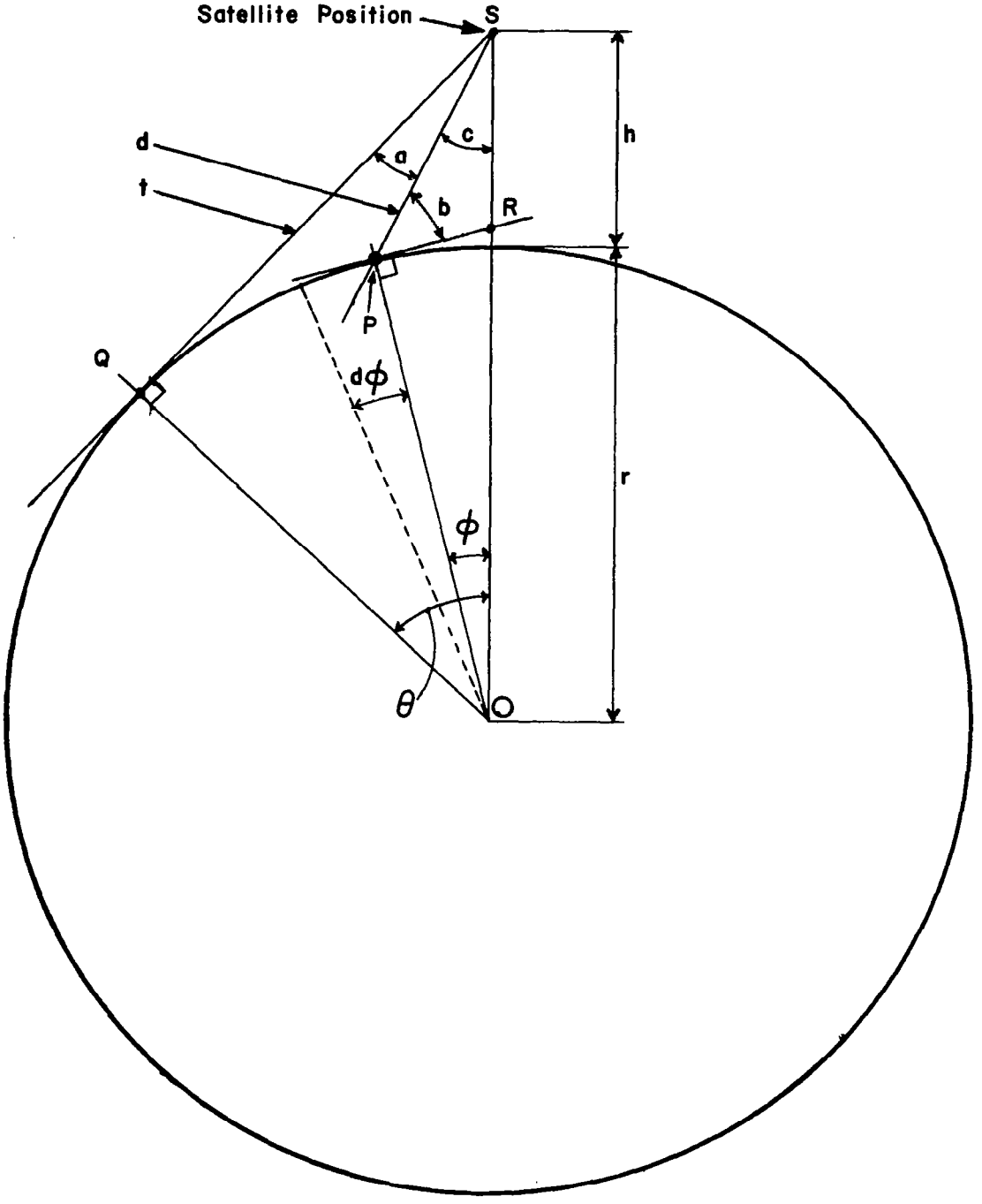

Figure II-1 Satellite Above Earth - Geometric Variables Defined

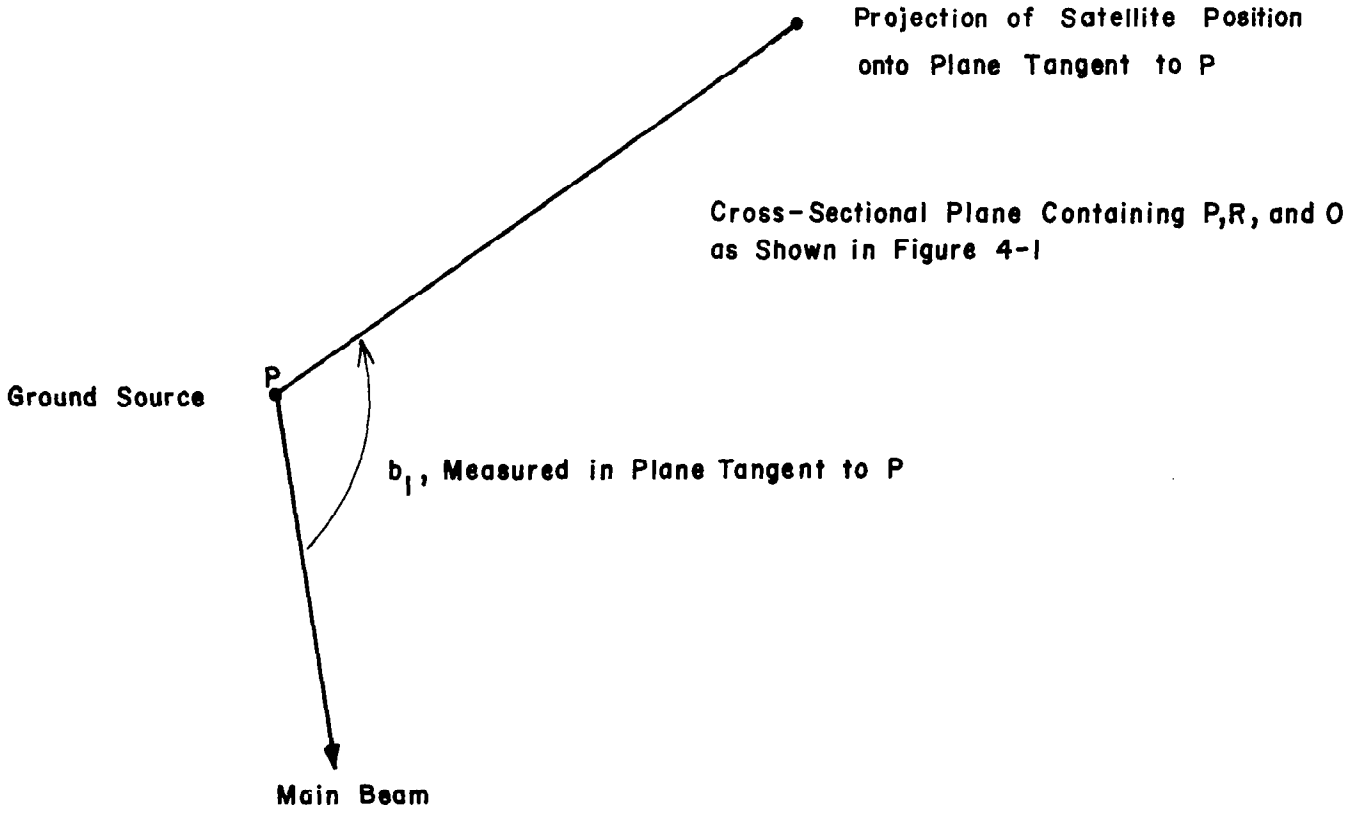

Figure III-2 Ground Source Orientation

where $f_\varphi(\varphi)$ is the probability density function of the random variable φ, k is a constant, and second factor on the right is the area of the surface in the interval $(\varphi, \varphi + d\varphi)$. That is, the uniform distribution implies that the probability of being in a specified area is proportional to the area. Since the source is assumed to be somewhere on the cap we must have

$$\int_0^\theta f_\varphi(\varphi)\, d\varphi = 1 = k \cdot 2\pi r^2 \int_0^\theta \sin\varphi \, d\varphi$$

$$= k \cdot 2\pi r^2 (1 - \cos\theta) \qquad \text{(II-2)}$$

so that

$$k = \frac{1}{2\pi r^2 (1 - \cos\theta)} \qquad \text{(II-3)}$$

and from (II-1)

$$f_\varphi(\varphi) = \frac{\sin\varphi}{1 - \cos\theta} \quad , \quad 0 < \varphi < \theta \qquad \text{(II-4)}$$

$$= 0 \quad , \quad \text{elsewhere}$$

We now determine the angles a and b defined in Fig.II-1 as a function of φ. From the work on p. 44 of the preliminary report (with some changes of notation)

$$\cos b = \frac{r + h}{r} \cos(\theta + a) \qquad \text{(II-5)}$$

From Fig.II-1

$$a + c + \theta = \frac{\pi}{2} \qquad \text{(II-6)}$$

and

$$\varphi + c + b = \frac{\pi}{2} \qquad \text{(II-7)}$$

Eliminating c between (II-6) and (II-7)

$$a - b - \varphi + \theta = 0 \qquad \text{(II-8)}$$

Substituting (II-8)into (II-5)to eliminate a

$$\cos b = \frac{r + h}{r} \cos (b + \varphi)$$

$$= (\cos b \cos \varphi - \sin b \sin \varphi)/\cos \theta$$

or

$$\cos b \, [\cos \theta - \cos \varphi] = -\sin b \sin \varphi$$

or

$$\frac{\sin b}{\cos b} = \tan b = \frac{\cos \varphi - \cos \theta}{\sin \varphi} \qquad \text{(II-9)}$$

From (II-8)

$$a = b + \varphi - \theta = \varphi - \theta - \arctan \frac{\cos \varphi - \cos \theta}{\sin \varphi} \qquad \text{(II-10)}$$

Equations II-9 and II-10 give a and b in terms of the known cap angle θ and the random variable angle φ.

The received power at the satellite is given by the formula

$$P_r = \frac{\lambda^2}{(4\pi d)^2} P_t G_t G_r \, , \qquad \text{(II-11)}$$

or in dB by,

$$P_r = P_t + G_t + G_r + \left[\frac{\lambda^2}{(4\pi d)^2}\right] \text{dB} \qquad \text{(II-12)}$$

where P_t = transmitted power

G_t = transmitter antenna gain in the direction of the receiver

G_r = receiver antenna gain in the direction of the transmitter.

The term $\left[\lambda^2/ (4\pi d)^2\right]$ dB, where λ is the wavelength, is the free space loss which depends on the distance d in Fig. II-1. In terms of φ, d is given by

$$d^2 = r^2 + (r + h)^2 - 2r(r + h)\cos\varphi$$

$$= h^2 \left[1 + \frac{4r(r + h)}{h^2} \sin^2 (\varphi/2) \right]$$

$$= t^2 \left[1 + \frac{2r^2 - 2r(r + h)\cos\varphi}{t^2} \right] \qquad \text{(II-13)}$$

Where t is the tangential distance as defined in Fig.II-1. Each of the terms on the right of(II-12) is a random variable, and the sum of these is the random variable of interest P_r. In many instances the services in operation at any one frequency are of one kind, all using the same transmitted power, P_t. P_t is therefore assumed fixed and the probability density of

$$P_r - P_t \equiv P_\delta = G_t + G_r + \left[\frac{\lambda^2}{(4\pi d)^2}\right] \text{dB} \qquad \text{(II-14)}$$

is found.

To determine the probability density of P_δ, denoted $f_p(p)$, the joint density of the two dimensional random variable (P_δ, φ), denoted $f_{p,\varphi}(p,\varphi)$ is found and marginalized:

$$f_{P_\delta}(p) = \int_{\varphi=0}^{\theta} f_{P_\delta,\varphi}(p, \varphi)\, d\varphi \qquad \text{(II-15)}$$

The joint density can be written

$$f_{P_\delta,\varphi}(p, \varphi) = f_{P_\delta|\varphi}(p, \varphi)\, f_\varphi(\varphi) \qquad \text{(II-16)}$$

where $f_\varphi(\varphi)$ is given by (II-4) and $f_{p_\delta|\varphi}(p,\varphi)$ is the conditional density of P_δ given φ. At a given value of φ, the free space loss in (II-14) ($= \lambda^2/(4\pi d)^2$) is constant but G_t and G_r are random variables which generally depend on φ. Antenna gain models are now described which will make it possible to determine this dependence.

The antenna gain model to be used for the ground antenna is shown in Fig. II-3. A similar model might be used for the satellite antenna but, for reasons given later, other models will be used for this case. The ground antenna is assumed to have a constant gain, G_m, over a region in the vicinity of the main beam as shown in Fig. II-3, and random gain as a function of position elsewhere. Models of this kind are described in the RADC Interference Notebook (Ref. 41) and by Johnson (Ref. 48). From tests on actual antennas it has been found that the back and sidelobe radiation patterns are approximately Gaussian random processes when the gain is measured in dB, with mean of about -10 dBi and a standard deviation ranging around 6 dB. The gain as a numerical ratio (rather than in dB) is therefore log-normally distributed. If a random variable x is normal then

$$y = e^{bx} \tag{II-17}$$

is log normal. With $b^{-1} = 10 \log_{10} e$, x is the value of y in dB. It can be shown that the mean and variance of y are given by

$$< y > = e^{bm_x + b^2\sigma_x^2/2} \tag{II-18}$$

$$\text{var } y = < y >^2 \left(e^{b^2\sigma_x^2} - 1\right) \tag{II-19}$$

where m_x and σ_x^2 are the mean and variance of the normal random variable, x. In our parlance x represents the gain in dB and y represents the unitless gain ratio. With m_x = -10 dB, σ_x = 6 dB, and b = 0.1 $\log_e 10$ = 0.23, the average value of y is

$$< y > \equiv G_b = e^{-2.3 + 18\,(0.23)^2} = 0.26 \ (= -5.8 \text{ dB}) \tag{II-20}$$

This is the mean value of the gain over the sphere surrounding the antenna except for the region of the main beam. It will be denoted by G_b. A value of 0.26 for G_b means that 26% of the transmitted power appears off the main lobes. The average gain over the entire sphere surrounding the antenna is unity for a 100% efficient radiator. (Losses

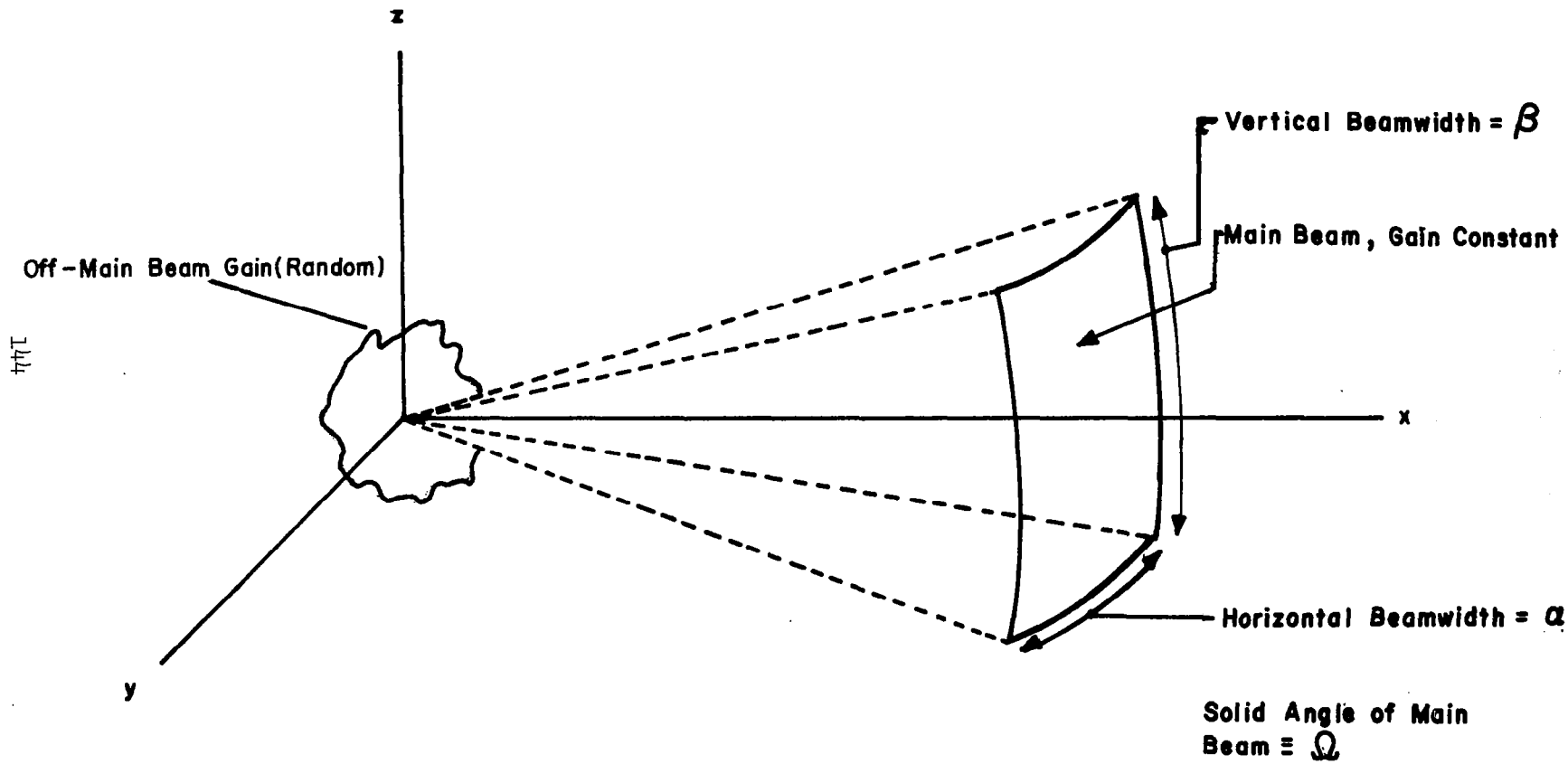

Figure II-3 Antenna Gain

may be assumed to reduce the transmitted power and the antenna may be treated as 100% efficient). Thus the average gain, G_{av}, is

$$G_{av} = \frac{1}{4\pi}\left[G_m \Omega + (4\pi - \Omega) G_b\right] = 1 \qquad \text{(II-21)}$$

where Ω is the solid angle of the main beam over which the gain is assumed to be the constant value G_m. The region of constancy will later be chosen based on the 3 dB beamwidths of the actual antennna modeled. Thus

$$G_b = \frac{1 - G_m\Omega/4\pi}{1 - \Omega/4\pi} \qquad \text{(II-22)}$$

For a narrow beamwidth antenna $\Omega/4\pi \ll 1$ so that

$$G_b \doteq 1 - G_m\Omega/4\pi \qquad \text{(II-23)}$$

Fig.II-3 shows a rectangular antenna beam -- a reasonable approximation for many radar antennas which have a fan beam. For small planar angles α and β the solid angle is

$$\Omega \doteq \alpha\,\beta \qquad \text{(II-24)}$$

so that

$$G_b \doteq 1 - G_m\,\alpha\beta/4\pi \qquad \text{(II-25)}$$

If the beam were of circular cross-section with planar beam angle α the solid angle would be approximately

$$\Omega = \frac{\pi}{4}\,\alpha^2 \qquad \text{(II-26)}$$

and

$$G_b = 1 - \frac{G_m\,\alpha^2}{16} \qquad \text{(II-27)}$$

The antenna gain pattern model described will be used in place of the actual three-dimensional antenna pattern, which is, in any event, usually unavailable. The antenna data commonly available are the 3 dB beamwidths and main beam gain. From the latter the parameters of the model are to be determined. The most obvious steps are to equate G_t with the given antenna's maximum gain and to equate α and β with the given antenna's 3 dB beamwidths and from these to determine suitable values of the mean and standard deviation of G_b when the latter is given in dB. This approach is, in fact, reasonable as we show for the case of a parabolic dish. Assuming the dish has a gain G the 3 dB beamwidth is approximately (Ref. 34, p. 12-14)

$$\alpha_{3\ dB} = \left(\frac{8.22}{G}\right)^{\frac{1}{2}} \text{ radians} \qquad \text{(II-28)}$$

Equating G and $\alpha_{3\ dB}$ with G_m and α in(II-27) we get

$$G_b = 1 - \frac{8.22}{16} \doteq 0.5 \qquad \text{(II-29)}$$

This value is larger than the value found in(II-20) where a mean of -10 dBi and a standard deviation 6 dB were used for the parameters of the random off main beam gain in dB. Had we used a value of standard deviation of 8 dB, retaining the mean value of -10 dBi, we would get a value of $G_b = 0.54$. This conforms well enough to the result of (II-29). The standard deviation of 8 dB is within the range experimentally observed (Ref. 41) and is typical of the patterns seen around antennas in crowded environments. A reasonable procedure would then be to equate the maximum gain and 3 dB beamwidths to G_m, α and β respectively, then to find G_b from (II-25)or(II-27) depending on whether a rectangular or circular beam cross section is more reasonable. Next, a suitable value for the standard deviation, σ_x, of the off main beam gain in dB is obtained using (II-18) with the mean,m_x, set to - 10 dBi.

As an example consider the fan-beam antenna used with the AN/SPS-10 radar. Its given characteristics are (Ref. 48)

Gain = 30 dB
Vertical 3 dB beamwdith = $\beta = 17^o$
Horizontal 3 dB beamwidth = $\alpha = 1.8^o$

The rectangular model is appropriate and from (II-25)

$$G_b = 0.26$$

Using (II-18), assuming that the mean off-axis gain is -10dBi and $y = G_b = 0.26$, the standard deviation of the off-axis gain σ_x, is 6 dB.

We now return to (II-14), the equation giving the difference between received and transmitted power, P_δ, as a function of antenna gains and free space loss. The probability density of the power difference, P_δ, is to be found as given by (II-15) and (II-16), and the conditional density $f_{p|\varphi}(p, \varphi)$. It will simplify matters if the ground antenna is assumed to have a rectangular pattern with horizontal beamwidth α and vertical beamwidth β. Then, from Fig. II-1

$$\begin{aligned} &\text{if } b < \beta, \quad G_t = G_m \text{ with probability } \frac{\alpha}{2\pi}, \\ &\qquad \text{and}^* \quad N(-10 \text{ dBi}, \overline{6 \text{ dB}}^2) \text{ with probability } \left(1 - \frac{\alpha}{2\pi}\right) \\ &\text{if } b > \beta, \quad G_t \text{ is } N(-10 \text{ dBi}, \overline{6}^2). \end{aligned} \tag{II-30}$$

The probability of encountering the main beam is assumed constant for all $b < B$. This is an approximation if the vertical beamwidth $B \ll \pi/2$. From (II-9) we can determine for any given φ what the corresponding value of b is. A curve of this function for a satellite altitude of 250 miles, for which $\theta = 19.75^\circ$ is shown in Fig. II-4. If, for instance, the ground antenna were the AN/SPS -10 antenna whose vertical beamwidth $\beta = 17^\circ$, $b < \beta$ implies $\varphi > 8.75^\circ$. Since $\alpha = 1.8^\circ$, and $G_m = 30$ dB,

$$\begin{aligned} G_t &= 30 \text{ dB with probability } 0.005 \\ &= N(-10 \text{ dBi}, \overline{6 \text{ dB}}^2) \text{ with probability } 0.995 \end{aligned} \Bigg\} \text{ for } 8.75 < \varphi < 19.75^\circ$$

$$= N(-10 \text{ dBi}, \overline{6 \text{ dB}}^2) \qquad \text{for } 0 < \varphi < 8.75^\circ$$

(II-31)

---

* The notation $N(m, \sigma^2)$ denoted a normally distributed random variable, x, with mean = m and variance = σ^2. That is,

$$N(m, \sigma^2) = \frac{1}{\sigma \sqrt{2\pi}} e^{-\frac{(x-m)^2}{2\sigma^2}}$$

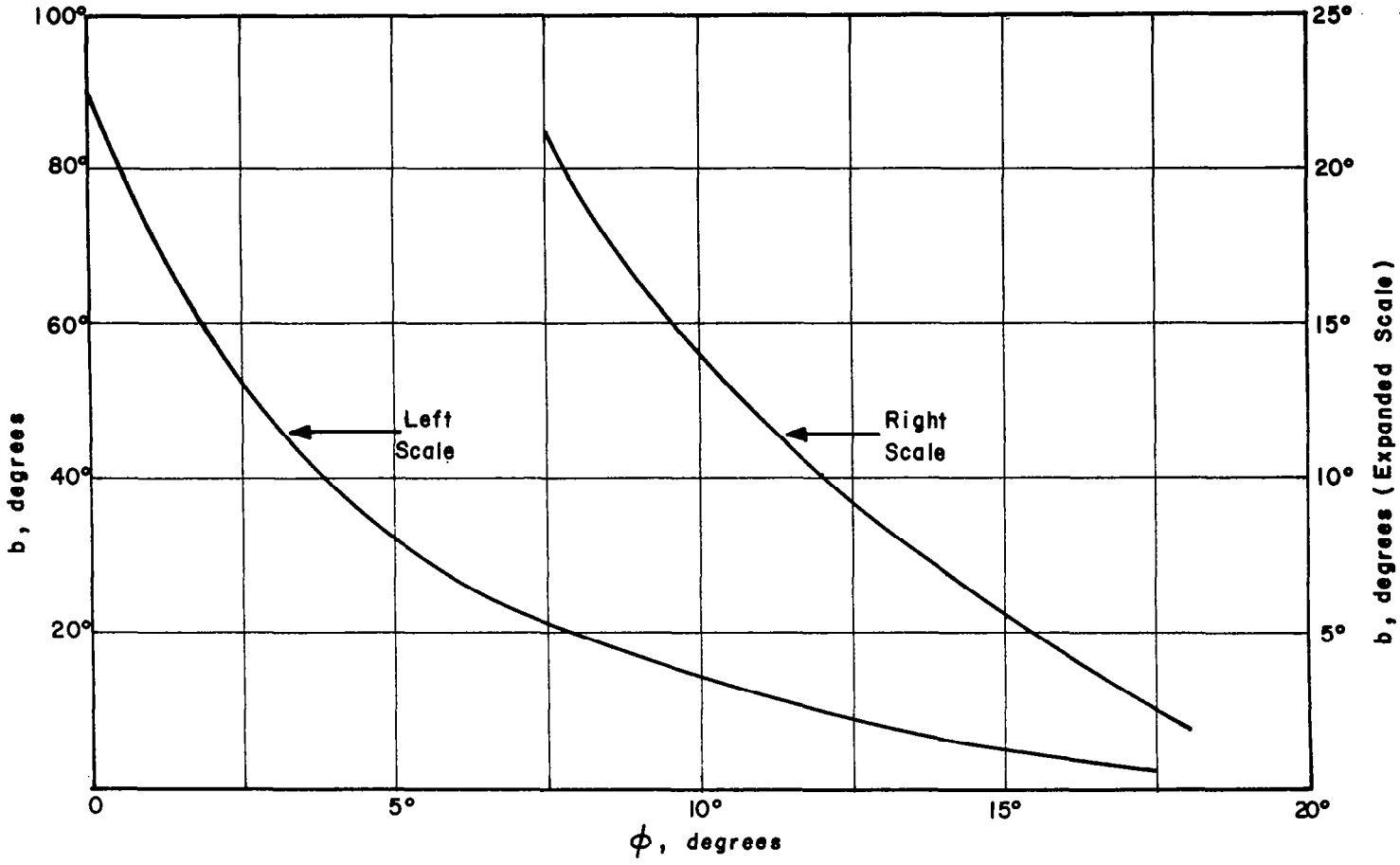

Figure II-4 Elevation Angle, b, as a Function of Angle off Nadir, ϕ (Equation II-9). Satellite Altitude = 250 mi, θ = 19.75°

G_r, the satellite receiver gain pattern, can be modeled in a simpler manner since we are, in this case, calculating the off main beam contributions. That is, the main beam part of the satellite antenna sensitivity is omitted leaving only the side and back lobe features to be simulated. Again here we may treat the gain in dB as a normal random variable with mean gain of -10 dBi and standard deviation which comforms to the procedure described above(II-29). As is discussed elsewhere in this report it will be advantageous to try to design a receiver antenna whose side and back lobe sensitivity is a relatively smooth function of the angle off the main beam. Ideally, the back and side lobe sensitivity would be a constant. A reasonable value would be $0.25 < G_b < 0.5$ or, in dB -6 dBi $< G_b <$-3 dBi. We will carry out a computation initially based on G_b a constant value of -3 dBi. Equation II-14 is therefore

$$P_\delta = G_t - 3 \text{ dB} + \left[\frac{\lambda^2}{(4\pi)^2}\right]_{dB} - \left[d^2\right]_{dB}$$

$$= G_t - 3 \text{ dB} + \left[\frac{\lambda^2}{(4\pi)^2}\right]_{dB} - \left[t^2\right]_{dB} - \left[1 + \frac{2r^2 - 2r(r+h)\cos\varphi}{t^2}\right]_{dB} \quad \text{(II-32)}$$

Use was made of (II-13) to replace d^2. Some of the constants with respect to φ are moved to the left of the equation giving

$$P_\delta - \left[\frac{\lambda^2}{(4\pi)^2}\right]_{dB} + \left[t^2\right]_{dB} \cong P = G_t - 3 \text{ dB} - \left[k_1 - k_2 \cos\varphi\right]_{dB} \quad \text{(II-33)}$$

where

$$k_1 = 1 + \frac{2r^2}{t^2} = 16.52$$

$$k_2 = \frac{2r(r+h)}{t^2} = 16.49 \quad \text{(II-34)}$$

for h = 402 km (250 miles), r = 6440 km (4000 miles). For $h \ll r$, k_1 is very nearly equal to k_2 and we will take it as such generally. Thus

$$k_1 = 1 + \frac{2r^2}{t^2} \doteq k_2 \tag{II-35}$$

and

$$\begin{aligned} P &= G_t - 3 - 10 \log_{10} k_1 - 10 \log_{10} (1 - \cos \varphi) \\ &= G_t - 15.18 - 10 \log_{10} (1 - \cos \varphi) \end{aligned} \tag{II-36}$$

Using (II-31) the conditional probability density of P given φ is*

$$\begin{aligned} f_{P|\varphi}(p, \varphi) &= \frac{1}{\sigma\sqrt{2\pi}} e^{-\frac{(p-m)^2}{2\sigma^2}}, \quad 0 < \varphi < 8.75^\circ \\ &= 0.005\ \delta\,[p - 30 + 15.18 + 10 \log_{10} (1 - \cos \varphi)] \\ &\quad + \frac{0.995}{\sigma\sqrt{2\pi}} e^{-\frac{(p-m)^2}{2\sigma^2}} \qquad 8.75^\circ < \varphi < 19.75^\circ \end{aligned} \tag{II-37}$$

where

$$\begin{aligned} m &= -10 \text{ dB} - 15.18 - 10 \log_{10} (1 - \cos \varphi) \\ \sigma &= 6 \text{ dB} \end{aligned} \tag{II-38}$$

Using (II-4) and (II-16) we have for (II-15)

---

* $f_P(p)$ can be found using expressions similar to (II-15) and (II-16) by using P rather than the difference in power P_δ.

$$f_p(p) = \int_0^{19.75^\circ} f_{p|\varphi}(p, \varphi) \frac{\sin\varphi}{1 - \cos\theta} \, d\varphi$$

$$= \int_0^{8.75^\circ} \frac{1}{6\sqrt{2\pi}} e^{-\frac{[p + 25.18 + 10 \log_{10}(1 - \cos\varphi)]^2}{2 \cdot 6^2}} \cdot \frac{\sin\varphi}{1 - \cos\theta} \, d\varphi$$

$$+ \int_{8.75^\circ}^{19.75^\circ} \frac{0.995}{6\sqrt{2\pi}} e^{-\frac{[p + 25.18 + 10 \log_{10}(1 - \cos\varphi)]^2}{2 \cdot 6^2}} \cdot \frac{\sin\varphi}{1 - \cos\theta} \, d\varphi$$

$$+ 0.005 \int_{8.75}^{19.75} \delta[p - 30 + 15.18 + 10 \log_{10}(1 - \cos\varphi)] \cdot \frac{\sin\varphi}{1 - \cos\theta} \, d\varphi \qquad \text{(II-39)}$$

The evaluation of the first two terms of (II-39) has been done numerically using a trapezoidal rule approximation to determine the integrals. The results obtained is shown in Fig. II-5.

The third term of II-39, identified as

$$I = 0.005 \int_{8.75^\circ}^{19.75} \delta[p - 14.82 + 10 \log_{10}(1 - \cos\varphi)] \frac{\sin\varphi}{1 - \cos\theta} \, d\varphi \qquad \text{(II-40)}$$

can be integrated in closed form. Since the integrand involves a delta function it contributes to the integral only when

$$p - 14.82 + 10 \log_{10}(1 - \cos\varphi) = 0 \qquad \text{(II-41)}$$

I will take on non-zero values for p in a range which satisfies (II-41) with φ in the range $(8.75^\circ, 19.75^\circ)$. To determine the range let $\varphi = 8.75^\circ$ in (II-41) to give

$$p = 34.16$$

and then let $\varphi = 19.75^{\circ}$ in (II-41)to give

$$p = 27.12$$

thus the non-zero values of I occur in the range of p given by the interval (27.12, 34.16).

To determine the value of the integral(II-40) let

$$x = 10 \log_{10} (1-\cos \varphi) = 10 \log_{10} e \ \log_e (1-\cos \varphi)$$

$$\frac{dx}{d\varphi} = 10 \log_{10} e \cdot \frac{\sin \varphi}{1-\cos \varphi}$$

$$1-\cos \varphi = 10^{\frac{x}{10}}$$

substituting(II-42) into(II-40) given

$$I = 0.005 \int \delta[p - 14.82 + x] \frac{10^{\frac{x}{10}} dx}{10 \log_{10} e.(1-\cos \varphi)} \qquad \text{(II-43)}$$

$$= 0.005 \frac{10^{\frac{(14.82 - p)}{10}}}{10 \log_{10} e. (1-\cos \varphi)} \quad , \ 27.12 < p < 34.16$$

This result is plotted in Fig.II-5 together with the numerically computed portions of (II-39).

Equation II-39 was set up to conform to a typical radar antenna. A corresponding result for a CW transmitter such as those used for line-of-sight microwave transmission is in order. We assume the typical case of a parabolic dish of about 6 ft. diameter operating at 3 GHz with a gain of 33 dB and a corresponding 3 dB beamwidth of about 3.6°. From(II-25) (with $\alpha = \beta$ = beamwidth) $G_b = 0.35$ so that the random off-main-beam gain will have a mean of -10 dBi and, from (II-18), the standard deviation would be 7 dB. From Fig.II-4 the value of φ at which $b = \beta$ is about 16.4°. For $16.4 < \varphi < 19.75$ the main beam of the ground source may be seen with probability 3.6/360 = 0.01. Thus the probability density of the received power for this case is

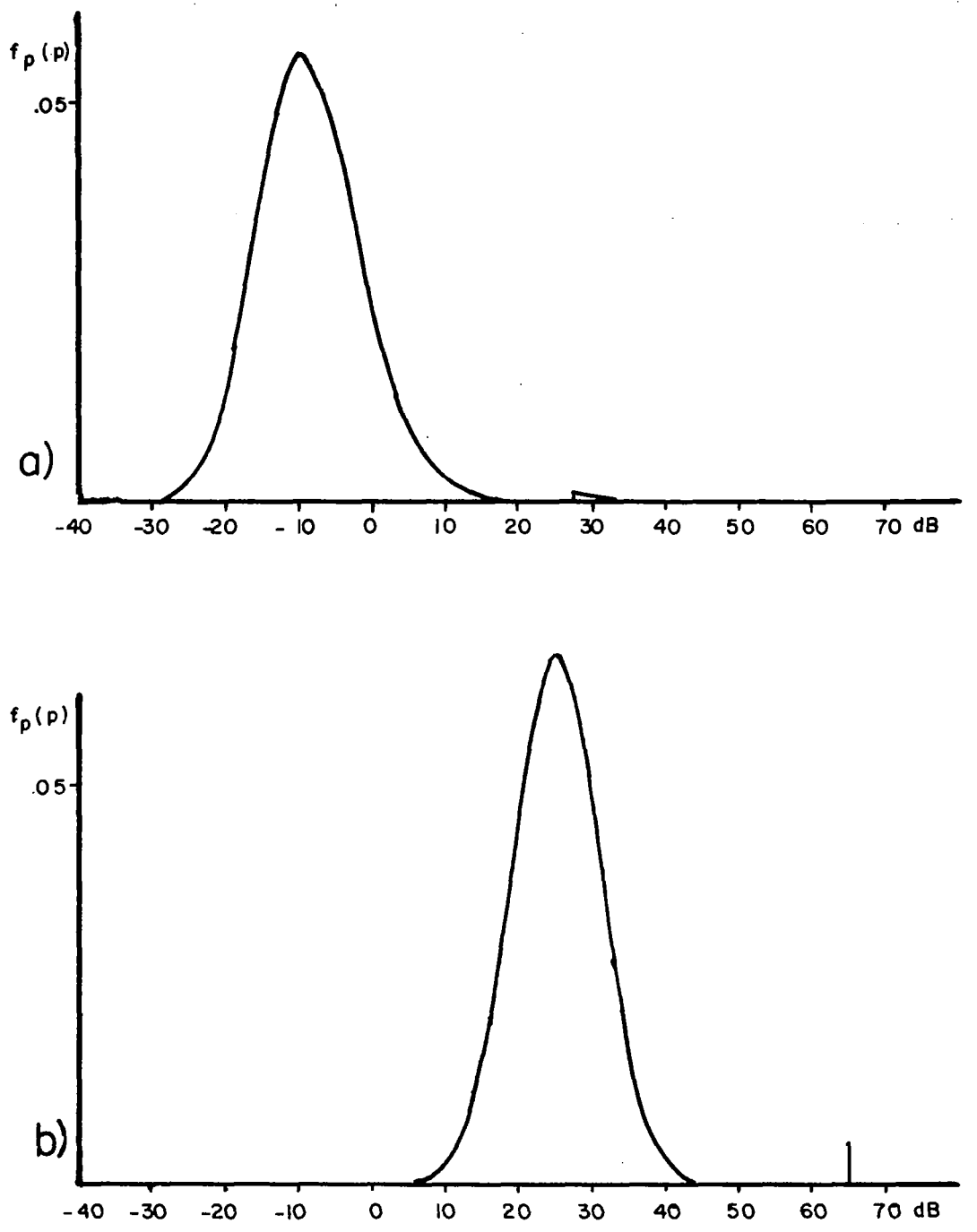

Figure II-5 Probability Density as a Function of $P_t - P_r$. (a) In the Receiver's Backlobe, (b) In its Mainbeam

$$f_p(p) = \int_0^{16.4} \frac{1}{7\sqrt{2\pi}} e^{-\frac{(p-m)^2}{2\cdot(7)^2}} \frac{\sin\varphi}{1-\cos\theta}\, d\varphi$$

$$+ \int_0^{19.75} \frac{0.99}{7\sqrt{2\pi}} e^{-\frac{(p-m)^2}{2\cdot(7)^2}} \frac{\sin\varphi}{1-\cos\theta}\, d\varphi$$

$$+ 0.01 \int_{16.4}^{19.75} \delta[p-33+15.18+10\log_{10}(1-\cos\varphi)] \frac{\sin\varphi}{1-\cos\theta}\, d\varphi \qquad \text{(II-44)}$$

where m is as given in (II-38). The solution to (II-44) is done in a manner similar to (II-39).

The next steps are (1) to account for the presence of more than one source on the ground if indeed the presence of more than one is likely, and (2) to compare the received amplitudes from the unwanted sources to the levels of typical desired sources. With regard to the effect of multiple sources we distinguish two cases as discussed in the introduction, namely,

1. The sources are all continuous and independent of one another. In that event the powers observed at the satellite are additive and the probability density of the sum is obtained by convolving the probability density of a single source as many times as there are sources. The number of sources may be treated as a known number or as a random number. We will treat it as a known number, the number based on the survey data presented elsewhere in this report.*

2. The sources are all low duty cycle radar emissions. In this case, the sum is of the form of random pulses in time with both interpulse interval and amplitude from pulse to pulse fluctuating. The statistics of the pulse to pulse interval has been studied (Ref.49) but the important point in our case is whether or not the pulses will obscure other desired signals. If, for instance, a radar emission is to be measured it is important that the emission stands above the undesired signals. Thus, we need the probability density of amplitudes of the largest of the unwanted signals. This is an order statistic which can be calculated from the probability density of amplitudes of any one undesired signal relatively simply. Denoting the distribution function of the signal received from each emitter by

$$F_p(p) = \text{Prob [Power received } P < p]$$

* The additivity applies to power in watts, not power measured logarithmically in dB.

The probability that $P < p$ for m emitters is

$$F_{mp}(p) = F_p^m(p)$$

This is also the probability that the largest power received is less than p. Thus, the probability density of the maximum power received from m sources is

$$f_{mp}(p) = \frac{dF_{mp}(p)}{dp} = m\, F_p^{m-1}(p)\, \frac{d\, F_p(p)}{dp}$$

$$= m\, F_p^{m-1}(p)\ \ f_p(p)$$

$$= \left[\int_o^p f_p(p_1)\, dp_1\right]^{m-1} \quad f_p(p) \qquad \text{(II-45)}$$

The comparison to levels of desired sources in the satellite antenna's main beam is made by determining the probability density of power received along the main beam. The received signal power is given by (II-12) where, in this case d = t, the distance from satellite to the horizon (horizon scan is being assumed). Thus, we write an expression which is analogous to (II-33)

$$P_\delta - \left[\frac{\lambda^2}{(4\pi)^2}\right]_{dB} + [t^2]_{dB} = P = G_t + G_r \qquad \text{(II-46)}$$

In (II-33) P was determined for unwanted signals; (II-46) is the corresponding value of P determined for the desired signals. G_r, the satellite receiver's main-beam gain, ranges around 35 dB and we will use this value as typical. G_t, the ground source gain, now being viewed in its main-beam plane, is either the high main beam gain or the random side and back lobe gain. The models adopted earlier in this section will again be used here. Thus, for the case of a fan beam radar emission, from (II-31)

$$G_t = 30 \text{ dB with probability } 0.005$$
$$= N(-10 \text{ dBi}, \overline{6 \text{ dB}}^{\,2}) \text{ with probability } 0.995 \qquad \text{(II-47)}$$

(No specification involving φ is needed here since the ground antenna is being examined in its emission plane.) Thus the random variable P is described probabilistically as follows:

$$\begin{aligned} P &= 65 \text{ dB with probability } 0.005 \\ &= N(25 \text{ dBi}, \overline{6 \text{ dB}}^{\,2}) \text{ with probability } 0.995. \end{aligned} \tag{II-48}$$

The two probability densities are shown superimposed in Figure II-5, the unwanted density having been determined for a single unwanted source. Denoting the desired signal power by P_d and the undesired signal power by P_n, with corresponding subscript notation for the probability densities (see Fig. II-5), the probability of the undesired power exceeding the desired power is given by

$$P[P_u > P_d] = \int_{p_2=0}^{\infty} \int_{p_1=p_2}^{\infty} f_{pu}(p_1) f_{pd}(p_2) dp_1 dp_2 \tag{II-49}$$

II.2 Reduction of Effect of Sidelobe Leakage

There are two ways for reducing the effect of side lobe leakage. The first is to reduce side lobe sensitivity and the second is to use signal processing techniques.

With regard to side lobe reduction, horn fed parabolic dish antennas have back and side lobe sensitivities of about 30 to 40 dB below the main beam. It may be possible, by the use of an oversized dish, to reduce these sensitivities; an aperture illumination with a more gradual taper, and a reduction of spill over from the feed horn, might be achieved. Antenna efficiency is, however, lowered and for space applications where size is important this approach does not seem fruitful. Low noise antennas are specifically designed for low back and side lobes sensitivity (to avoid seeing too much of the high temperature earth) and these are either of the Cassegranian feed type or the horn reflector type. The latter has been said to give the lowest noise (Ref. 50., p.336) and from the typical pattern shown in Fig. II-6 (Ref. 51) it is seen to have side and back lobe sensitivity better than 45 dB below the main lobe. Techniques have furthermore been found (Refs. 52 and 53) for reducing the off-main beam gain in selected regions by the use of blinders and resistive edge lining. In our application the horizon is $\pm 70^{\circ}$ away from nadir. In the tangential scanning mode it is therefore only necessary to control sidelobes 140° away from the main lobe measured in the plane defined by the main lobe axis and the center of the earth, and $\pm 70^{\circ}$ measured from nadir in a perpendicular

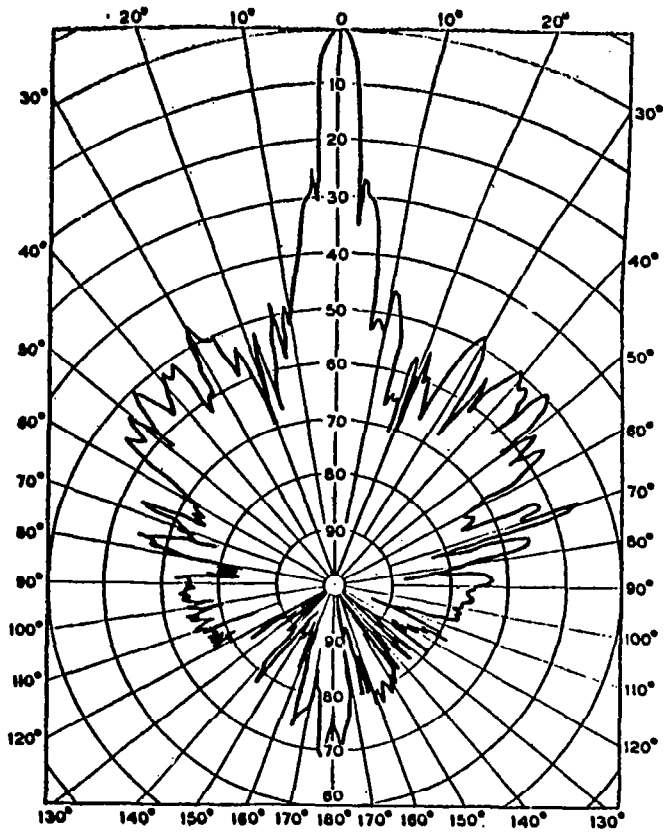

Fig. II-6 Measured Pattern in dB of Horn-Reflector Antenna at 3740 MHz.

plane also going through the earth's center. The greatest danger to the measuring system is expected to come from emitters on the horizon because (a) the ground source main beam may be directed toward the satellite, and (b) the circle at the horizon is of maximum length, giving high probability of sources in this vicinity. Thus, antenna sensitivity in the direction of the horizon should be as low as it can be. If the pattern shown in Fig. II-6 were the vertical pattern, the 140° point would be looking at the opposite horizon from the main beam. The sensitivity of this antenna at the opposite horizon is more than 80 dB below the main beam gain and a source located here, even 70 dB above one on the main beam, would have little effect on the measurement. Thus, the horn reflector has good side lobe characteristics and should be considered as a candidate for this application. It is, however, a bulky structure, and other possibilities, including array systems and cassegranian structures, should be considered.

As pointed out at the beginning of section II-1, with no source on the main beam, readings obtained are a result of side lobe leakage (and internal system noise) and means are required for recognizing such cases. We may imagine a completely quiet condition where the output reading is the result of internal noise only. Readings above the noise level represent ground sources but they may come from sources on or off the main beam. Several means for distinguishing between on- and off-main-beam sources are discussed below.

In the preliminary report a scheme was described for viewing a horizon source for 0.21 seconds in a 1° beamwidth antenna [see eq. (31) of that report]. Every 0.21 seconds the receiver again sweeps through the range of frequencies being observed and thus periodically observes every frequency slot. To be specific, if the receiver were scanning a range from 1 to 2 GHz then according to eq. (32) of the preliminary report, with T = 0.21 seconds, F = 1 GHz, the observation bandwidth would be 577 kHz and the dwell time would be 156 microseconds in each 577 kHz bandwidth slot. A given source would be examined for 156 microseconds in contiguous 577 kHz bands and the observation would be repeated 0.21 seconds later. If the first observation were made with the source in the main beam, the second observation would be made with the source off the main beam because of the antenna motion. The succession of measurements in a particular bandwidth slot, as the satellite moves, will follow the gain pattern of the satellite antenna if the ground source remains constant. Thus, constant on-beam sources can be identified from the sequence of measurements, provided that off-beam sources do not see side lobe variations which look like the main beam pattern variations. Ideally, the pattern off the main beam ought to be constant. In that case, the succession of off-beam measurements should show little or no variation while the on-beam measurements will show a great variation as the main beam sweeps over the source. It would appear though that low and constant off main beam sensitivity are not consistent. Antennas with low side lobe sensitivity like the one shown in Fig. II-6 have side lobe sensitivities that vary markedly with the off-axis angle. Nevertheless,

the main beam variation with angle is expected to be a recognizable feature and should make identification possible for stationary sources. Radar sources with moving antennas pose a problem. In 0.21 seconds a radar antenna rotating at 4 rps will have turned through approximately 20°. The radar antenna gains seen on successive scans separated by 0.21 seconds, may be very different, thus making recognition by this scheme difficult.

Figure II-7 shows sections of a plot of $P_t - P_r$ versus time as given by (II-14) drawn by a computer program that simulates a rotating receiver moving past a rotating transmitter in the same horizontal plane. In this particular simulation, the 6.5 GHz transmitter is rotating clockwise at 12 rpm and the receiver is rotating clockwise at 1 rpm. The hypothetical transmitter has a main beam with 30 dB gain within a 2° angle and -8 dB gain elsewhere, while the receiver pattern is similar to that of the ten-foot dish shown in Fig. 39(b). Initially, both transmitter and receiver are pointing due east, and the receiver is 2500 km due east of the transmitter, traveling south at 7.24 km/s.

In this simulation, the receiver "looks" for a single instant in time every 0.2 seconds, and does not see the transmitter in the intervening time intervals.

The three spikes at the beginning represent the main beam of the transmitter looking at the back lobe of the receiver; the spacing between the peaks within the set is the time for a single rotation of the transmitter. Because the transmitter main beam is so narrow, subsequent peaks do not appear because the main beam passes the receiver during the interval between observations. How many spikes appear in each series and the time between appearances of sets of spikes depends on the relationship between the rotation rate of the transmitter and the time interval between successive observations by the receiver.

The broad symmetrical peak is an image of the receiver's antenna pattern, drawn as it scans the relatively uniform back lobe of the transmitter. On a subsequent rotation of the receiver, we see the spikes of the transmitter pattern superimposed on the receiver pattern. The way the receiver gain pattern dominates the record suggests that one might be able to accurately locate transmitters by processing the received data through a filter that represents the gain pattern of the receiver.

Even in the rotating antenna case, the sequence of measurements shows unusual features which may aid in identifying on-beam sources.

An alternative is to make use of a broad-beam, low gain, auxiliary antenna with its own receiver. The identification of on-beam sources in the narrow-beam antenna would be made by observing differences

between the readings in the two systems. On-beam sources will read substantially higher in the narrow-beam system than in the wide-beam system by an amount equal to the difference in the gains. Off-beam sources will give pairs of readings which are sometimes equal and sometimes such that the wide-beam antenna reading is greater than the narrow-beam antenna reading. With multiple sources, one of which is in the main beam, the difference may be smaller and identification would be less certain. This scheme overcomes the problem found with rotating antennas but it has the disadvantage of multiplying the hardware needs. In the continuing study these alternatives will be more fully developed and a recommendation will be made on the scheme which is judged to be most appropriate.

INITIAL CONDITIONS

TRANSMITTTER PATTERN

ANGLE	GAIN(DB)
0.00	30.0
1.00	30.0
2.00	-6.0
358.00	-8.0
359.00	30.0
360.00	44.1

RECEIVER PATTERN

ANGLE	GAIN(DB)
0.00	44.1
2.00	21.0
15.00	7.0
20.00	0.0
70.00	0.0
100.00	-26.0
260.00	-26.0
290.00	0.0
340.00	0.0
345.00	7.0
358.00	21.0
360.00	44.1

ROTATION RATES

TRANSMITTTER12.000 RPM
RECEIVER 1.000 RPM

INITIAL ORIENTATIONS

TRANSMITTER:90.000DEGREES; RECEIVER: 90.000DEGREES

RECEIVER IS TRAVELLLING 180.000 DEGREES AT 7.240 KM/S

TRANSMITTER IS AT 270.000 DEGREES, 2500.0 KM AWAY

TRANSMISSION FREQUENCY IS 6.500 GHZ

Figure II-7(a) Computer Simulation of a Moving Rotating Receiver Looking at a Rotating Transmitter in the Same Horizontal Plane (Initial Conditions)

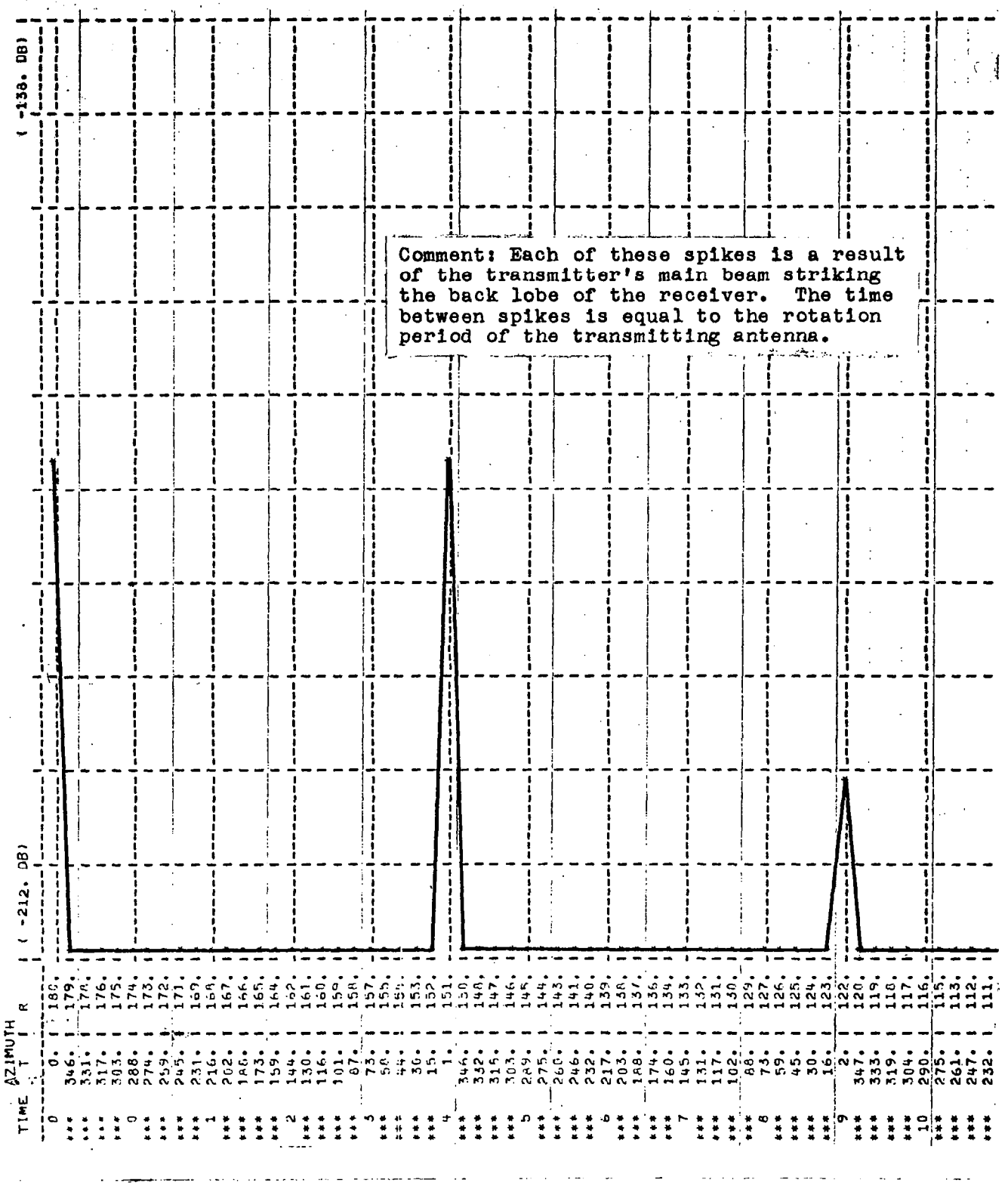

Figure II-7(b) Computer Simulation of a Moving Rotating Receiver Looking at a Rotating Transmitter in the Same Horizontal Plane (Time Zero Through Time 10)

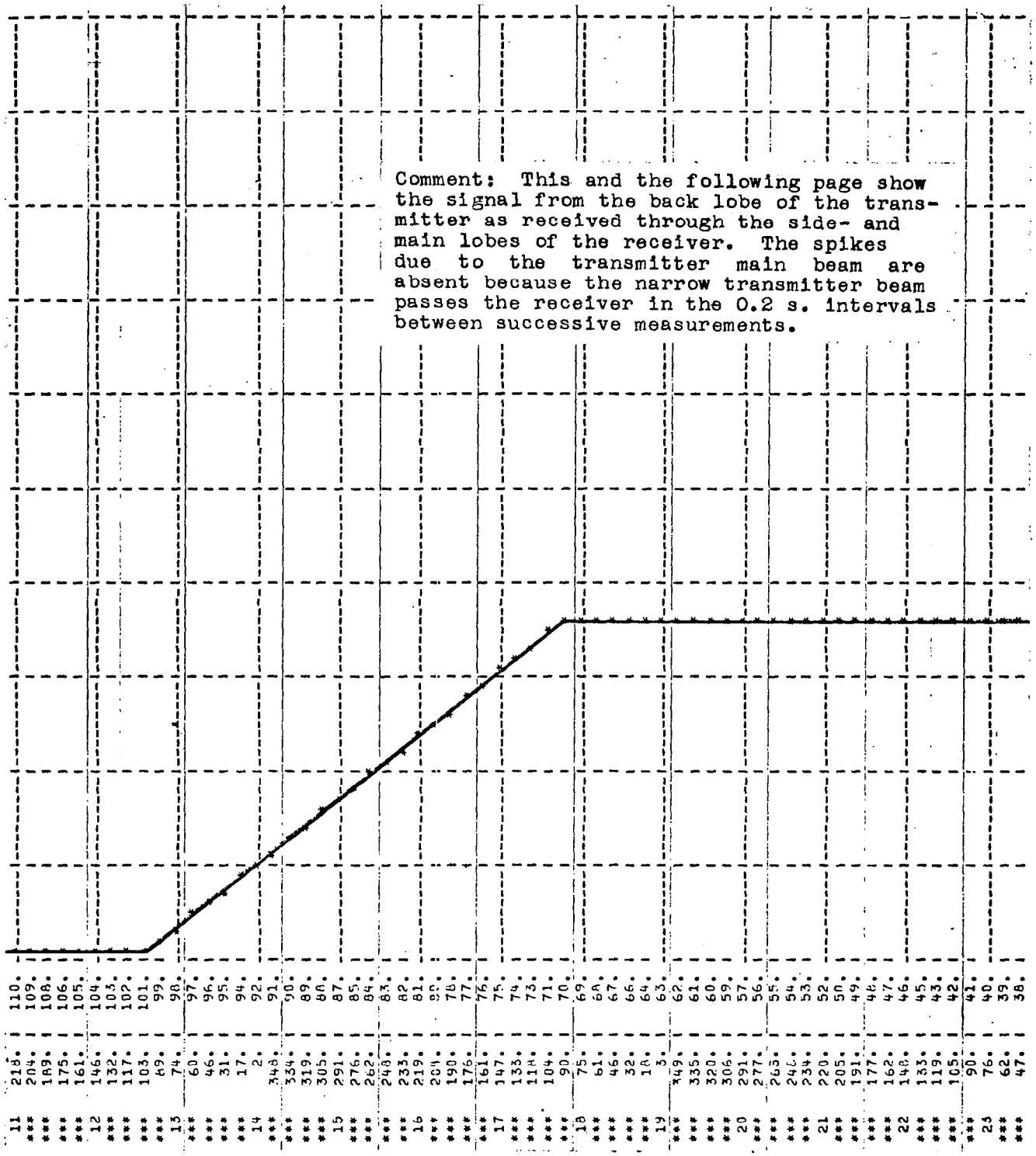

Figure II-7(c) Computer Simulation of a Moving Rotating Receiver Looking at a Rotating Transmitter in the Same Horizontal Plane (Time 11 Through Time 23)

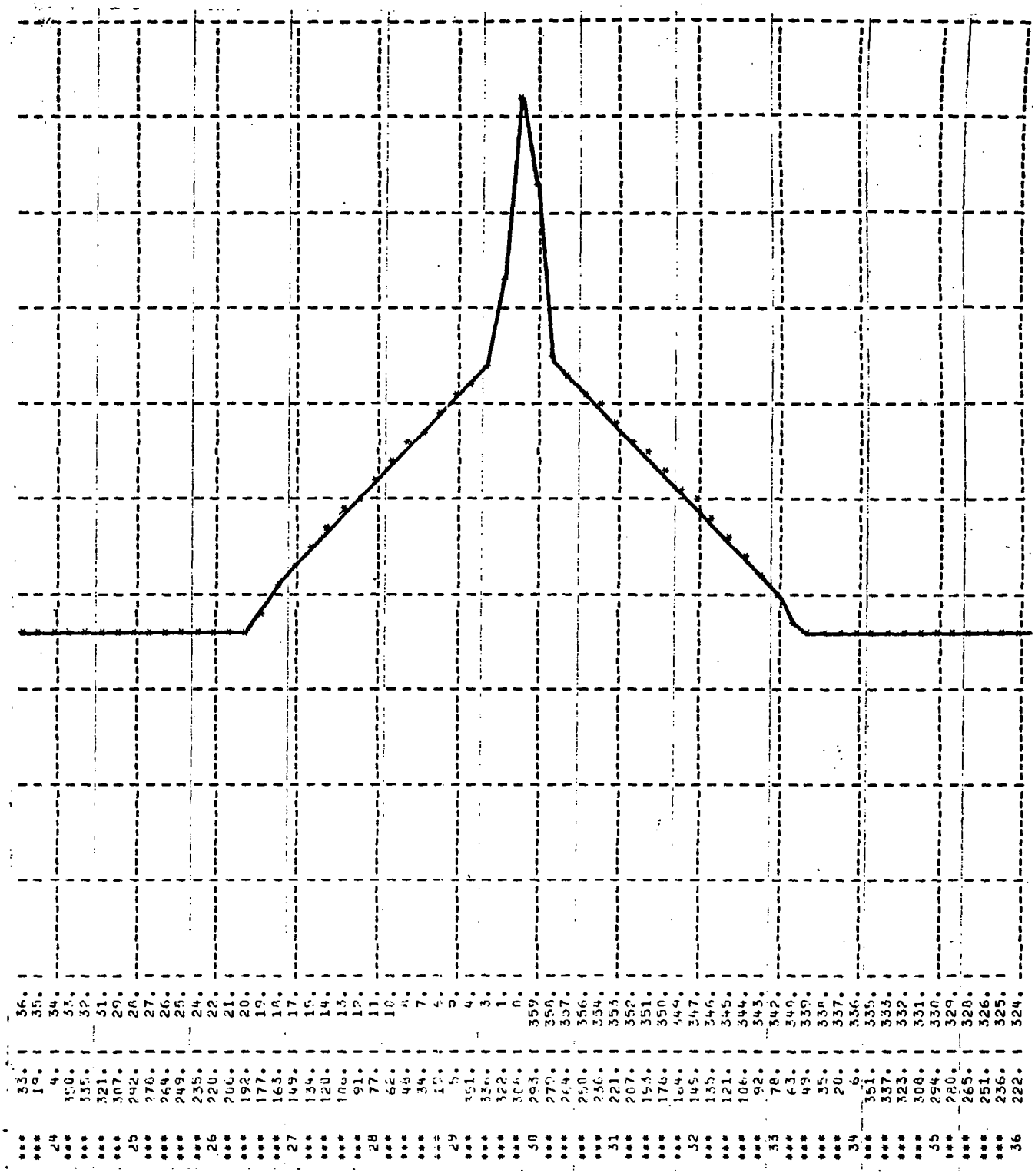

Figure II-7(d) Computer Simulation of a Moving Rotating Receiver Looking at a Rotating Transmitter in the Same Horizontal Plane
(Time 23 Through Time 36)

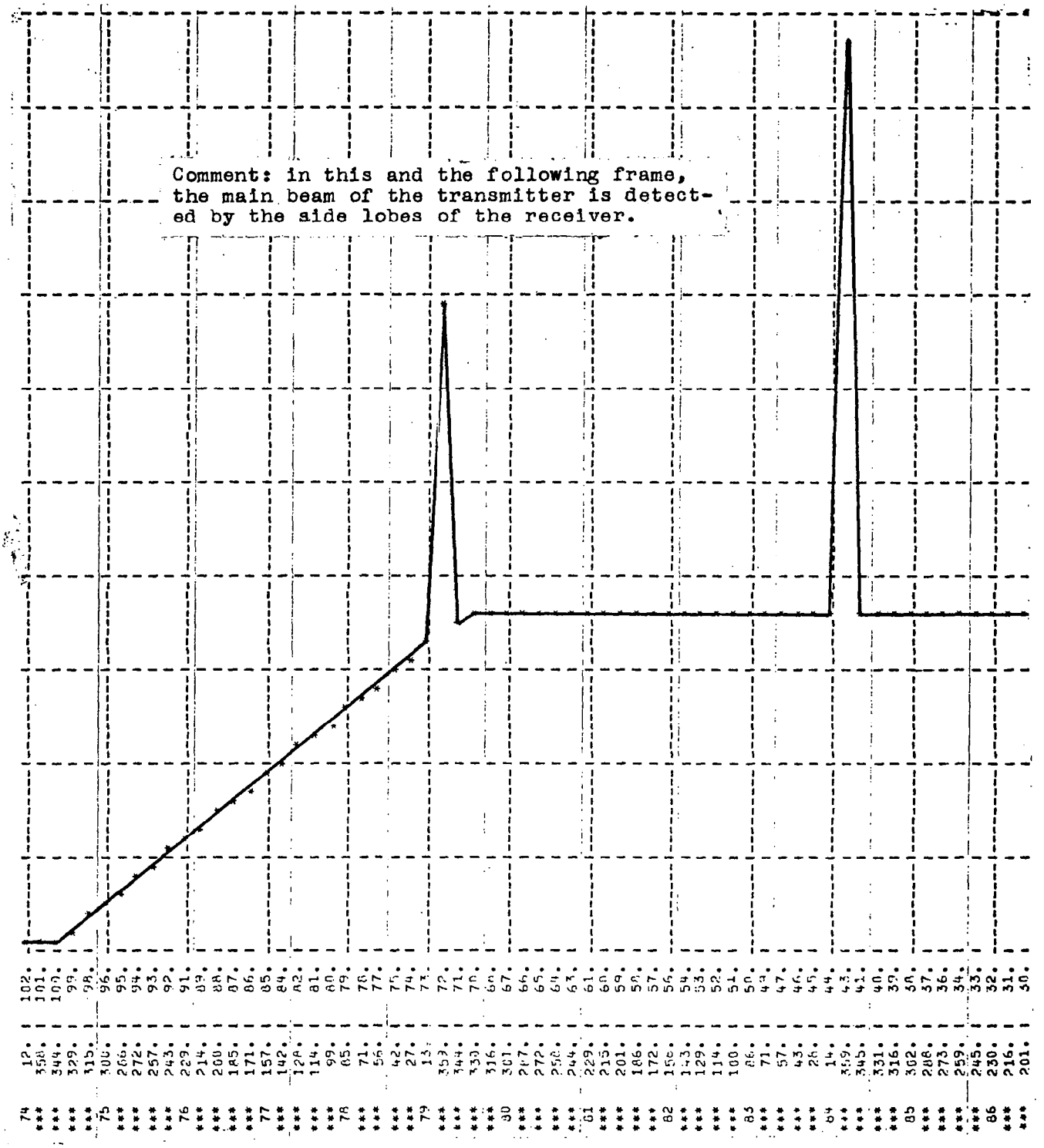

Figure II-7(e) Computer Simulation of a Moving Rotating Receiver Looking at a Rotating Transmitter in the Same Horizontal Plane
(Time 74 Through Time 86)

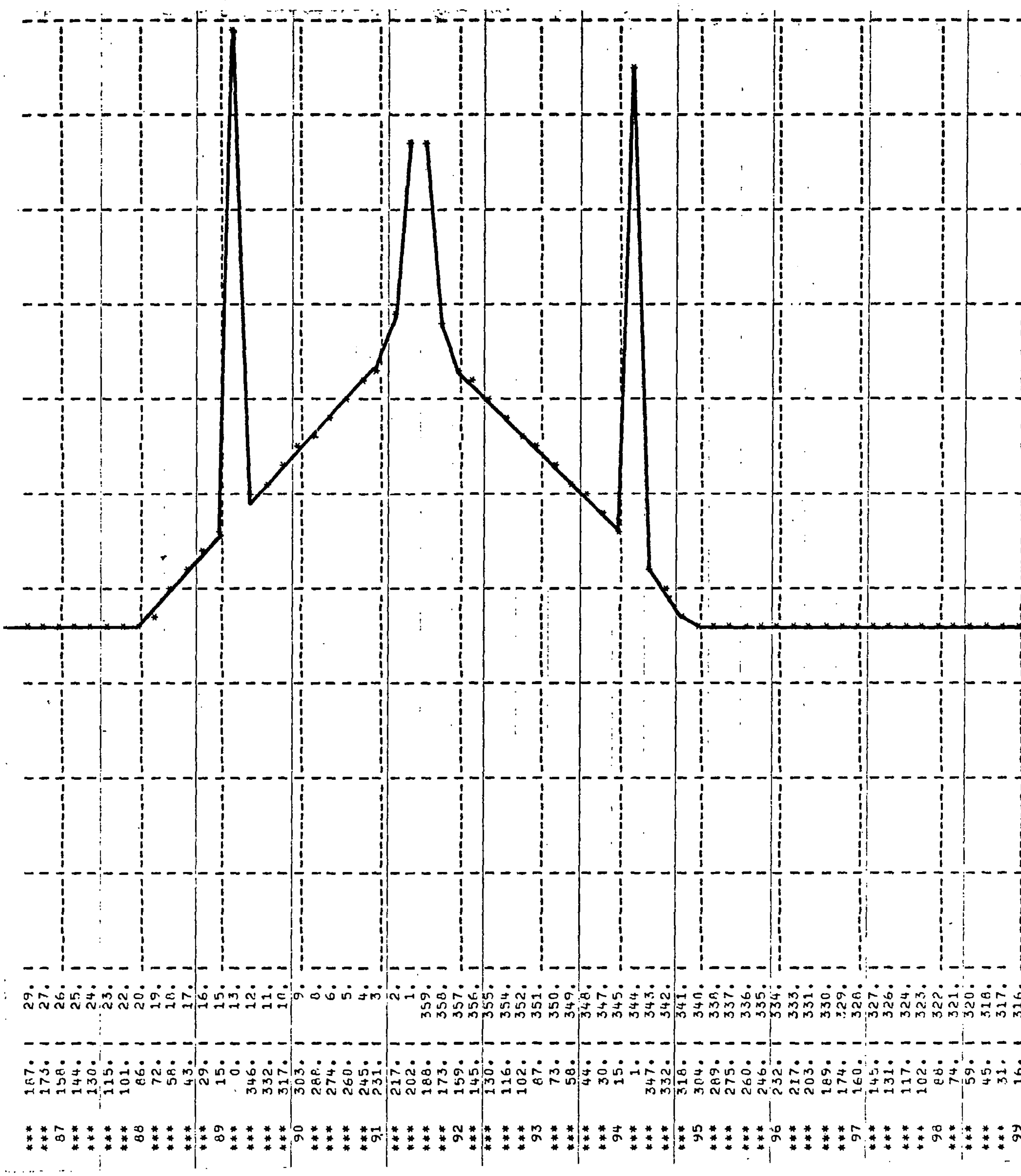

Figure II-7(f) Computer Simulation of a Moving Rotating Receiver Looking at a Rotating Transmitter in the Same Horizontal Plan
(Time 86 Through Time 99)

*U.S. GOVERNMENT PRINTING OFFICE: 1976 - 635-275/104